The Effect of Time-Varying Boundary Conditions on the Generation of Sum and Difference Frequency Tones in a Coaxial Loudspeaker

by

Eddie Dupont

A thesis
presented to the University of Waterloo
in fulfillment of the
thesis requirement for the degree of
Master of Mathematics
in
Applied Mathematics

Waterloo, Ontario, Canada, 2009

I hereby declare that I am the sole author of this thesis. This is a true copy of the thesis, including any required final revisions, as accepted by my examiners.

I understand that my thesis may be made electronically available to the public.

Abstract

A coaxial loudspeaker in which the woofer and tweeter oscillate at angular frequencies ω_1 and ω_2 respectively, is known to produce sum and difference frequencies $\omega_\pm = \omega_1 \pm \omega_2$ [1]. The generation of these can be attributed to both the nonlinearity of the equations of motion and the Lagrangian boundary behaviour of the low-frequency transducer. In order to characterize the phenomena of interest a perturbation expansion of the field variables is introduced (sometimes called quasi-linear approximation). After deriving a second-order equation for pressure, from which the intermodulation frequencies are obtained, an attempt is made to justify the dominance of the boundary mechanism over that of the fluid nonlinearity. An exact integral solution is then given for the spatial factor of the $\omega_\pm$ pressure terms. In the special case of a farfield on-axis observer an analytic solution is obtained. Several numerical investigations are performed and compared with experiment.

Acknowledgments

First and foremost I thank God, and, no less important is Jesus who has always been my inspiration for everything I do.

I am indebted to my supervisor Stan Lipshitz who has helped me develop as a mathematician over the years. I also give thanks to his lab counterpart John Vanderkooy for our enlightening three-way discussions and his acoustical tech savvy. I hope to be able to continue working alongside their unending knowledge.

I am forever grateful to Kevin Lamb for all of the opportunities he has given me as well as Helen Warren for her unwavering support. I thank the whole of the Applied Math department for the encouragement and assistance that I was so generously given through the somewhat rocky study period.

Special thanks to Kevin Krauel for his comments during the many meetings with Stan and especially his motivational sensibility. I am also extremely grateful to his wife Jayne for her corrections to my written work.

Finally, I thank John Wainwright who, several years ago, set me on a better path.

Dedication

No amount of work is trivial or time is wasted when you are supported by love. I have lived every moment because of the love of my friends and family. To them all.

Contents

List of Tables

List of Figures

Chapter 1

Introduction

1.1 Preamble

Before we begin our investigation, the following quote by Beyer [2] is worth mentioning:

"The analysis of a finite-amplitude wave in a real medium involves such a large number of complications that it is not possible to carry the problem through to solution without making an equally large number of mathematical approximations."

1.2 History

While there exist various electro-acoustic transducer technologies [3, 4] the most common type of loudspeaker driver comes in the form of a (typically) circular diaphragm which oscillates as a result of the interaction between a permanent magnet and a varying electromagnetic coil. Although a full study of a loudspeaker would include the physics of the electrical/mechanical components themselves, here we are only interested in the modulation of the air surrounding the speaker and thus, for the sake of tractability, abstract the physical object into a simplified mathematical model.

Although typical electro-dynamic drivers have a conical shape, the standard representative model is that of a flat vibrating piston in an infinite baffle as shown in figure 1.1. According to Chernof [5] this model provides a valid approximation of a loudspeaker up to frequencies of 1kHz.

The solution for the pressure anywhere in the field (based on the first-order wave equation) was given by Rayleigh [6] over a century ago

$$p(x,y,z,t) = \rho_0 \int_{S_w} \frac{\dot{u}_p(\xi,\eta,t-r/c)}{2\pi r} dS_w \tag{1.1}$$

where u_p is the velocity of the piston, ρ_0 is the density of air and c is the speed of sound. The surface S_w is shown in figure 1.1 and need not be circular but must lie on the $z = 0$ plane for (1.1) to be valid. The distance r, also shown in the figure, is given by $r = \sqrt{(x-\xi)^2 + (y-\eta)^2 + z^2}$. While analytic solutions to this equation can only be obtained in special cases (e.g. farfield, on axis of a circular piston) the method used to obtain it is present in much of this thesis. For other results based on non-circular geometries, off-axis observations and various solution methods the reader is directed to [7–13].

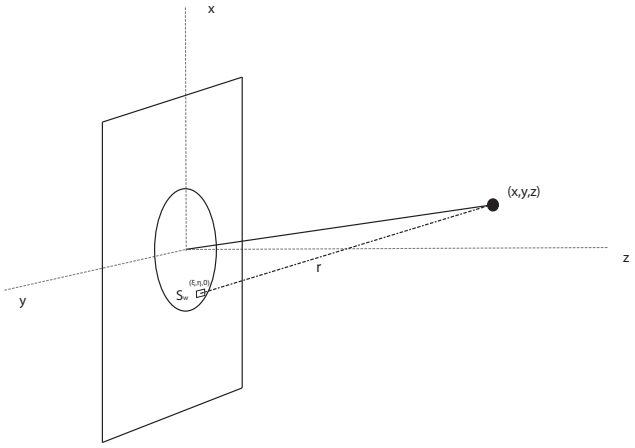

Figure 1.1: Vibrating piston in infinite baffle.

For a more accurate investigation of a very specific structural/acoustic profile a boundary element method would be required. The point here, however, is not to

determine the output of any particular loudspeaker brand but to see if a simplified mathematical model is a good representation of reality. If it is then we also seek to determine what predictions can be made from varying the parameters within the model. If it is not then there should be an attempt to justify any discrepancies between theory and practice.

At this point we should clarify the specifics of the current undertaking. As was mentioned, there is no shortage of investigations on modeling of a simple woofer type loudspeaker. Often however, speaker systems contain both a low-frequency woofer and high-frequency tweeter. Many, if not most, consumer models have these two transducers located at two different positions on the baffle (typically the front of the cabinet). An alternative is to have both transducers performing coaxially with the high-frequency tweeter centered on the woofer (as it's typically the smaller of the two). This setup was previously examined internally by Timko [14] and Gutfraind [15]. Unfortunately there aren't many in-depth scientific investigations of the benefits of one type versus the other. A technical document [16](white paper) released by Frazier Loudspeakers lists some of the following features of coaxial designs:

- Symmetry - Signals arrive at the same time regardless of listener position.
- Equal Phase - Due to the symmetry and the difficulty in building perfect cutoff filters, varying phase profiles at different positions causes amplitude distortions that are uniform as compared with a component setup.
- Seamless Crossover - With both tweeter and woofer at the same location it is difficult to tell when the signal switches between the two.
- Size - The total size of the speaker system is reduced due to transducer coincidence.

Note that these are simply characteristics of coaxial speakers and do not necessarily represent absolute benefits. Depending on the required use of the transducer

one may be inclined to choose a component setup over a coaxial design. Assuming the aforementioned model-to-reality condition is satisfied, the purpose here is to investigate in a mathematical fashion how the proximity of the tweeter to the woofer is affected by the finite moving boundary.

Although many problems in acoustics are solved using the standard linear wave equation, as we will see, these equations are in fact approximations derived from nonlinear constitutive equations for fluids. Because of this, certain phenomena can only be explained using the full nonlinear description. Moreover, when moving boundaries are present there exists an additional source of complication within the mathematics. Deciding which factor plays a more dominant role in any given situation is a non-trivial task. There have been extensive debates over the importance of moving boundaries versus fluid nonlinearities as regards acoustic motion [17, 18].

As with several other studies, we choose to use a quasi-linear approximation to the equations of motion in order to characterize the second-order behaviour from both the boundaries and the fluid. Such an approach is based on Lighthill's work [19] on aerodynamics and its current form is due to many early investigations of the scattering of sound by sound from Ingard & Pridmore-Brown [20] and Westervelt [21] among others.

According to [20] it has been known since at least the 19th century that when sound propagates through air the nonlinearity of the air not only distorts the wave but also generates harmonics of the fundamental tone. Likewise, when multiple sources are present in the medium, the same mechanism will generate sum and difference frequencies of the underlying tones. Experiments by Thuras et al. [22] confirm this. However, this type of generation requires intense acoustic pressures of the order of 200 MPa to get harmonics which are between 36 to 24 decibels lower than the fundamental. Since Thuras concludes that the combination tones are proportional to the product of the magnitudes of the pressures of the individual tones and since normal listening environments are between 0.002 to 0.02 Pa it seems very unlikely that the nonlinearities of the air should contribute much. The moving

boundary should be the main generator of sum and difference frequencies.

Nonetheless as we shall see, we present a method of solution which presupposes the existence of both types of combination tone generation in order to be as general as possible. Only then do we neglect certain terms based on the arguments above and those to follow. Much of the forthcoming work will be concerned with time harmonic vibrations generated by physical boundaries and as such will depend more on these boundary values than initial values. Thus, we assume a steady state of fluctuations and focus on solutions to boundary value problems with little interest in the initial values and transient terms.

Chapter 2 will present the necessary background to and derivation of the quasi-linear approximation method in order to obtain equations that are used throughout this thesis. Chapter 3 introduces the method of solution based on Green's functions as well as certain mathematical concepts which will assist in the formulation of the problem at hand. Chapter 4 gives various solutions, both analytical and numerical, to the equations presented in Chapter 2 and establishes an integral solution to the original problem from which various results are obtained and compared with experimental setups.

Chapter 2

Fundamentals

2.1 Fluid Equations

We begin by establishing the basic equations often used in acoustics. These stem from the fundamental equations of fluid dynamics (with no sources), taken here from Blackstock [23], namely

$$\begin{aligned} \frac{D\rho}{Dt} + \rho\nabla\cdot\mathbf{u} &= 0 \quad \text{(continuity)}, \\ \rho\frac{Du}{Dt} + \nabla p &= (\lambda+2\mu)\nabla(\nabla\cdot\mathbf{u}) - \mu\nabla\times\nabla\times\mathbf{u} \quad \text{(momentum)}, \\ \rho C_v\frac{DT}{Dt} + p\nabla\cdot\mathbf{u} &= \Phi(\lambda,\mu,\mathbf{u}) + \kappa\nabla^2 T \quad \text{(energy)}, \\ p &= R\rho T \quad \text{(ideal gas)}. \end{aligned} \tag{2.1}$$

The derivation of these can be found in any standard text on acoustics or fluid mechanics[1]

The operator D/Dt is the standard material or advective derivative and the variables have their conventional meanings:

[1]See for example the books by Kundu [24] or Kinsler [25]. A very detailed derivation (albeit without any images) is given by Hunt [26]

ρ - density

$\mathbf{u} = (u(\mathbf{x}), v(\mathbf{x}), w(\mathbf{x}))$ - fluid particle velocity

p - pressure

T - temperature

R - ideal gas constant

λ, μ - dilatational and shear viscosity coefficients

κ - heat conduction coefficient

C_v - specific heat at constant volume.

The function Φ represents viscous dissipation. It is customary [27] to assume that, in air, acoustic waves are non-viscous and adiabatic (no heat flow, see footnote below) so that $\lambda = \mu = \kappa = 0$. Also, the function Φ, as given in [23], vanishes when $\lambda = \mu = 0$. With these assumptions, and using the ideal gas law, the energy equation becomes

$$\rho \frac{C_v}{R} \frac{D}{Dt} \left(\frac{p}{\rho} \right) + p \nabla \cdot \mathbf{u} = 0. \tag{2.2}$$

Then, using the fact that $R = C_p - C_v$ and defining $\gamma = \frac{C_p}{C_v}$ and applying the continuity equation, (2.2) becomes

$$\frac{\rho}{\gamma - 1} \frac{D}{Dt} \left(\frac{p}{\rho} \right) - \frac{p}{\rho} \frac{D\rho}{Dt} = 0 \tag{2.3}$$

which reduces, after several lines of algebra, to

$$\frac{D}{Dt}(p\rho^{-\gamma}) = 0 \quad \text{or} \quad \frac{p}{\rho^\gamma} = \text{constant} = \frac{p_0}{\rho_0^\gamma} \tag{2.4}$$

so for inviscid ($\lambda = \mu = 0$) nonconducting ($\kappa = 0$) fluids, assuming an ideal gas, we have the homentropic[2] gas law

$$\frac{p}{p_0} = \left(\frac{\rho}{\rho_0} \right)^\gamma \tag{2.5}$$

so that with the given assumptions, equation (2.5) and the continuity and momentum equations of (2.1) form a set of 3 equations in 3 unknowns (5 if you consider each component of $\mathbf{u}$ separately).

[2]The entropy s of the system is governed by $\rho T \frac{Ds}{Dt} = \Phi + \kappa \nabla^2 T$. The adiabatic assumption simply implies $\kappa = 0$ and so when we also have $\Phi = 0$ we see that $\frac{Ds}{Dt} = 0$ and therefore entropy is constant, hence homentropic.

2.2 Derivations

2.2.1 Speed of Sound

In the next sections we will be deriving the quasi-linear equations via successive approximations using non-dimensional variables. Before doing so however, we must establish the scalings to be used for each of the field variables. The notion of sound speed is an important tool towards this development.

Generally, the speed of sound, in any medium, is proportional to its stiffness and inversely proportional to its density [28]. Also, in a given material, temperature has a significant effect on propagation speed. Since the equation of state describes the relationship between these three quantities it seems plausible that it would characterize the speed of sound. We will see later that in fact[3] the speed of sound in any fluid is given by

$$c^2 = \frac{dp}{d\rho} \tag{2.6}$$

which, with our current equation of state yields

$$\frac{dp}{d\rho} = \gamma \frac{p_0}{\rho_0} \left(\frac{\rho}{\rho_0} \right)^{\gamma}. \tag{2.7}$$

Although we will be using a perturbation style technique in order to gain information about the various field quantities at different orders, we use a constant speed of sound at all orders, namely the equilibrium value c_0 . According to Borwick [29], this assumption is valid so long as the magnitude of the pressure disturbance is small relative to atmospheric pressure.

To obtain the equilibrium sound speed then, one need only assume $\rho = \rho_0$ in (2.7) to arrive at

$$c_0 = \sqrt{\frac{\gamma p_0}{\rho_0}}. \tag{2.8}$$

As was mentioned at the outset, we are trying to obtain appropriate scalings for the field variables to use in our non-dimensional expansion. Even though we choose to

[3]The quantity c^2 represents the advective term in the equations to follow.

use a constant speed of sound we will develop the expansion for all field quantities in order to maintain generality.

2.2.2 Scaling Quantities

Assuming typical listening situations, coaxial speakers, like any other acoustic transducer, produce field disturbances (e.g., pressure, density) much smaller than the ambient pressure. Because of this, perturbation techniques can be used to separate different orders of the field variables. This approach has been taken by various authors in differing forms. Morse and Ingard [30] use a generic expansion

$$\psi = \psi_0 + \psi_1 + \psi_2 + \cdots$$

for any field quantity ψ. Blackstock [23] uses a similar method but is more careful in stating the restrictions between quantities at each order. The investigation by van Wulfften Palthe [31] provides a dimensionless approach, however it is applied to the spherically symmetric case. In the above studies there are no explanations as to the validity of the expansions in terms of a perturbative framework. Since it was not immediately clear to the author that the combination of two first-order[4] quantities (say pressure and velocity) would yield the same order as two other quantities (say density and pressure) a full investigation was undertaken to ensure that no other "middle orders" were possible. To do this as accurately as possible a dimensionless approach was used.

First we attempt to find appropriate scalings to create the non-dimensional parameters in order to pursue with the investigation mentioned in the previous paragraph. We assume that the field quantities obey an expansion of the form

$$\begin{aligned} \rho &= \rho_0 + \rho_1 + \rho_2 + \cdots \\ p &= p_0 + p_1 + p_2 + \cdots \\ \mathbf{u} &= 0 + \mathbf{u}_1 + \mathbf{u}_2 + \cdots \end{aligned} \tag{2.9}$$

[4]The convention from here on is that the equilibrium conditions are considered zeroth order

According to Morse & Ingard [30], for normal acoustic pressures it is reasonable to impose the conditions

$$\rho_0 \gg \rho_1 \gg \rho_2 \cdots, p_0 \gg p_1 \gg p_2 \cdots, \mathbf{u}_1 \gg \mathbf{u}_2 \gg \cdots \tag{2.10}$$

with

$$\rho_1^2 = O(\rho_2), \quad p_1^2 = O(p_2), \quad |u_1|^2 = O(|u_2|) \quad \text{etc.} \tag{2.11}$$

meaning that each quantity is in and of itself a series of successively decreasing terms. To establish that products of different field quantities are of the same magnitude as products of the same field quantities (e.g., $p_1\rho_2 = O(|\mathbf{u}_1|^3)$) we proceed to establish the scalings for each of the variables. We arbitrarily choose to use density as a starting point to give us our first scaling ρ_0.

To find the scaling for the pressure we first expand p in a Taylor series about the equilibrium density ρ_0

$$p = p(\rho_0) + \frac{dp}{d\rho}(\rho_0)(\rho - \rho_0) + \frac{1}{2}\frac{d^2p}{d\rho^2}(\rho_0)(\rho - \rho_0)^2 + \frac{1}{6}\frac{d^3p}{d\rho^3}(\rho_0)(\rho - \rho_0)^3 + \cdots \tag{2.12}$$

then using the equation of state (2.5) to evaluate we obtain

$$p = p_0 + \gamma p_0 \left(\frac{\rho - \rho_0}{\rho_0}\right) + \frac{\gamma(\gamma-1)p_0}{2}\left(\frac{\rho - \rho_0}{\rho_0}\right)^2 + \frac{\gamma(\gamma-1)(\gamma-2)p_0}{6}\left(\frac{\rho - \rho_0}{\rho_0}\right)^3 + \cdots \tag{2.13}$$

If we now replace the difference quantities $\rho - \rho_0, p - p_0$ with their subsequent order terms (up to second-order for brevity) using (2.9) and do some factoring we can arrive at the following

$$p_1\left(1 + \frac{p_2}{p_1}\right) = \frac{\gamma p_0}{\rho_0}\rho_1\left(1 + \frac{\rho_2}{\rho_1}\right)\left[1 + \frac{(\gamma-1)\rho_1}{2}\left(\frac{1 + \frac{\rho_2}{\rho_1}}{\rho_0}\right) + \frac{(\gamma-1)(\gamma-2)\rho_1^2}{6}\left(\frac{1 + \frac{\rho_2}{\rho_1}}{\rho_0}\right)^2 + \cdots\right] \tag{2.14}$$

then by assumptions (2.10) we arrive, quite concisely, at

$$p_1 \ll \gamma p_0 \tag{2.15}$$

so that γp_0 can be used as our scaling for the pressure. Before proceeding in the same fashion with the particle velocity we mention that, given equation (2.13) we

can use the definition (2.6) to obtain a series expansion for the speed of sound

$$c^2 = \frac{\gamma p_0}{\rho_0} + \frac{\gamma(\gamma-1)p_0}{\rho_0^2}(\rho-\rho_0) + \frac{\gamma(\gamma-1)(\gamma-2)}{2\rho_0^3}(\rho-\rho_0)^2 + \cdots \tag{2.16}$$

which at equilibrium reduces to (2.8). With this we can rewrite (2.15) as

$$p_1 \ll c_0^2 \rho_0. \tag{2.17}$$

Finally, to find a characteristic measure for the fluid particle velocity we introduce the notion of specific acoustic impedance[5], denoted by Z, which relates the sound pressure to the fluid particle velocity. The specific acoustic impedance will depend on the type of wave that is produced and the medium through which it propagates but the point here is merely to obtain some measure of scale in the particle velocity. For this we resort to the impedance of a plane wave in air which is simply[6] [23]

$$Z = \frac{p - p_0}{u} = \rho_0 c_0. \tag{2.18}$$

Then by using the same idea as before we can relate the particle velocity and pressure via

$$u_1\left(1 + \frac{u_2}{u_1}\right) = \frac{p_1}{\rho_0 c_0}\left(1 + \frac{p_2}{p_1}\right) \tag{2.19}$$

which again, under the assumptions (2.10) reduces to $u_1 = \frac{p_1}{\rho_0 c_0}$ and finally, using (2.17) gives

$$u_1 \ll c_0. \tag{2.20}$$

Therefore, in assuming a decreasing perturbation series for the field variables and the first condition for the density, we arrive at the following restrictions

$$\begin{aligned} \rho_1 &\ll \rho_0, \\ p_1 &\ll \gamma p_0, \\ |\mathbf{u}| &\ll c_0. \end{aligned} \tag{2.21}$$

[5]Impedance is an important concept in many acoustical settings. The purpose here however is to simply use it as a tool to find an appropriate scale.

[6]Recall we are assuming a plane wave so that in an appropriate coordinate system $\mathbf{u} = u$

2.3 Non-dimensional Equations

We now introduce dimensionless variables in order to gain a better understanding of the magnitudes of the disturbances under the conditions (2.21). According to Fahy [32], for small enough disturbances, a fractional change in one of the field variables results in a similar fractional change in the others. That is to say, relative to their equilibrium states, each field quantity deviates by an equal percentage. This implies that the dimensionless quantities

$$\frac{\mathbf{u}}{c_0} = \epsilon\tilde{\mathbf{u}}, \quad \frac{\rho-\rho_0}{\rho_0} = \epsilon\tilde{\rho}, \quad \frac{p-p_0}{\gamma p_0} = \epsilon\tilde{p}, \tag{2.22}$$

all share a common value[7] of $\epsilon \ll 1$ where each of the tilde quantities are $O(1)$.

2.3.1 Continuity

Putting these variables first into the continuity equation of (2.1) we obtain

$$\rho_0\epsilon\frac{\partial\tilde{\rho}}{\partial t} + \epsilon^2 c_0\rho_0\tilde{\mathbf{u}}\cdot\nabla\tilde{\rho} + \epsilon c_0\rho_0\nabla\cdot\tilde{\mathbf{u}} + \epsilon^2\rho_0 c_0\tilde{\rho}\nabla\cdot\tilde{\mathbf{u}} = 0. \tag{2.23}$$

In order to ensure that the magnitudes of derivatives of the variables are comparable to the variables themselves we introduce a characteristic time, t_c and a characteristic length, $c_0 t_c$ so that we may define $\tau = \frac{t}{t_c}$ and $\tilde{\nabla} = c_0 t_c \nabla$ to give

$$\epsilon\tilde{\rho}_\tau + \epsilon^2\tilde{\mathbf{u}}\cdot\tilde{\nabla}\tilde{\rho} + \epsilon\tilde{\nabla}\cdot\tilde{\mathbf{u}} + \epsilon^2\tilde{\rho}\tilde{\nabla}\cdot\tilde{\mathbf{u}} = 0. \tag{2.24}$$

Note that we have not yet introduced any series expansions and that the inherent nonlinearities of the continuity equation are characterized by the ϵ^2 terms. To obtain the successive approximations (stopping at third order) we let

$$\tilde{\rho} = \tilde{\rho}_1 + \epsilon\tilde{\rho}_2 + \epsilon^2\tilde{\rho}_3, \quad \tilde{\mathbf{u}} = \tilde{\mathbf{u}}_1 + \epsilon\tilde{\mathbf{u}}_2 + \epsilon^2\tilde{\mathbf{u}}_3 \tag{2.25}$$

and substitute into (2.24) to obtain

$$\begin{aligned}\epsilon(\tilde{\rho}_{1_\tau} + \epsilon\tilde{\rho}_{2_\tau} + \epsilon^2\tilde{\rho}_{3_\tau}) + \epsilon^2(\tilde{\mathbf{u}}_1 + \epsilon\tilde{\mathbf{u}}_2 + \epsilon^2\tilde{\mathbf{u}}_3)\cdot\tilde{\nabla}(\tilde{\rho}_1 + \epsilon\tilde{\rho}_2 + \epsilon^2\tilde{\rho}_3) + \\ \epsilon\tilde{\nabla}\cdot(\tilde{\mathbf{u}}_1 + \epsilon\tilde{\mathbf{u}}_2 + \epsilon^2\tilde{\mathbf{u}}_3) + \epsilon^2(\tilde{\rho}_1 + \epsilon\tilde{\rho}_2 + \epsilon^2\tilde{\rho}_3)\tilde{\nabla}\cdot(\tilde{\mathbf{u}}_1 + \epsilon\tilde{\mathbf{u}}_2 + \epsilon^2\tilde{\mathbf{u}}_3) &= 0,\end{aligned} \tag{2.26}$$

[7] ϵ is often characterized by the first of (2.22); the so called Mach Number

from which we can pick off the first-, second- and third-order equations

$$O(\epsilon) \qquad \tilde{\rho}_{1_\tau} + \tilde{\nabla} \cdot \tilde{\mathbf{u}}_1 = 0 \tag{2.27}$$

$$O(\epsilon^2) \qquad \tilde{\rho}_{2_\tau} + \tilde{\mathbf{u}}_1 \cdot \tilde{\nabla}\tilde{\rho}_1 + \tilde{\nabla} \cdot \tilde{\mathbf{u}}_2 + \tilde{\rho}_1 \tilde{\nabla} \cdot \tilde{\mathbf{u}}_1 = 0 \tag{2.28}$$

$$O(\epsilon^3) \qquad \tilde{\rho}_{3_\tau} + \tilde{\mathbf{u}}_2 \cdot \tilde{\nabla}\tilde{\rho}_1 + \tilde{\mathbf{u}}_1 \cdot \tilde{\nabla}\tilde{\rho}_2 + \tilde{\nabla} \cdot \tilde{\mathbf{u}}_3 + \rho_1 \tilde{\nabla} \cdot \tilde{\mathbf{u}}_2 + \tilde{\rho}_2 \tilde{\nabla} \cdot \tilde{\mathbf{u}}_1 = 0. \tag{2.29}$$

2.3.2 Momentum

Substitution of (2.22) into the momentum equation of (2.1) under the current assumptions ($\lambda = \mu = 0$) yields

$$(\rho_0 + \epsilon\rho_0\tilde{\rho})(\epsilon c_0 \tilde{\mathbf{u}}_t + \epsilon^2 c_0^2 (\tilde{\mathbf{u}} \cdot \nabla)\tilde{\mathbf{u}}) + \nabla(p_0 + \gamma\epsilon p_0 \tilde{p}) = 0. \tag{2.30}$$

Again, using the characteristic length and time of the previous section, this equation reduces to

$$\epsilon\tilde{\mathbf{u}}_\tau + \epsilon^2(\tilde{\mathbf{u}} \cdot \tilde{\nabla})\tilde{\mathbf{u}} + \epsilon\tilde{\rho}\tilde{\mathbf{u}}_\tau + \epsilon^3\tilde{\rho}(\tilde{\mathbf{u}} \cdot \tilde{\nabla})\tilde{\mathbf{u}} + \epsilon\tilde{\nabla}\tilde{p} = 0. \tag{2.31}$$

From here we can use the expansions (2.25) along with a similar ansatz for the pressure, $\tilde{p} = \tilde{p}_1 + \epsilon\tilde{p}_2 + \epsilon^2\tilde{p}_3$ to obtain a rather large equation which, after order separation becomes [8]

$$O(\epsilon) \qquad \tilde{\mathbf{u}}_{1_\tau} + \tilde{\nabla}\tilde{p}_1 = 0, \tag{2.33}$$

$$O(\epsilon^2) \qquad \tilde{\mathbf{u}}_{2_\tau} + (\tilde{\mathbf{u}}_1 \cdot \tilde{\nabla})\tilde{\mathbf{u}}_1 + \tilde{\rho}\tilde{\mathbf{u}}_{1_\tau} + \tilde{\nabla}\tilde{p}_2 = 0, \tag{2.34}$$

$$O(\epsilon^3) \qquad \tilde{\mathbf{u}}_{3_\tau} + (\tilde{\mathbf{u}}_1 \cdot \tilde{\nabla})\tilde{\mathbf{u}}_2 + (\tilde{\mathbf{u}}_2 \cdot \tilde{\nabla})\tilde{\mathbf{u}}_1 + \tilde{\rho}_1\tilde{\mathbf{u}}_{2_\tau} + \tilde{\rho}_2\tilde{\mathbf{u}}_{1_\tau} + \tilde{\rho}(\tilde{\mathbf{u}}_1 \cdot \tilde{\nabla})\tilde{\mathbf{u}}_1 + \tilde{\nabla}\tilde{p}_3 = 0$$

. (2.35)

[8] If one assumes irrotational flow (which we will in the forthcoming section) the last of these equations can be simplified using the vector identity

$$\nabla(\mathbf{F} \cdot \mathbf{G}) = (\mathbf{F} \cdot \nabla)\mathbf{G} + (\mathbf{G} \cdot \nabla)\mathbf{F} + \mathbf{F} \times (\nabla \times \mathbf{G}) + \mathbf{G} \times (\nabla \times \mathbf{F}) \tag{2.32}$$

where the last two terms vanish under irrotationality.

2.3.3 State

The ordered equations of state materialize rather quickly from the pressure expansion (2.13). After substituting the dimensionless quantities (2.22) into (2.13) to get

$$\epsilon\tilde{p} = \epsilon\tilde{\rho} + \left(\frac{\gamma-1}{2}\right)\epsilon^2\tilde{\rho}^2 + \frac{(\gamma-1)(\gamma-2)}{6}\epsilon^3\tilde{\rho}^3\ldots \tag{2.36}$$

and using the expansions for pressure and density, followed by order separation, we arrive at

$$O(\epsilon) \qquad \tilde{p}_1 = \tilde{\rho}_1 \tag{2.37}$$

$$O(\epsilon^2) \qquad \tilde{p}_2 = \tilde{\rho}_2 + \left(\frac{\gamma-1}{2}\right)\tilde{\rho}_1^2 \tag{2.38}$$

$$O(\epsilon^3) \qquad \tilde{p}_3 = \tilde{\rho}_3 + (\gamma-1)\tilde{\rho}_1\tilde{\rho}_2 + \frac{(\gamma-1)(\gamma-2)}{6}\tilde{\rho}_1^3. \tag{2.39}$$

2.4 Wave Equations

To solve these equations we reduce each order from 3 variables to 1 variable. The first-order equations are easily reduced to any variable of choice however the higher order expressions are quite cumbersome. Since pressure is easily measured in the lab (and commonly used in acoustic theory) we will solve the equations in terms of pressure p.

2.4.1 First-Order

Combining the time derivative ($\frac{\partial}{\partial\tau}$) of (2.27) and the divergence ($\tilde{\nabla}\cdot$) of (2.33) we obtain

$$\begin{aligned} & \tilde{\rho}_{1_{\tau\tau}} + \tilde{\nabla}\cdot\mathbf{u}_{1_\tau} = 0, \quad \tilde{\nabla}\cdot\mathbf{u}_{1_\tau} + \tilde{\nabla}^2\tilde{p}_1 = 0, \\ \Rightarrow \quad & \tilde{\rho}_{1_{\tau\tau}} - \tilde{\nabla}^2\tilde{p}_1 = 0, \end{aligned} \tag{2.40}$$

and using (2.37) we derive the standard first-order non-dimensional wave equation for pressure

$$\boxed{\tilde{p}_{1_{\tau\tau}} - \tilde{\nabla}^2\tilde{p}_1 = 0}. \tag{2.41}$$

Note that a similar equation can be derived for density using (2.37). That for particle velocity is obtained by taking the time derivative of (2.33) and the gradient of (2.27) to obtain (using a vector identity)

$$\mathbf{u}_{1_{\tau\tau}} - [\tilde{\nabla} \times (\tilde{\nabla} \times \mathbf{u}_1) + \tilde{\nabla}^2 \mathbf{u}_1] = 0. \tag{2.42}$$

Vorticity

According to Blackstock [23] acoustic phenomena are generally irrotational and vorticity is only significant when shear stresses along boundaries are important. Irrotational flow is represented mathematically [24] as $\nabla \times \mathbf{u} = 0$ so that when a flow is vorticity-free the equation for velocity reduces to the standard wave equation

$$\mathbf{u}_{1_{\tau\tau}} - \tilde{\nabla}^2 \mathbf{u}_1 = 0. \tag{2.43}$$

Since we have ignored shear stresses at the outset (thus giving us a zero right hand side for the momentum equation), we can obtain a time evolution equation for the first-order vorticity by taking the curl of (2.33) and noting that $\tilde{\nabla} \times \tilde{\nabla} \tilde{p}_1 \equiv 0$ to get

$$(\tilde{\nabla} \times \tilde{\mathbf{u}}_1)_\tau = 0 \tag{2.44}$$

and since we assumed the equilibrium condition $\tilde{\mathbf{u}} = 0$, meaning each order of the velocity expansion (2.25) is initially 0, then we have that $\tilde{\nabla} \times \tilde{\mathbf{u}}_1 = 0$. A similar argument applies to the second-order velocity field. Taking the curl of (2.34) and using several vector identities along with (2.37) and (2.33) we arrive at

$$(\tilde{\nabla} \times \tilde{\mathbf{u}}_2)_\tau = -\tilde{\rho}_1 (\tilde{\nabla} \times \tilde{\mathbf{u}}_1)_\tau + \tilde{\nabla} \times (\tilde{\mathbf{u}}_1 \times (\tilde{\nabla} \times \tilde{\mathbf{u}}_1)) \tag{2.45}$$

which, after using the result of (2.44) and the zero initial state, we obtain $\tilde{\nabla} \times \tilde{\mathbf{u}}_2 = 0$. We can continue in this fashion for third and higher order but it is perhaps more convenient to point out that these results can alternatively be obtained using the the fundamental equation of momentum (2.1) for an inviscid, barotropic flow (an ideal gas satisfies this condition). This result is famously referred to as Kelvin's circulation theorem [24].

In the following section and indeed throughout the rest of this thesis we will focus on the acoustic pressure p. When necessary, quantities such as particle velocity $\mathbf{u}$ will be derived from the equations of momentum or continuity once the solution for the pressure has been obtained.

2.4.2 Higher-Orders

The wave equation for pressure at second-order follows much the same procedure as in the previous section. Combining the τ derivative of (2.28) with the divergence of (2.34) and using some vector identities along with the irrotational assumption gives, after much simplification

$$\tilde{\rho}_{2_{\tau\tau}} + \tilde{\nabla} \cdot (\tilde{\rho}_{1_\tau} \tilde{\mathbf{u}}_1) - \frac{1}{2}\tilde{\nabla}^2 |\tilde{\mathbf{u}}_1|^2 - \tilde{\nabla}^2 \tilde{p}_2 = 0. \tag{2.46}$$

Then using (2.37), (2.38) and (2.27) we arrive at the non-dimensional second-order wave equation for pressure

$$\boxed{\tilde{p}_{2_{\tau\tau}} - \tilde{\nabla}^2 \tilde{p}_2 = \left(\tfrac{\gamma-1}{2}\right)(\tilde{p}_1^2)_{\tau\tau} + (\tilde{p}_{1_\tau})^2 - \tilde{\nabla}\tilde{p}_{1_\tau} \cdot \tilde{\mathbf{u}}_1 + \tfrac{1}{2}\tilde{\nabla}^2 |\tilde{\mathbf{u}}_1|^2}. \tag{2.47}$$

Although we will not use it in this thesis, we state the third-order non-dimensional wave equation for pressure which, as was done previously, can be obtained by taking the τ derivative of (2.29) and the divergence of (2.35). After numerous substitutions of the equations of state, continuity and momentum we obtain

$$\begin{aligned} \tilde{p}_{3_{\tau\tau}} - \tilde{\nabla}^2 \tilde{p}_3 \;=\; & (\gamma-1)(\tilde{p}_1 \tilde{p}_2)_{\tau\tau} + \frac{(\gamma-1)(1-2\gamma)}{6}(\tilde{p}_1^2)_{\tau\tau} + \tilde{\nabla}^2(\tilde{\mathbf{u}}_1 \cdot \tilde{\mathbf{u}}_2) \\ & + \frac{\tilde{p}_1}{2}\tilde{\nabla}^2 |\tilde{\mathbf{u}}_1|^2 + \frac{\tilde{\nabla}\tilde{p}_1}{2} \cdot \tilde{\nabla}|\tilde{\mathbf{u}}_1|^2 - \tilde{\nabla} \cdot (\tilde{p}_{1_\tau} \tilde{\mathbf{u}}_2) - \tilde{\nabla} \cdot (\tilde{p}_{2_\tau} \tilde{\mathbf{u}}_1) \\ & + \left(\frac{\gamma-1}{2}\right)(\tilde{p}_1^2)_\tau \tilde{\nabla} \cdot \tilde{\mathbf{u}}_1 + \left(\frac{\gamma-1}{2}\right)\tilde{\mathbf{u}}_1 \cdot \tilde{\nabla}(\tilde{p}_1^2). \end{aligned} \tag{2.48}$$

We have derived the wave equations that will be used in much of the forthcoming sections. It should be noted that these equations are assuming no physical sources within the medium. Later we will modify these slightly to include sources once we have introduced the notion of acoustic monopole.

As is typical with a perturbation approach we note that (2.47) has terms on the right hand side that only depend upon the solution of (2.41). Similarly, (2.48) can be solved (in principle) once the first two wave equation solutions have been obtained.

The benefit of this approach compared to using the full nonlinear equations in (2.1) is that analytic solutions to the wave equation are well established for certain geometries [33]. In other cases if we can obtain a formal solution to the general inhomogeneous wave equation $p_{tt} - c^2\nabla^2 p = f$ then since we can write both (2.47) and (2.48) in this form, we can arrive at the corresponding formulas for p_2 and p_3 (in the dimensional case). Indeed due to the linearity of the wave equation a formal solution exists in the form of an integral with a specific kernel often called the Green's function (or fundamental solution [34]). The subsequent chapter will delve into the foregoing method, which as we will see, relies heavily on boundary conditions.

2.5 Boundary Conditions

The final expansion that we require is one for the boundary condition. Whereas the previous derivations were rather general and can be used for a variety of physical problems we now specify conditions for the problem at hand.

We are to investigate the modulation of a high frequency wave due to the motion of a nearby woofer. As was mentioned in the introduction, the woofer is modeled by a flat moving piston located on an infinite plane baffle coinciding with the xy plane (see Figure 1.1). We assume that all points on the piston $(x, y, z) \in S_w$ move in unison such that $z = B_1(t)$ where the function B_1 prescribes the motion (position) of the boundary in time, i.e., the piston moves parallel to the z-axis. Every other point $(x, y) \notin S_w$ on the baffle is assumed to have zero velocity. This allows us to

establish the boundary condition for the particle velocity

$$\begin{aligned} \mathbf{u}(x,y,B(t),t)\cdot\mathbf{n} &= -\dot{B}_1(t) \quad \text{for } (x,y)\in S_w \\ \mathbf{u}(x,y,0,t)\cdot\mathbf{n} &= 0 \quad \text{for } (x,y)\notin S_w \end{aligned} \tag{2.49}$$

where $\mathbf{n}=(0,0,-1)$ is normal to the boundary[9]. Since $\mathbf{u}=(u,v,w)$ the non-trivial boundary condition (2.49) implies

$$w(x,y,B_1(t),t)=\dot{B}_1(t), \quad \text{for } (x,y)\in S_w \tag{2.50}$$

which essentially says that the particle velocity in the z direction at the position $z=B_1(t)$ is equal to the velocity of the woofer $\dot{B}_1(t)$. Prescribing the boundary condition at $z=B_1(t)$ instead of the more convenient (and often used $z=0$) is essential to the method of solution. It is in fact because of this requirement that we are able to obtain the results that will follow.

Since we assume that the boundary (and the tweeter) are the only sources of disturbance in an otherwise quiescent medium, it must be a small boundary disturbance that causes the respective perturbative disturbances in the field variables. Seeing that B_1 is a length we can nondimensionalize as[10]

$$\frac{B_1(t)}{c_0 t_c}=\epsilon\tilde{B}_1(\tau) \tag{2.51}$$

where $\tilde{B}_1$ is order 1. Applying $\tau=\frac{t}{t_c}$ gives

$$\dot{B}_1(t)=\epsilon c_0\tilde{B}_{1_\tau}(\tau). \tag{2.52}$$

For notational convenience we omit the x and y dependence in the following since it is only our z dimension which is of interest.

[9]The sign of the normal here is rather arbitrary in that we could use $-\mathbf{n}$ and change the sign of the function B_1 (assuming periodic motion) to accommodate the situation. In the next chapter it is convenient to use this normal.

[10]A reasonable choice for c_0t_c for oscillatory motion would be the wavelength λ (making t_c the period). For woofer amplitudes less than 1cm with frequencies below 100Hz, $\lambda>3$m so that $\epsilon\ll 1$.

Defining $w(z,t) = \tilde{w}(\tilde{z},\tau)$ where $\tilde{z} = \frac{z}{c_0 t_c}$ and using the fact that $\frac{\mathbf{u}}{c_0} = \epsilon\tilde{\mathbf{u}}$ and the expansion for $\tilde{\mathbf{u}}$ (2.25) we have, from (2.49)-(2.52)

$$\begin{aligned} \epsilon c_0(\tilde{\mathbf{u}}_1 + \epsilon\tilde{\mathbf{u}}_2 + \epsilon^2\tilde{\mathbf{u}}_3 \ldots)\cdot\mathbf{n} &= -\epsilon c_0 \tilde{B}_{1_\tau}(\tau), \\ \epsilon\tilde{w}_1(\epsilon\tilde{B}_1(\tau),\tau) + \epsilon^2\tilde{w}_2(\epsilon\tilde{B}_1(\tau),\tau) + \epsilon^3\tilde{w}_3(\epsilon\tilde{B}_1(\tau),\tau) &= \epsilon\tilde{B}_{1_\tau}(\tau). \end{aligned} \tag{2.53}$$

To obtain conditions at each order we expand (2.53) in a Taylor series about $z = 0$, again, suppressing the x and y dependence

$$\begin{aligned} &\epsilon\left[\tilde{w}_1(0,\tau) + \tilde{w}_{1\tilde{z}}(0,\tau)\epsilon\tilde{B}_1(\tau) + \frac{1}{2}\tilde{w}_{1\tilde{z}\tilde{z}}(0,\tau)\epsilon^2\tilde{B}_1^2(\tau) + \frac{1}{6}\tilde{w}_{1\tilde{z}\tilde{z}\tilde{z}}(0,\tau)\epsilon^3\tilde{B}_1^3(\tau) + \cdots\right] \\ +\ &\epsilon^2\left[\tilde{w}_2(0,\tau) + \tilde{w}_{2\tilde{z}}(0,\tau)\epsilon\tilde{B}_1(\tau) + \frac{1}{2}\tilde{w}_{2\tilde{z}\tilde{z}}(0,\tau)\epsilon^2\tilde{B}_1^2(\tau) + \frac{1}{6}\tilde{w}_{2\tilde{z}\tilde{z}\tilde{z}}(0,\tau)\epsilon^3\tilde{B}_1^3(\tau) + \cdots\right] \\ +\ &\epsilon^3\left[\tilde{w}_3(0,\tau) + \tilde{w}_{3\tilde{z}}(0,\tau)\epsilon\tilde{B}_1(\tau) + \frac{1}{2}\tilde{w}_{3\tilde{z}\tilde{z}}(0,\tau)\epsilon^2\tilde{B}_1^2(\tau) + \frac{1}{6}\tilde{w}_{3\tilde{z}\tilde{z}\tilde{z}}(0,\tau)\epsilon^3\tilde{B}_1^3(\tau) + \cdots\right] \\ =\ &\epsilon\tilde{B}_{1_\tau}(\tau). \end{aligned} \tag{2.54}$$

Once the orders have been separated we arrive at the following conditions

$$O(\epsilon) \qquad \tilde{w}_1(0,\tau) = \tilde{B}_{1_\tau}(\tau), \tag{2.55}$$

$$O(\epsilon^2) \qquad \tilde{w}_2(0,\tau) = -\tilde{w}_{1\tilde{z}}\tilde{B}_1(\tau), \tag{2.56}$$

$$O(\epsilon^3) \qquad \tilde{w}_3(0,\tau) = -\frac{1}{2}\tilde{w}_{1\tilde{z}\tilde{z}}(0,\tau)\tilde{B}_1^2(\tau) - \tilde{w}_{2\tilde{z}}(0,\tau)\tilde{B}_1(\tau).. \tag{2.57}$$

The meaning behind these expressions is not very mysterious. At first-order we expect that the particle velocity in the z direction be identical to that of the moving piston (albeit at the position $z = 0$). The second of these is a correction for the fact that at first-order we assume the motion to be strictly at $z = 0$. It attempts to compensate for how much the first-order particle velocity varies with position($\tilde{w}_{1\tilde{z}}$) and then multiplies this quantity by the position that we are currently at ($\tilde{B}_1$). The third-order condition has a similar dependence although it is compensating for the second-order position and thus has a second term to deal with the first-order changes as well.

As we will see, it is in fact the second of these, (2.56), which gives us much of the information about how nearby acoustic sources are affected by the non-zero boundary position.

2.6 Final Dimensional Equations

The previous sections were meant to derive, in a somewhat rigorous fashion, the perturbation expansions of the equations of fluid motion as well as of the boundary problem. To achieve this we used a non-dimensional approach in order to quell any concerns about the relative magnitudes of various quantities and their derivatives. In doing so, we established the wave equations to be used in the forthcoming sections. At this point however, it is easier (for both notational and reference purposes) to revert to dimensional quantities within these equations. Doing so is simply a matter of algebra and so we state, without display of procedure, the equivalent equations to those presented in the previous sections. Also, as was noted in section 2.2.1, we will be using a constant speed of sound $c_0 = \sqrt{\frac{\gamma p_0}{\rho_0}}$. Because of this, we shall suppress the subscript 0 and simply write $c_0 = c$.

The following is a summary of the equations that will be used, separated by order

0^{th} order:

$$p = p_0, \quad \rho = \rho_0, \quad \mathbf{u} = 0. \tag{2.58}$$

1^{st} order

$$\begin{aligned} \rho_{1t} + \rho_0 \nabla \cdot \mathbf{u}_1 &= 0 \quad \text{(continuity)}, && (2.59)\\ \rho_0 \mathbf{u}_{1t} + \nabla p_1 &= 0 \quad \text{(momentum)}, && (2.60)\\ p_1 - c^2 \rho_1 &= 0 \quad \text{(state)}, && (2.61)\\ p_{1tt} - c^2 \nabla^2 p_1 &= 0 \quad \text{(wave)}. && (2.62) \end{aligned}$$

2nd order

$$\rho_{2t} + \rho_0 \nabla \cdot \mathbf{u}_2 = -\rho_1 \nabla \cdot \mathbf{u}_1 - \nabla \rho_1 \cdot \mathbf{u}_1 \quad \text{(continuity)}, \tag{2.63}$$

$$\rho_0 \mathbf{u}_{2t} + \nabla p_2 = -\rho_1 \mathbf{u}_{1t} - \rho_0 (\mathbf{u}_1 \cdot \nabla)\mathbf{u}_1 \quad \text{(momentum)}, \tag{2.64}$$

$$p_2 - c^2 \rho_2 = \frac{(\gamma - 1)c^2}{2\rho_0} \rho_1^2 \quad \text{(state)}, \tag{2.65}$$

$$p_{2tt} - c^2 \nabla^2 p_2 = \frac{(\gamma - 1)}{2\rho_0 c^2} (p_1^2)_{tt} + \frac{1}{\rho_0 c^2} (p_{1t})^2 - \nabla p_{1t} \cdot \mathbf{u}_1 + \frac{\rho_0 c^2}{2} \nabla^2 |\mathbf{u}_1|^2 \quad \text{(wave)}. \tag{2.66}$$

Boundary conditions

$$1^{st} \text{ order} \quad w_1(x, y, 0, t) = \dot{B}_1(t), \text{for } (x, y) \in S_w \tag{2.67}$$

$$2^{nd} \text{ order} \quad w_2(x, y, 0, t) = -w_{1z}(x, y, 0, t) B_1(t), \text{for } (x, y) \in S_w \tag{2.68}$$

$$w(x, y, 0, t) = 0 \quad \text{for } (x, y) \notin S_w$$

Chapter 3

Tools

3.1 Sources

3.1.1 Point Source

The concept of a point source is common to many fields of applied mathematics. Here we will derive the notion of an acoustic monopole which will be used as the model for the high-frequency tweeter. Generally, a source is a region of space that by contact with the medium converts mechanical (or other forms of) energy to acoustic energy which is radiated through the medium [30]. According to Pierce [27], any small source which can be enclosed in a small time varying volume has all the attributes of a point source, so long as the dimensions of the source are small compared with the wavelength produced. Note that this behaviour applies to sources of any shape, not necessarily spherical in any way.[1] In the current situation, we are dealing with a high-frequency transducer that is typically circular and rather tiny. Although tweeter sizes do vary, for the frequencies of interest here the wavelengths produced in air are an order of magnitude greater than the dimensions of the source. It should also be pointed out that we must restrict our investigation to distances that are several characteristic lengths (of the source, not

[1] See page 163 of [27].

to be confused with the characteristic length given in the preceding chapter) away from the source. This poses no difficulty however since the compact size of the tweeter would only create measurement problems within a few centimetres of the speaker; not a typical listening situation. As we will see, the concept of a point source also plays an important role outside its obvious realm of applicability. In fact, situations which cannot be modelled by a single point source can be viewed as a distribution of point sources [23]. Also, solutions to the general theory of acoustic radiation and diffraction governed by the inhomogeneous wave equation are based on the idea of a simple source.[2]

Mathematically a point source is essentially the limiting case of a pulsating spherical radiator as the radius goes to zero. To compensate for the diminishing radius however, the velocity of the boundary motion must increase so as to maintain the source strength of the original pulsating sphere [27]. To do this in a rigorous fashion we first find the solution for the finite sized sphere. The following process is adapted from the knowledge in [23, 27, 30].

In an unbounded medium, a pulsating sphere will produce an acoustic field which is spherically symmetric. To solve for this pressure field we use (2.62) with the Laplacian modified for spherical coordinates

$$\nabla^2 = \frac{1}{r^2}\frac{\partial}{\partial r}\left(r^2\frac{\partial}{\partial r}\right) + \frac{1}{r^2\sin\phi}\frac{\partial}{\partial\phi}\left(\sin\phi\frac{\partial}{\partial\phi}\right) + \frac{1}{r^2\sin^2\phi}\frac{\partial^2}{\partial\theta^2} \tag{3.1}$$

where ϕ is the zenith angle and θ the azimuth angle.[3] For spherically symmetric waves the solution only depends on the radial distance r so that the last two terms drop which gives, upon applying (2.62)

$$p_{1tt} - c^2\left(p_{1rr} + \frac{2}{r}p_{1r}\right) = 0. \tag{3.2}$$

A clever substitution of $h = rp_1$ turns (3.2) into

$$h_{tt} - c^2 h_{rr} = 0 \tag{3.3}$$

[2]The terminology varies between authors. Some use point source, others use simple source and still others use acoustic monopole.

[3]According to [35] this is the American mathematical convention. It is common to switch the roles of θ and ϕ.

which has the famous d'Alembert solution

$$h = f(t - \frac{r}{c}) + g(t + \frac{r}{c}) \quad \Rightarrow \quad p_1 = \frac{f(t - \frac{r}{c})}{r} + \frac{g(t + \frac{r}{c})}{r} \tag{3.4}$$

for arbitrary functions f and g. The first term represents outgoing spherical waves while the second represents incoming spherical waves. Since we have assumed an unbounded medium so that only outgoing waves exist the pressure field can be described by only the first term so that

$$p_1 = \frac{f(t - \frac{r}{c})}{r}. \tag{3.5}$$

In order to find the function f we must match the solution to boundary conditions on the surface of the sphere.

For a pulsating sphere of radius a, we call $Q(t)$ the volume flow of air (often called the 'volume velocity') which is given mathematically by

$$Q(t) = 4\pi a^2 u^{(r)}(a, t) \tag{3.6}$$

where $u^{(r)}$ is the radial component of velocity (the only non-zero component in this case). To relate the particle velocity to the pressure p_1 we can use (2.60) which in spherical coordinates[4] gives

$$\rho_0 u_t^{(r)} + \frac{\partial p_1}{\partial r} = 0 \tag{3.7}$$

With our solution (3.5) we obtain

$$u_t^{(r)}(r, t) = \frac{f(t - \frac{r}{c})}{\rho_0 r^2} + \frac{f'(t - \frac{r}{c})}{\rho_0 c r}. \tag{3.8}$$

Up until now we have not made any assumptions other than spherical symmetry. To obtain the solution for a point source we let $r = a$ and substitute our particle velocity from (3.6) into the above equation to get

$$\frac{Q'(t)}{4\pi a^2} = \frac{f(t - \frac{a}{c})}{\rho_0 a^2} + \frac{f'(t - \frac{a}{c})}{\rho_0 c a}. \tag{3.9}$$

[4] $\nabla = \mathbf{r}\frac{\partial}{\partial r} + \boldsymbol{\phi}\frac{1}{r}\frac{\partial}{\partial \phi} + \boldsymbol{\theta}\frac{1}{r \sin\phi}\frac{\partial}{\partial \theta}$ in spherical coordinates. The last two drop in spherically symmetric cases.

Multiplying both sides by a^2 and then taking the limit as $a \to 0$ causes the second term on the right-hand side to drop out leaving

$$f(t) = \frac{\rho_0 Q'(t)}{4\pi} \tag{3.10}$$

which upon substitution into (3.5) shows how the pressure is related to the rate of volume flow

$$p_1 = \frac{\rho_0 Q'(t - \frac{r}{c})}{4\pi r}. \tag{3.11}$$

Since Q represents volume per unit time or "volume velocity", then $Q'(t)$ is the "volume acceleration". We see then that the pressure field is proportional to the acceleration of the boundary and not the velocity. In other words, it is only a change in flow which affects the change in pressure. This should make sense since if we were to put ourselves within a medium undergoing a strict mean flow (constant velocity) we would hear no sound.

For a real physical source to be represented by a mathematical point in space we must be able to characterize the physical source by some quantity. Indeed it is the magnitude of this value Q, often called the "source strength", which allows us to do this. For example in time harmonic motion the idea is that we assume $u^{(r)} = b_0 \cos(\omega t)$ so that $Q(t) = 4\pi a^2 b_0 \cos(\omega t) = Q_0 \cos(\omega t)$ so that for various radii, the magnitude of the boundary velocity b_0 adjusts to keep the source strength Q_0 constant. There is a caveat however; as can be seen from (3.6) a vanishing radius requires a radial velocity which tends to infinity. Mathematically this is fine, however clearly not physically realizable. On the other hand a sphere whose radius shrinks to zero but still generates an acoustic field is equally absurd. However, as Pierce points out

"Although an extremely small source of sufficiently large strength to generate audible sound at appreciable distances would in actuality require consideration of nonlinear terms, the concept of a point source generating waves governed by the linear acoustic equations is a convenient extrapolation consistent with the general framework of linear acoustic theory".[5]

[5]Taken from [27] p.160.

Despite its physical impossibility we will indeed be using the notion of a point source to represent the high-frequency tweeter as under the appropriate conditions it is a valid approximation and mathematically simple to apply.

In the next section we will determine what modifications to the equations given in Chapter (2) are required in order to account for sources within the region. With respect to the aforementioned point sources, to describe their location in a three dimensional setting we add a spatial component given by the Dirac Delta[6] function so that the volume flow is given by

$$q(\mathbf{x} - \mathbf{x_0}, t) = Q_0[s(t)\delta(\mathbf{x} - \mathbf{x_0})] \tag{3.12}$$

where $\mathbf{x_0}$ is the location of the point source in space and $s(t)$ is an $O(1)$ function describing the signal .

3.1.2 Modification to Wave Equations to Include Sources

When an object oscillates within a medium it creates a volume flow of air. A specific example is found in the previous section where we had a pulsating sphere creating the changes in volume denoted by $Q(t)$. Since Q is measured in units of volume per unit time (or volume flow), multiplying this quantity by the density ρ gives units of mass per unit time. Of the fundamental equations given by (2.1) it is the continuity equation that deals with mass generation. It is in fact a statement of the conservation of mass which says

$$\begin{array}{ccccc} \text{Rate of change} & & \text{Mass flow through} & & \text{Mass generation} \\ \text{of mass in a} & = & \text{the boundaries} & + & \text{within the volume} \\ \text{fixed volume} & & \text{of the volume} & & \text{per unit time} \end{array} \tag{3.13}$$

with the corresponding integral relationship (see figure 3.1 for notation)

$$\frac{d}{dt}\int_V \rho dV = -\int_S \rho \mathbf{u}\cdot\mathbf{n} dS + \int_V \rho q(\mathbf{x}, t) dV. \tag{3.14}$$

[6]A derivation of sorts is given in [27] beginning with a general distributed source over a small region.

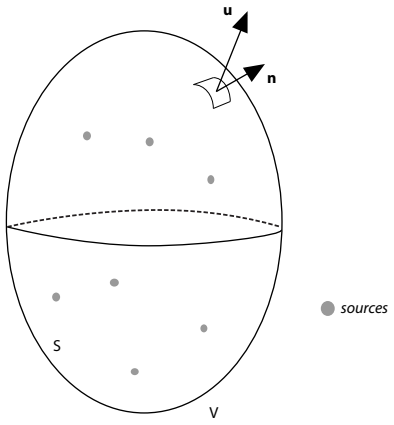

Figure 3.1: Arbitrary fixed volume within the medium. Here there are a finite number of point sources that could be represented by a summation of amplitude varying delta functions. The general case of mass generation would have a continuum function within the whole of the region, such as in Equation (2.66) which will be discussed in chapter 4.

The function $q(\mathbf{x}, t)$ represents the volume velocity generated by all sources and is measured in units of volume per unit time per unit volume, or, volume flow density (also called source strength density).

Assuming all field variables are continuous, the integral form (3.14) can be converted to differential form by taking the time integral inside (for a time independent region) using the divergence theorem and the fact that V is arbitrary within the medium, yielding

$$\frac{\partial \rho}{\partial t} + \nabla \cdot (\rho \mathbf{u}) = \rho q(\mathbf{x}, t) \tag{3.15}$$

which can be converted to that in (2.1) by using the material derivative $\frac{D}{Dt}$. To obtain order relations based on (3.15) we make the assumption that our function Q is given by (3.12) where Q_0 is of the same order as ϵ based on the argument given in the paragraph above equation (2.51). That is to say, we assume that the woofer and the tweeter, being the only acoustic sources in the medium, produce sound pressures which are of the same order of magnitude.

We can then write (suppressing the spatial dependence)[7] $q(t) = \epsilon\tilde{q}(\tau)$ and, using (2.25) for the density obtain the modified continuity equations

$$O(\epsilon) \qquad \tilde{\rho}_{1_\tau} + \tilde{\nabla}\cdot\tilde{\mathbf{u}}_1 = \tilde{q}(\tau), \tag{3.16}$$

$$O(\epsilon^2) \qquad \tilde{\rho}_{2_\tau} + \tilde{\mathbf{u}}_1\cdot\tilde{\nabla}\tilde{\rho}_1 + \tilde{\nabla}\cdot\tilde{\mathbf{u}}_2 + \tilde{\rho}_1\tilde{\nabla}\cdot\tilde{\mathbf{u}}_1 = \rho_1\tilde{q}(\tau), \tag{3.17}$$

$$\tag{3.18}$$

with modified wave equations

$$O(\epsilon) \quad \tilde{p}_{1_{\tau\tau}} - \tilde{\nabla}^2\tilde{p}_1 = \tilde{q}_\tau(\tau), \tag{3.19}$$

$$O(\epsilon^2) \quad \tilde{p}_{2_{\tau\tau}} - \tilde{\nabla}^2\tilde{p}_2 = \left(\frac{\gamma-1}{2}\right)(\tilde{p}_1^2)_{\tau\tau} + (\tilde{p}_{1_\tau})^2 - \tilde{\nabla}\tilde{p}_{1_\tau}\cdot\tilde{\mathbf{u}}_1,$$
$$+ \frac{1}{2}\tilde{\nabla}^2|\tilde{\mathbf{u}}_1|^2 + \tilde{p}_{1_\tau}\tilde{q}(\tau) + \tilde{p}_1\tilde{q}_\tau(\tau), \tag{3.20}$$

whose full dimensional versions become

$$O(\epsilon) \qquad p_{1tt} - c^2\nabla^2 p_1 = \rho_0 c^2\dot{q}(\mathbf{x},t), \tag{3.21}$$

$$O(\epsilon^2) \qquad p_{2tt} - c^2\nabla^2 p_2 = \frac{(\gamma-1)}{2\rho_0 c^2}(p_1^2)_{tt} + \frac{1}{\rho_0 c^2}(p_{1t})^2$$
$$- \nabla p_{1t}\cdot\mathbf{u}_1 + \frac{\rho_0 c^2}{2}\nabla^2|\mathbf{u}_1|^2 + p_{1t}q(\mathbf{x},t) + p_1\dot{q}(\mathbf{x},t). \tag{3.22}$$

3.2 Fundamental Solution of the Wave Equation

Similar to the notion of impulse response for linear, time-invariant systems, partial differential equations have what is called a fundamental solution. General PDEs are not guaranteed to have a fundamental solution [36]; however, for an equation which

[7] Although this equation is completely valid one may note that unless that tweeter and woofer are radiating at the same frequency, one of the non-dimensional functions $\tilde{B}_1(\tau)$ and $\tilde{q}(\tau)$ will contain the ratio of the two frequencies. This is not an immediate issue however since the amplitudes of the functions will not change. The issue arises upon derivation of the wave equation when a time derivative is necessary. The author did in fact create a system of equations based on different time scales but for the purposes of estimating relative magnitudes it was found to be more cumbersome than useful. We therefore classified the source q based solely on amplitude and investigated its importance after solutions were obtained. See Chapter 4.

is both linear and has constant coefficients, existence of the fundamental solution (from here on referred to as the Green's function) is assured by the Malgrange-Ehrenpreis Theorem [37]. Fortunately the wave equation satisfies these criteria.

The purpose of the Green's function (which we will denote by G and which is sometimes called the influence function) is to determine how much of an "influence" points surrounding an observation point contribute to the overall solution. The function G therefore, accepts twice the number of parameters as the original function we seek to find, that is $G = G(\xi, \eta, \zeta, \tau, x, y, z, t)$ where the Greek variables represent the influence points and the Roman variables represent the observation point. Based on this description one might suspect that, in order to determine the influence of all points in a region on a single point (x, y, z, t), a four-dimensional integral is required; this is indeed the case.

Before performing this integration we must first find the function G. To do so, in general, we are required to solve the equation

$$\mathbf{L}G(\boldsymbol{\chi} - \mathbf{x}) = \delta(\boldsymbol{\chi} - \mathbf{x}) \tag{3.23}$$

where $\mathbf{L}$ is the linear differential operator associated with the PDE. In our case we have [8]

$$\mathbf{L} = \frac{\partial^2}{\partial \tau^2} - c^2 \nabla^2 \tag{3.24}$$

and $\mathbf{x} = (x, y, z, t)$, $\boldsymbol{\chi} = (\xi, \eta, \zeta, \tau)$ so that we are attempting to solve

$$G_{\tau\tau} - c^2 \nabla^2 G = \delta(\xi - x, \eta - y, \zeta - z, \tau - t) \tag{3.25}$$

with $G = 0$ for $\tau > t$. That is, we assume future events do not influence the present; the standard causality condition. We also assume we are in an unbounded medium so that we are finding what is called the free-space Green's function. What is important here is that G satisfies the homogeneous version of (3.25) everywhere other than the point (x, y, z, t). To determine G we use a method that, while not

[8]Note that this τ is unrelated to the dimensionless τ given above and in Chapter 2. Also, the Laplacian is with respect to the influence variables.

terribly rigorous, is rather intelligible. An alternative and more pedantic derivation is provided in Appendix B.

A physical way to interpret (3.25) is to note that, in the absence of any boundaries, the only disturbance comes from the delta function on the right-hand side. There is no activity until $\tau = t$ at which time there is an impulse at the point (x, y, z). If we assume a homogeneous medium then it is reasonable to seek G as a function of r alone [38], where $r = \sqrt{(\xi - x)^2 + (\eta - y)^2 + (\zeta - z)^2}$.

We know from dealing with the point source in section 3.1.1 that the homogeneous wave equation in spherical coordinates admits solutions of the form

$$G = \frac{f(\tau - \frac{r}{c})}{r} + \frac{g(\tau + \frac{r}{c})}{r} \tag{3.26}$$

for arbitrary functions f and g. Given a unit pulse disturbance, we expect only outgoing waves meaning $g = 0$.

To find the form of the function f we integrate equation (3.25) using an epsilon ball (unrelated to the dimensionless ϵ used previously, see Figure 3.2) surrounding the point (x, y, z)

$$\int_V G_{\tau\tau}\, dV - c^2 \int_V \nabla^2 G\, dV = \int_V \delta(\xi - x, \eta - y, \zeta - z, \tau - t)\, dV. \tag{3.27}$$

Using the sifting property[9] of the delta function, the right-hand side reduces to

$$\int_V G_{\tau\tau} dV - c^2 \int_V \nabla^2 G dV = \delta(\tau - t). \tag{3.28}$$

The next step involves using the divergence theorem on the second term on the left which, as Greenberg points out, is not actually valid due to the nature of G around the point $r = 0$. The method is mostly formal though since, strictly speaking, equation (3.25) is also invalid as the delta function is a distribution and

[9]The reader can find ample resources on the delta function if not in self-contained volumes then certainly in almost any book about differential equations. A fine treatment, with regard to its uses in finding Green's functions, is given by Greenberg in section 3 of [38]

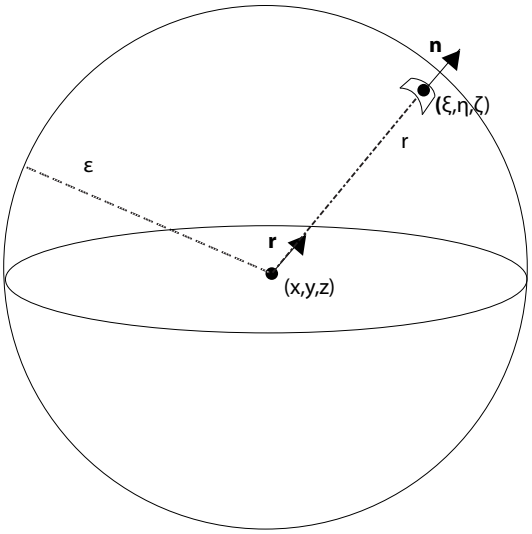

Figure 3.2: Epsilon ball used in finding the Green's function for the wave operator, $\epsilon > 0$.

should be acting on a suitable test function[10].

Proceeding with the theorem therefore and using our ansatz $G = \frac{f(\tau - \frac{r}{c})}{r}$ gives

$$\int_V \frac{f''}{r} dV - c^2 \int_S \nabla G \cdot \mathbf{n}\, dS = \delta(\tau - t). \tag{3.29}$$

In spherical coordinates ∇ is given in the footnote after equation (3.10) which for radial-only dependence yields $\nabla G = \frac{\partial G}{\partial r}\mathbf{r}$ with $\mathbf{r}$ being a unit vector. Also, $dS = r^2 \sin\phi\, d\phi\, d\theta$ and, for a sphere surrounding (x, y, z), we have $\mathbf{n} = \mathbf{r}$ so that $\nabla G \cdot \mathbf{n} dS = \frac{\partial G}{\partial r}(r^2 \sin\phi d\phi d\theta)$. Then since $\frac{\partial G}{\partial r} = -\frac{f'}{rc} - \frac{f}{r^2}$ we obtain

$$\int_V \frac{f''}{r} dV + c^2 \int_S \left(\frac{f'}{rc} + \frac{f}{r^2} \right) r^2 \sin\phi\, d\phi\, d\theta = \delta(\tau - t). \tag{3.30}$$

When the functions in question do not depend on the angles ϕ and θ we have

[10]It should be pointed out that not performing this step would lead to the rather peculiar result $0 = \delta(\tau - t)$ since our guess for G satisfies the homogenous wave equation. It would seem therefore that the divergence theorem is helping us determine the nature of the singularity. Again, we refer the reader to Appendix B for a rigorous derivation. The author finds it interesting however that the result can be obtained by the method used above despite the lax approach.

$dV = 4\pi r^2 dr$ so that the first term above becomes

$$\int_V \frac{f''}{r} dV = \int_0^\epsilon 4\pi r f'' \, dr \tag{3.31}$$

which can be made arbitrarily small and therefore we neglect it. On the surface S we have that $r = \epsilon$ is constant so that after simplifying we obtain

$$\int_S \left(\frac{f'}{rc} + \frac{f}{r^2} \right) r^2 \sin\phi \, d\phi \, d\theta = 4\pi \left(\frac{f'\epsilon}{c} + f \right) \tag{3.32}$$

so that for arbitrarily small ϵ we arrive at

$$c^2 4\pi f(\tau) = \delta(\tau - t) \quad \Rightarrow \quad f(\tau - \frac{r}{c}) = \frac{\delta(\tau - t - \frac{r}{c})}{4\pi c^2} \tag{3.33}$$

which gives us a Green's function of

$$G = \frac{\delta(\tau - t - \frac{r}{c})}{4\pi r c^2}. \tag{3.34}$$

Unfortunately this formula doesn't satisfy our causality condition $G = 0$ for $\tau > t$. To get the result we desire note that if $G(\tau - t, \cdot)$ is a solution to (3.25) we have

$$\mathbf{L}G(\tau - t, \cdot) = \delta(\tau - t, \cdot). \tag{3.35}$$

Let $G^* = G(t - \tau, \cdot)$ then since $G_{\tau\tau} = G_{(-\tau)(-\tau)}$ the operator $\mathbf{L}$ does not change under this transformation so that we have

$$\mathbf{L}G^* = \delta(t - \tau, \cdot) \tag{3.36}$$

and since $\delta(t - \tau) = \delta(\tau - t)$ we see that G^* satisfies (3.25). With that we have our final free-space Green's function

$$G(\xi, \eta, \zeta, \tau, x, y, z, t) = \frac{\delta(t - \tau - \frac{r}{c})}{4\pi r c^2} \tag{3.37}$$

which satisfies $G = 0$ for $\tau > t$ since $r = \sqrt{(\xi - x)^2 + (\eta - y)^2 + (\zeta - z)^2} \geq 0$.

We see from this that G is not a standard function but in fact, like the delta function from which it was created, a distribution. As such it must act on some test function to be fully exploited. Indeed, along with obtaining the solution for the inhomogeneous wave equation, the next section will reveal exactly which functions our Green's function G will influence.

3.3 General Solution to Inhomogeneous Wave Equation

As we have demonstrated, using the quasi-linear approximation (perturbation expansions) to the basic equations of fluids (2.1) reduces the system to an ordered collection of inhomogeneous wave equations. Therefore, if we can solve the general inhomogeneous wave equation then we can, in principle, obtain solutions to any order of the field variables.

To do this we start with a generic inhomogeneous wave equation

$$p_{tt} - c^2\nabla^2 p = f(x, y, z, t) \tag{3.38}$$

and multiply by our Green's function $G(\xi, \eta, \zeta, \tau, x, y, z, t)$. The next step is to create a four-dimensional integral in time and space. The time integral is taken to some arbitrary time $T > t$ where t is our current time. The integral in space has 3 separate cases (see figure 3.3):

- the volume of interest includes our observation point (x, y, z)
- the volume of interest doesn't include the point (x, y, z). This will be discussed in the subsequent chapter when we deal with the solution to the second-order wave equation.
- the volume of interest includes our observation point on its boundary. Not used in this thesis.

It should be stated that for all three cases, the volumes of integration can be arbitrarily chosen and need not be bounded by physical surfaces; it is typically, however, convenient to do so.

For our purposes we will work out the details of the first case since this is the one which we will be using. The other two cases are mentioned in Appendix C.

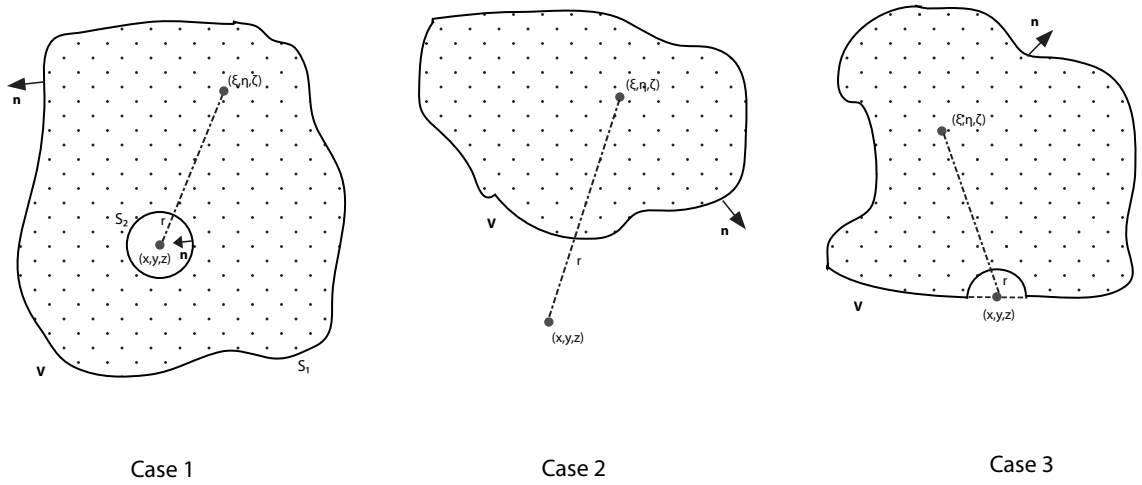

Figure 3.3: Volumes of various regions used in three separate cases to derive integral solution of inhomogeneous wave equation. Note in Case 1 that the ball around our observation point is used to keep the functions sufficiently smooth in the dotted region. This ball (like the half-ball in case 3) is shrunk to 0 so that our observation point is included, unlike in Case 2.

Upon multiplying (3.38) by G and integrating over our region we have

$$\int_V \int_0^T G p_{\tau\tau}\, d\tau\, dV - c^2 \int_V \int_0^T G \nabla^2 p\, d\tau\, dV = \int_V \int_0^T G f\, d\tau\, dV \tag{3.39}$$

with $dV = d\xi\, d\eta\, d\zeta$ and $T > t$.

The main method behind using Green's functions is to break down the left hand side using integration by parts. This will require taking derivatives of the Green's function G which is not straightforward since G is in fact a distribution (even though in solving for G we implictly assumed it could be differentiated since it was the solution to a PDE).

The theory behind distributions and how they can be manipulated is beyond the scope of this thesis. Suffice it to say that the delta function is at least as differentiable as the function upon which it acts. Since we are using it to act on physical quantities such as pressure and particle velocity we assume they are sufficiently smooth to allow this operation. For a detailed investigation of the delta

function and other generalized functions used as mathematical tools in the context of acoustics see Chapter 2 of [39].

Proceeding with the derivation, the first term of (3.39) becomes (suppressing the differentials)

$$\begin{aligned}\int_V \int_0^T G p_{\tau\tau} &= \int_V G p_\tau |_0^T - \int_V \int_0^T G_\tau p_\tau \\ &= \int_V G p_\tau |_0^T - \int_V G_\tau p |_0^T + \int_V \int_0^T G_{\tau\tau} p \\ &= \int_V (G p_\tau - G_\tau p) |_0^T + \int_V \int_0^T G_{\tau\tau} p. \end{aligned} \tag{3.40}$$

To transform the second term of (3.39) we use the vector identity

$$G\nabla^2 p = \nabla \cdot (G\nabla p - p\nabla G) + p\nabla^2 G \tag{3.41}$$

and the divergence theorem on the first term (which is valid in the regions given by Figure 3.3) to obtain [11]

$$\int_V \int_0^T G\nabla^2 p = \int_S \int_0^T (G\nabla p - p\nabla G) \cdot \mathbf{n} + \int_0^T \int_V p\nabla^2 G \tag{3.42}$$

where the surface $S = S_1 \cup S_2$ and the normal $\mathbf{n}$ is as shown in Figure 3.3. The term on the right hand side of (3.39) is considered known. Combining all of this information gives us the integral equation

$$\int_V (G p_\tau - G_\tau p) |_0^T - c^2 \int_S \int_0^T (G\nabla p - p\nabla G)\cdot\mathbf{n} + \int_V \int_0^T p \left(G_{\tau\tau} - c^2\nabla^2 G\right) = \int_V \int_0^T G f. \tag{3.43}$$

In the volume V, the Green's function satisfies the homogeneous version of (3.25) so that the third term above is identically zero. The second term can be broken up as follows

$$\int_0^T \int_{S_1} (G\nabla p - p\nabla G) \cdot \mathbf{n} + \int_0^T \int_{S_2} (G\nabla p - p\nabla G) \cdot \mathbf{n}. \tag{3.44}$$

[11] Since there is a hole in the region we are technically applying the generalized divergence theorem as given in section 4.2.3 of [40].

The surface given by S_2 is meant to approach 0 so as to include all the points surrounding our observation point (x, y, z). To do this in a rigorous fashion we examine the second integral above in more detail. Since we have chosen an arbitrarily small ϵ-sphere we can write this integral as

$$-\int_0^T \int_{S_2} G\frac{\partial p}{\partial \epsilon} - p\frac{\partial G}{\partial \epsilon} dS_2\, d\tau \tag{3.45}$$

since $r = \epsilon$ on the surface of S_2 and $\mathbf{n} = -\mathbf{r}$ (unit vector). Upon substitution of our Green's function (3.37) we get

$$-\int_0^T \int_{S_2} \left[\frac{\delta(t-\tau-\frac{\epsilon}{c})}{4\pi\epsilon c^2}\frac{\partial p}{\partial \epsilon} + p\frac{\delta'(t-\tau-\frac{\epsilon}{c})}{4\pi\epsilon c^3} + p\frac{\delta(t-\tau-\frac{\epsilon}{c})}{4\pi\epsilon^2 c^2}\right] dS_2\, d\tau. \tag{3.46}$$

Next we let $t^* = t - \frac{\epsilon}{c}$ and, using the fact that $T > t$ and the following property of derivatives of delta functions [39]

$$\int_0^T p(\tau)\delta'(t^*-\tau)d\tau = \int_0^T \frac{\partial p}{\partial \tau}\delta(t^*-\tau)d\tau = \frac{\partial p}{\partial t}|_{t^*} \tag{3.47}$$

we evaluate the time integral to arrive at

$$-\int_{S_2} \left[\frac{1}{4\pi\epsilon c^2}\frac{\partial p}{\partial \epsilon}|_{t^*} + \frac{1}{4\pi\epsilon c^3}\frac{\partial p}{\partial t}|_{t^*} + \frac{1}{4\pi\epsilon^2 c^2}p|_{t^*}\right] dS_2. \tag{3.48}$$

Assuming now that our function p and its derivatives are continuous at our observation point we can approximate each of them by using the value at (x, y, z) and take them out of the integral. Using the fact that $dS_2 = \epsilon^2 \sin\phi\, d\phi\, d\theta$ we see that as $\epsilon \to 0$ only the third term above will remain. Also, $t^* \to t$ which leaves us with

$$-p(x, y, z, t)\int_0^{2\pi}\int_0^{\pi} \frac{1}{4\pi c^2}\sin\phi\, d\phi\, d\theta. \tag{3.49}$$

The integration trivially gives 4π so that we finally conclude that

$$\int_0^T \int_{S_2} (G\nabla p - p\nabla G)\cdot\mathbf{n} = -\frac{1}{c^2}p(x, y, z, t). \tag{3.50}$$

Substituting this result into (3.43) and moving all the integral terms to the right-hand side yields the general integral solution

$$p(x, y, z, t) = \int_V \int_0^T G f d\tau dV + c^2 \int_{S_1}\int_0^T (G\nabla p - p\nabla G)\cdot\mathbf{n} dS_1 d\tau - \int_V (Gp_\tau - G_\tau p)\,|_0^T. \tag{3.51}$$

This is the most general solution to the wave equation (3.38). This solution can be used for interior problems (where S_1 is some finite shape) or for exterior problems (where the surface S_1 extends out to infinity).

Unfortunately, none of this work has made the problem any easier since our unknown function p appears under the integral sign on the right. Nonetheless, the integral solution does give light to the factors influencing the function p. The first integral represents the contribution from the forcing term f throughout the whole volume V. The third integral represents the contributions from initial conditions. The second integral is the most interesting of the three. It says that in the absence of any forcing and initial conditions the solution for p anywhere in the region is obtained by knowledge of p and $\nabla p \cdot \mathbf{n}$ on the boundary. The term $\nabla p \cdot \mathbf{n}$ is often converted to normal particle acceleration using a momentum equation (see Section 2.6). That is, if we know the pressure and the velocity on the boundary (so that we can compute the acceleration) then computing p anywhere in the field is a matter of quadrature. Unfortunately, we typically require one of these quantities to get the other and so in its full generality there is no other option but to solve the integral equation numerically.

All is not lost however. It is possible to remove some of the terms of (3.51) in cases with simplifying geometry. Indeed for our original model of a piston in an infinite baffle the geometry of the volume V will help us achieve these simplifications.

3.4 Geometry of Problem and Simplifying Conditions

The volume V for our problem can be defined as the semi-infinite volume $z \geq 0$ in Figure 3.4. The baffle (solid line) is located at $z = 0$ and is given by S_b. The woofer is the surface S_w which we assume to be flat and circular (the figure below is a cross-section so the woofer is drawn to be noticeable). Conditions on S_b and S_w are given by equations (2.67) and (2.68) restated here using the current notation:

$$1^{st} \text{ order} \quad w_1(x,y,0,t) = \dot{B}_1(t) \text{ on } S_w, \tag{3.52}$$

$$2^{nd} \text{ order} \quad w_2(x,y,0,t) = -w_{1z}(x,y,0,t)B_1(t) \text{ on } S_w, \tag{3.53}$$

$$\text{all orders} \quad w(x,y,0,t) = 0 \text{ on } S_b. \tag{3.54}$$

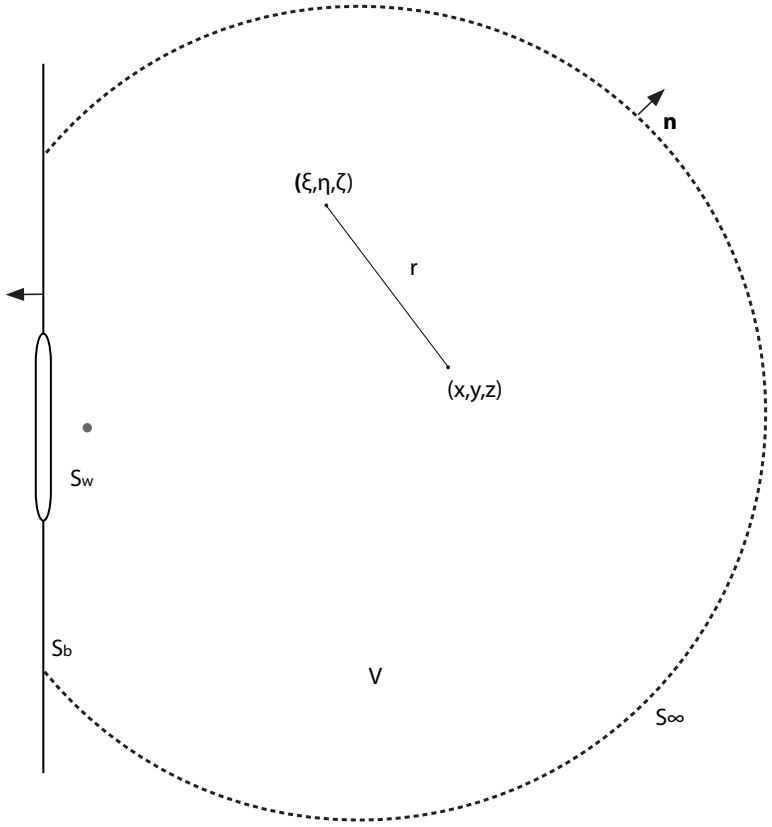

Figure 3.4: Volume V and associated surfaces for use in baffled piston model. For an unbounded medium, surface S_∞ extends to infinity. The grey dot represents the point source tweeter. The point (x, y, z) is our fixed observation point while (ξ, η, ζ), the integration point, moves throughout the region.

We wish to establish conditions on the surface S_∞ so that as the surface is extended to infinity it provides no contribution to the solution.

3.4.1 Radiation Condition at Infinity

Our surface integral in (3.51) is taken over $S_1 = S_b \cup S_w \cup S_\infty$. Here we investigate that over S_∞. In the limit as the surface goes to infinity the normal derivative is replaced with the radial derivative, however this time the unit vectors $\mathbf{n}$ and $\mathbf{r}$ are in the same direction giving us

$$\int_0^T \int_{S_\infty} \left[\frac{\delta(t-\tau-\frac{r}{c})}{4\pi r c^2} \frac{\partial p}{\partial r} + \frac{\partial p}{\partial \tau} \frac{\delta(t-\tau-\frac{r}{c})}{4\pi r c^3} + p \frac{\delta(t-\tau-\frac{r}{c})}{4\pi r^2 c^2} \right] dS_\infty \, d\tau. \tag{3.55}$$

Now in writing the lower bound of 0 for our time integration we were implicitly assuming $r < ct$, that is, that we are waiting long enough for contributions from anywhere in the region to reach our observation point. This is expressed in the argument of the delta function $\delta((t-\frac{r}{c})-\tau)$ so that $r < ct \Rightarrow T > t > t - \frac{r}{c} > 0$ and our τ integration is nontrivial. However as r tends to infinity, there will be no time t so that $r < ct$ and the argument of the delta function will never be 0 giving us a trivial integration.

Now an argument could be made towards our lower bound of 0 and taking the r limit before evaluating the integral. Indeed, we should start our time integration as far back as possible so as to include all contributions for any given value of r. We thus assume

$$\varphi(t, \cdot) \equiv 0 \quad \text{for } t < t_0 \tag{3.56}$$

for any given field quantity φ. The lower limit on the time integral will then be replaced by $t_0 \in \mathbb{R}$ and, using a finite value of $r < c(t-t_0)$ we can write the limiting behaviour as

$$\lim_{r\to\infty} \int_{t_0}^T \varphi(\tau)\delta(t - \frac{r}{c} - \tau) d\tau = \lim_{r\to\infty} \varphi(t - \frac{r}{c}). \tag{3.57}$$

As it stands, since $r < c(t-t_0)$ then $t - \frac{r}{c} > t_0$ so that our function φ is nonzero (not identically zero anyway) before the limit is taken. However, being a field quantity, φ is assumed continuous yielding

$$\lim_{r\to\infty} \varphi(t - \frac{r}{c}, \cdot) = \varphi(-\infty, \cdot) = 0 \tag{3.58}$$

from our assumption (3.56) so that all integrations give 0 again.

The final situation worth considering is that of time-harmonic behaviour. Truly, the approach above is still valid because in principle there must be some time t_0 before which there was no activity. Nonetheless it is worth mentioning since much of the literature only considers the analysis below.

For time-harmonic behaviour (that we assume has been going on indefinitely) the equivalent of the wave equation is the Helmholtz equation

$$\nabla^2 P + k^2 P = F(x, y, z) \tag{3.59}$$

where $k = \frac{\omega}{c}$ with ω the harmonic frequency (i.e., $p(x, y, z, t) = P(x, y, z)e^{j\omega t}$). This PDE has a corresponding Green's function [41]

$$\bar{G} = \frac{e^{-jkr}}{4\pi r}, \quad r = \sqrt{(x-\xi)^2 + (y-\eta)^2 + (z-\zeta)^2} \tag{3.60}$$

and a general solution given by [30]

$$P(x, y, z) = \int_V F\bar{G} dV + \int_S \left(\bar{G}\nabla P - P\nabla\bar{G}\right) \cdot \mathbf{n}\, dS. \tag{3.61}$$

Again, we are to investigate the integral over the surface which tends to infinity

$$\lim_{r\to\infty} \int_{S_\infty} \frac{e^{-jkr}}{4\pi r}\frac{\partial P}{\partial r} - P\frac{\partial}{\partial r}(\frac{e^{-jkr}}{4\pi r})\, dS_\infty. \tag{3.62}$$

Since $\frac{\partial}{\partial r}(\frac{e^{-jkr}}{4\pi r}) = -jk\left(\frac{e^{-jkr}}{4\pi r}\right) - \frac{e^{-jkr}}{4\pi r^2}$ and $dS_\infty = \Omega r^2$ (with Ω being the solid angle subtended by S_∞), in the limit of large r the first term of $\frac{\partial\bar{G}}{\partial r}$ dominates and we arrive at

$$\frac{\Omega}{4\pi}\lim_{r\to\infty} e^{-jkr} r\left(\frac{\partial P}{\partial r} + jkP\right). \tag{3.63}$$

In order for this term to disappear we require that

$$\lim_{r\to\infty} r\left(\frac{\partial P}{\partial r} + jkP\right) = 0, \tag{3.64}$$

which is famously known as the Sommerfeld radiation condition. According to Skudrzyk [33] this will be satisfied so long as the function P goes as r^{-1} in the farfield (see example below). As we will see in the next chapter, the pressure from our woofer acts like a point source in the farfield so that this requirement

is satisfied for the pressure generated by both the woofer and tweeter. Therefore, even for time-harmonic behaviour the surface integral over S_∞ tends to 0.

The difference between the methods amounts to a time condition vs. a radiation/spreading condition. In the first method we insist that contributions from the expanding boundary will not reach the observation point in finite time whereas the second case says that we should only consider sufficiently behaved outgoing waves from the sources; incoming waves are meaningless. As Sommerfeld [42] himself put it, no energy may be radiated inward from infinity towards the sources. For example, a time harmonic solution to the spherical wave equation (3.2) is

$$p = \frac{e^{j\omega(t-\frac{r}{c})}}{r} + \frac{e^{j\omega(t+\frac{r}{c})}}{r} \tag{3.65}$$

but a quick check will show that only the first of these (representing outgoing waves) satisfies (3.64). The conclusion from all of this is that, regardless of the method used, the integral over S_∞ in (3.51) is discarded and we are left with those over S_b and S_w.

3.4.2 Woofer and Baffle Conditions

Computing the surface integral in 3.51 requires knowledge of $\nabla p \cdot \mathbf{n}$ and p over the given surface. For the case where $S_1 = S_b \cup S_w$ we can obtain the former by using the momentum equations to write the pressure gradient in terms of particle velocity and then use the boundary conditions given in Section 3.4. Alas, we do not have knowledge of pressure p on these surfaces for this is what we are trying to solve.

The beauty of the Green's function method is that for simple geometries (or if one is clever enough to work with more difficult arrangements, see for example [43]) we can modify our function G so as to cause one of the two terms (G or $\nabla G \cdot \mathbf{n}$) to vanish over the surface of interest. In our case we wish to find the required modification so that $\nabla G \cdot \mathbf{n} = 0$ on S_w and S_b.

To do this we must add a term to our Green's function which satisfies the homogeneous version of (3.25) everywhere in the volume V so that its only contribution

occurs at the boundary in question. Since our surfaces S_b and S_w are essentially the plane $z = 0$ a standard approach is to use an image source on the other side of the plane for each integration point. That is, add a second Green's function, identical to the first, except reflect the ζ variable in the xy-plane giving us

$$G = G(\xi, \eta, \zeta, \tau, x, y, z, t) + G(\xi, \eta, -\zeta, \tau, x, y, z, t) = G_1 + G_2. \tag{3.66}$$

To show that this gives $\nabla G \cdot \mathbf{n}$ on the $z = 0$ plane note that

$$\nabla G = \nabla G_1 + \nabla G_2 = (\frac{\partial G_1}{\partial \xi}, \frac{\partial G_1}{\partial \eta}, \frac{\partial G_1}{\partial \zeta}) + (\frac{\partial G_2}{\partial \xi}, \frac{\partial G_2}{\partial \eta}, \frac{\partial G_2}{\partial \zeta}) \tag{3.67}$$

but, using either the Helmholtz or wave equation Green's functions, on the surfaces $S_b \cup S_w$ we have $\frac{\partial G_1}{\partial \xi} = \frac{\partial G_2}{\partial \xi}$, $\frac{\partial G_1}{\partial \eta} = \frac{\partial G_2}{\partial \eta}$, $\frac{\partial G_1}{\partial \zeta} = -\frac{\partial G_2}{\partial \zeta}$ and $\mathbf{n} = (0, 0, -1)$ (recall the Footnote 2.5) so that

$$\nabla G \cdot \mathbf{n} = 0, \quad \text{on } S_b \cup S_w. \tag{3.68}$$

Indeed the infinite plane baffle helps reduce our integral equation rather substantially since condition (3.68) transforms our problem from an integral equation into an integration with a known integrand.

From this result we can write our solution thus far

$$p(x, y, z, t) = \int_V \int_0^T Gf \, d\tau \, dV + c^2 \int_{S_w \cup S_b} \int_0^T G \nabla p \cdot \mathbf{n} \, dS_1 \, d\tau - \int_V (Gp_\tau - G_\tau p) \, |_0^T \, dV. \tag{3.69}$$

As was mentioned at the beginning of this section, the function $\nabla p \cdot \mathbf{n}$ is known from the momentum equations (2.60) and (2.64) and the boundary conditions (3.52),(3.53) and (3.54). Solving for this quantity at first- and second-order we get

$$\nabla p_1 = -\rho_0 \mathbf{u}_{1t} \tag{3.70}$$

$$\nabla p_2 = -\rho_0 \mathbf{u}_{2t} - \rho_1 \mathbf{u}_{1t} - \rho_0 [(\mathbf{u}_1 \cdot \nabla) \mathbf{u}_1] \tag{3.71}$$

so that on our baffle (S_b), when computing $\nabla p \cdot \mathbf{n}$ with our normal $\mathbf{n} = (0, 0, -1)$, the first-order equation yields

$$\nabla p_1 \cdot \mathbf{n} = -\rho_0 (\mathbf{u}_1 \cdot \mathbf{n})_t = \rho_0 w_{1t}(x, y, 0, t) = 0 \tag{3.72}$$

using the fact that the normal is time-invariant and invoking (3.54) at the end. At second-order the calculation is similar but not as straightforward. We can see immediately from looking at (3.71) that the first and second terms will be 0 by a similar argument to that given above. The third term when dotted with the normal gives

$$\begin{aligned} -\left[(\mathbf{u}_1 \cdot \nabla)\mathbf{u}_1\right] \cdot \mathbf{n} &= -\left[\left((u_1, v_1, w_1) \cdot (\frac{\partial}{\partial x}, \frac{\partial}{\partial y}, \frac{\partial}{\partial z})\right)(u_1, v_1, w_1)\right] \cdot (0, 0, -1) \\ &= -\left[(u_1 \frac{\partial}{\partial x} + v_1 \frac{\partial}{\partial y} + w_1 \frac{\partial}{\partial z})(u_1, v_1, w_1)\right] \cdot (0, 0, -1) \\ &= u_1 \frac{\partial w_1}{\partial x} + v_1 \frac{\partial w_1}{\partial y} + w_1 \frac{\partial w_1}{\partial z}. \end{aligned} \tag{3.73}$$

On the baffle the first two derivative terms are zero because by (3.54) $w_1(x, y, 0, t) = 0$ for all x and y so there is no change along those axes. The third derivative term is unknown since we must take the derivative before evaluating $z = 0$. However the function w_1 is 0 for $z = 0$ so that all three terms indeed vanish and we get the conclusion that

$$\nabla p \cdot \mathbf{n} = 0, \quad \text{on } S_b \text{ for } p = p_1 \text{ or } p_2. \tag{3.74}$$

Our solution is therefore

$$p(x, y, z, t) = \int_V \int_0^T G f \, d\tau \, dV + c^2 \int_{S_w} \int_0^T G \nabla p \cdot \mathbf{n} \, dS_1 \, d\tau - \int_V (G p_\tau - G_\tau p) \, |_0^T dV. \tag{3.75}$$

3.4.3 Time Conditions

The final simplification that can be made is on the last term of our solution above. With the following established property of the Green's function

$$G = G_\tau = 0, \quad \tau > t \tag{3.76}$$

and the assumption that (see Section 3.4.1) there is no disturbance for $t \leq 0$ (or more generally $t \leq t_0$)

$$\varphi(t, \cdot) = 0, \quad t \leq 0 \tag{3.77}$$

for any field variable φ, the last integral in (3.75) vanishes upon evaluation at the boundary values $\tau = 0$ and $\tau = T > t$.

3.5 Final Solution and Remarks

After using the many geometrical and temporal simplifications, our general solution to the wave equation (3.51) has been reduced to

$$\boxed{p(x,y,z,t) = \int_V \int_0^T Gf \, d\tau \, dV + c^2 \int_{S_w} \int_0^T G\nabla p \cdot \mathbf{n} \, d\tau \, dS_w} \tag{3.78}$$

with our modified Green's function $G = G_1 + G_2$ as given by (3.66).

3.5.1 Point Source Equivalence

It should be mentioned that we have avoided the boundary of the tweeter in our domain V. We have assumed the tweeter to be a mass source of negligible size which is included in our function f. An alternative approach would be to alter the region V so as to include the boundary of a finite sphere representing the tweeter and then take the limit as the boundary shrinks to 0. The mathematics are nontrivial however since, in this case, we do not have the spherical symmetry surrounding our observation point (x, y, z) that we had for the boundary integrals given prior. Indeed we can show that[12]

$$\lim_{a\to 0} c^2 \int_{S_t} \int_0^T (G\nabla p - p\nabla G)\cdot\mathbf{n} \, dS_T \, d\tau = \rho_0 c^2 \int_0^T \int_V G\dot{Q}(\tau)\delta(\boldsymbol{\chi} - \mathbf{x_0}) \, dV \, d\tau, \tag{3.79}$$

that is to say, the pressure at (x, y, z) generated by the boundary integral of S_T (see Figure 3.5) whose radius shrinks to 0 is the same as that given by the volume integral where the forcing term is solely due to a point mass source.

Essentially, we are going to show the equivalence of two methods of solution: either we assume a no-source situation where the only contribution comes from a finite sphere

$$p(x,y,z,t) = \lim_{a\to 0} c^2 \int_{S_T} \int_0^T (G\nabla p - p\nabla G) \cdot \mathbf{n} \, dS_T \, d\tau, \tag{3.80}$$

[12]Here we have chosen $f = \rho_0 c^2 \dot{Q}(t)\delta(\mathbf{x} - \mathbf{x_0})$, as seen in (3.21).

or assume there are no boundaries (other than infinity) in the medium and we only have a point source

$$p(x,y,z,t) = \rho_0 c^2 \int_0^T \int_V G\dot{Q}(\tau)\delta(\boldsymbol{\chi} - \mathbf{x_0})\, dV\, d\tau. \tag{3.81}$$

The reason for investigating this is that in deriving (3.78) we used the divergence theorem in our volume V (see Figure 3.4). However this was not strictly valid since having a point source in the medium should not allow the theorem to be used. Therefore, the correct approach requires the use of a finite boundary. We can however show the equivalence of the methods which allows us to use the point source formulation alongside the divergence theorem as it is much simpler.

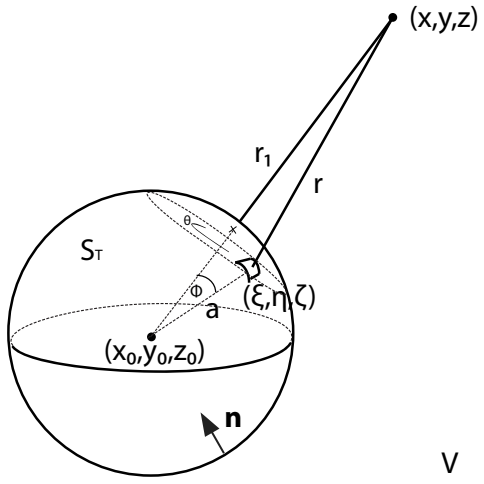

Figure 3.5: Sphere with surface S_T in unbounded volume V. The relationship between the lengths is given by $r^2 = r_1^2 + a^2 - 2r_1 a\cos\phi$. Note r is independent of θ.

To evaluate the integrals in closed form we assume a time harmonic radial vibration such that $u^{(r)} = b_0 e^{j\omega t}$ which gives us a source function $Q(t) = 4\pi a^2 b_0 e^{j\omega t} = Q_0 e^{j\omega t}$(see the paragraph after (3.11)). The second method (3.81) then gives [13]

$$p(x,y,z,t) = j\omega\rho_0 c^2 Q_0 \int_0^T \int_V \frac{\delta(t-\tau-\frac{r}{c})}{4\pi r c^2} e^{j\omega\tau}\delta(\boldsymbol{\chi} - \mathbf{x_0}) dV d\tau. \tag{3.82}$$

[13]Since we are assuming no boundaries we use the regular Green's function (3.37).

Now as r is integrated over the volume its only contribution will come when $\boldsymbol{\chi}= \mathbf{x_0}$ so that $r \to r_1$ and we have

$$p(x,y,z,t) = \frac{j\omega\rho_0 Q_0}{4\pi r_1}\int_0^T \delta(t-\tau-\frac{r_1}{c})e^{j\omega\tau}d\tau. \tag{3.83}$$

Again, this is easily evaluated to give a final solution of

$$p(x,y,z,t) = \frac{j\omega\rho_0 Q_0}{4\pi r_1}e^{j(\omega t-kr_1)} \tag{3.84}$$

identical to (3.11), derived using the differential form.

The first method (3.80) requires knowledge of both p and $\nabla p\cdot\mathbf{n}$ on the surface S_T. Again, we have knowledge of the latter by equation (3.7) and our prescribed boundary velocity. We could, as with the case for the plane boundary, create a modified Green's function which would eliminate $\nabla G\cdot\mathbf{n}$ on the surface of the sphere. However, constructing such a function is not a straightforward affair (see [43]). Instead it is much easier to compute p using the same approach given in Section 3.1.1.

The solution for a finite pulsating sphere is given by (3.5)

$$p = \frac{f(t-\frac{r_1}{c})}{r_1}, \tag{3.85}$$

where f satisfies the ODE (3.8):

$$u_t^{(r_1)}(r_1,t) = \frac{f(t-\frac{r_1}{c})}{\rho_0 r_1^2} + \frac{f'(t-\frac{r_1}{c})}{\rho_0 c r_1}. \tag{3.86}$$

At $r_1 = a$ we have $u^{(r_1)}(a,t) = b_0 e^{j\omega t}$ so that we can solve the ODE to get

$$f(t) = \rho_0 b_0 c\left(\frac{jka^2}{1+jka}\right)e^{j(\omega t+ka)} \tag{3.87}$$

which gives our solution for p in the region $r_1 \geq a$ as

$$p = \rho_0 b_0 c\left(\frac{jka^2}{1+jka}\right)\frac{e^{j(\omega t-k(r_1-a))}}{r_1}. \tag{3.88}$$

We next compute $G\nabla p\cdot\mathbf{n}$ recalling that $\nabla p\cdot\mathbf{n}$ is the normal acceleration of the boundary from our momentum equation (2.60). Noting the orientation of the normal from Figure 3.5 and using our function $u^{(r)} = b_0 e^{j\omega t}$ we obtain

$$\int_{S_T}\int_0^T G\nabla p\cdot\mathbf{n} = \frac{\rho_0 b_0 j\omega}{4\pi c^2}\int_{S_T}\frac{e^{j(\omega t-kr)}}{r}dS_T. \tag{3.89}$$

Now $dS_T = a^2 \sin\phi \, d\phi \, d\theta$ so that the integration would be taken over $\int_0^{2\pi}\int_0^{\pi}$. However, using the fact that $r^2 = a^2 + r_1^2 - 2r_1 a\cos\phi$ we get $dr = \frac{ar_1 \sin\phi d\phi}{r}$ so that $dS_T = \frac{ar}{r_1} dr \, d\theta$ and the integral becomes

$$\frac{\rho_0 b_0 j\omega a}{4\pi r_1 c^2} \int_0^{2\pi} \int_{r_1-a}^{r_1+a} e^{j(\omega t - kr)} \, dr \, d\theta \tag{3.90}$$

which evaluates to

$$\frac{j\omega\rho_0 b_0 a}{kc^2 r_1} e^{j(\omega t - kr_1)} \sin(ka). \tag{3.91}$$

To get $p\nabla G \cdot \mathbf{n}$ we evaluate (3.88) at $r_1 = a$ giving

$$p = \frac{A}{a} e^{j\omega t}, \quad A = \rho_0 b_0 c \left(\frac{jka^2}{1+jka} \right). \tag{3.92}$$

Unfortunately, as can be seen in Figure 3.5, $\nabla G \cdot \mathbf{n}$ (equivalently $\frac{\partial G}{\partial n}$) is no longer equal to $\frac{\partial G}{\partial r}$ but rather $-\frac{\partial G}{\partial a}$. The integral of $p\nabla G \cdot \mathbf{n}$ over the surface S_T is then

$$-\frac{A}{a} \int_{S_T} \int_0^T e^{j\omega\tau} \frac{\partial G}{\partial a} d\tau dS_T. \tag{3.93}$$

Then, evaluating the time integral and using the following:

- $\frac{\partial G}{\partial a} = \frac{\partial G}{\partial r}\frac{\partial r}{\partial a}$,
- $\frac{\partial G}{\partial r} = -\frac{\delta'(t-\tau-\frac{r}{c})}{4\pi r c^3} - \frac{\delta(t-\tau-\frac{r}{c})}{4\pi r^2 c^2}$,
- $\frac{\partial r}{\partial a} = \frac{a - r_1\cos\phi}{r}$,
- $dS_T = a^2 \sin\phi \, d\phi \, d\theta$,

our integral becomes

$$\frac{A}{4\pi a c^2} e^{j\omega t} \int_0^{2\pi} \int_0^{\pi} \left[jk\frac{e^{-jkr}}{r} + \frac{e^{-jkr}}{r^2} \right] \left(\frac{a - r_1\cos\phi}{r} \right) a^2 \sin\phi \, d\phi \, d\theta. \tag{3.94}$$

The appearance of the $\cos\phi$ term removes the benefit of our previous substitution $dS_T = \frac{ar}{r_1} \, dr \, d\theta$ and we are left to integrate over θ and ϕ with $r = \sqrt{a^2 + r_1^2 - 2r_1 a\cos\phi}$. Somewhat remarkably, the integral itself has a closed form solution of

$$\frac{-4\pi a}{r_1} e^{-jkr_1} \left[\cos(ka) - \frac{\sin(ka)}{ka} \right] \tag{3.95}$$

so that our term $\int_{S_T} p\nabla G \cdot \mathbf{n}$ is

$$-\frac{A}{c^2 r_1} e^{j(\omega t - kr_1)} \left[\cos(ka) - \frac{\sin(ka)}{ka}\right]. \tag{3.96}$$

Combining (3.91) with (3.96) gives our full solution

$$p = c^2 \int_{S_T} \int_0^T (G\nabla p - p\nabla G) \cdot \mathbf{n}\, dS_T\, d\tau \tag{3.97}$$

as

$$p = \frac{j\omega\rho_0 b_0 a}{kr_1} e^{j(\omega t - kr_1)} \sin(ka) + \frac{A}{r_1} e^{j(\omega t - kr_1)} \left[\cos(ka) - \frac{\sin(ka)}{ka}\right]. \tag{3.98}$$

Recalling that we defined $Q_0 = 4\pi a^2 b_0$ we can rewrite this as

$$p = \frac{j\omega\rho_0 Q_0}{4\pi r_1} e^{j(\omega t - kr_1)} \frac{\sin(ka)}{ka} + \frac{jk\rho_0 Q_0 c}{4\pi r_1 (1 + jka)} e^{j(\omega t - kr_1)} \left[\cos(ka) - \frac{\sin(ka)}{ka}\right] \tag{3.99}$$

and then in the limit as $a \to 0$ the value of Q_0 is held constant (see Section 3.1.1) and the second term drops out (since $\lim_{x\to 0} \frac{\sin(x)}{x} = 1$) and we are left with

$$p = \frac{j\omega\rho_0 Q_0}{4\pi r_1} e^{j(\omega t - kr_1)} \tag{3.100}$$

matching both (3.84) and (3.11).

As we have seen, the surface integral solution is not the easiest way to solve for the pressure of a simple point source. Indeed the simplest way to compute a purely radial field is to either follow the method given in Section 3.1.1 or to note that our solution for the finite sphere (3.88) reduces to those given in (3.84) and (3.100) in the limit of $a \to 0$.

The reason for carrying out these integrations is to show the equivalence of the methods so as to justify the form of our main solution (3.78). In the next chapter we will be using this formula to compute the second-order field and it is much simpler to do so in its current form than to include a finite shaped sphere with vanishing boundary.

Chapter 4

Solutions

In this chapter we obtain both approximate and exact analytic solutions for both the first- and second-order wave equations based on (3.78). We also derive an integral solution for p_2 which we solve numerically and compare with experiments performed in a lab. Finally, we determine the effects of varying the parameters using our theoretical model since they are not so easily measured in practice.

4.1 First-Order

We assume that our woofer is vibrating with frequency ω_1 such that $B_1(t) = B\sin(\omega_1 t)$ with B the amplitude of vibration. To simplify calculations we use exponentials so that $B_1(t) = \Re\{\frac{B}{j}e^{j\omega_1 t}\}$ and our woofer velocity is then $\dot{B}_1(t) = \Re\{b_w e^{j\omega_1 t}\}$ where $b_w = B\omega_1$ is the velocity amplitude. Likewise, our tweeter is assumed to satisfy (3.12) such that $s(t) = e^{j\omega_2 t}$ so that $Q(\mathbf{x}, t) = \Re\{Q_0 e^{j\omega_2 t}\delta(\mathbf{x} - \mathbf{x_0})\}$.

From here on we omit taking the real part assuming that this operation is done at the very end to get meaningful results. Note however that this is only valid at first-order since at second-order we have quadratic terms and in general $\Re(z_1 z_2) \neq \Re(z_1)\Re(z_2)$. We will deal with this in section 4.2.3.

Our first-order problem is to solve

$$p_{1tt} - c^2\nabla^2 p_1 = \rho_0 c^2 \dot{Q}(\mathbf{x}, t). \tag{4.1}$$

From our work in the previous chapter we know that this equation has solution

$$p_1 = \rho_0 c^2 \int_V \int_0^T G\dot{Q}(\boldsymbol{\chi}, t)\, d\tau\, dV + c^2 \int_{S_w} \int_0^T G\nabla p_1 \cdot \mathbf{n}\, d\tau\, dS_w \tag{4.2}$$

with G given by (3.66). For our purposes G will be written as

$$G = \frac{\delta(t - \tau - \frac{r_a}{c})}{4\pi r_a c^2} + \frac{\delta(t - \tau - \frac{r_b}{c})}{4\pi r_b c^2}, \tag{4.3}$$

where

$$r_a = \sqrt{(x-\xi)^2 + (y-\eta)^2 + (z-\zeta)^2}, \tag{4.4}$$

$$r_b = \sqrt{(x-\xi)^2 + (y-\eta)^2 + (z+\zeta)^2}, \tag{4.5}$$

and our tweeter point $\mathbf{x_0} = (0, 0, d)$ (see Figure 4.1)

4.1.1 Volume Integral - Tweeter

With our choice of function Q the volume integral in (4.2) becomes

$$j\omega_2\rho_0 Q_0 \int_V \int_0^T \left[\frac{\delta(t - \tau - \frac{r_a}{c})}{4\pi r_a} + \frac{\delta(t - \tau - \frac{r_b}{c})}{4\pi r_b}\right] e^{j\omega_2\tau}\delta(\boldsymbol{\chi} - \mathbf{x_0})\, d\tau\, dV. \tag{4.6}$$

As the integration point $\boldsymbol{\chi}= (\xi, \eta, \zeta)$ (see Figure 4.1) moves throughout the region, the only contribution occurs when $\boldsymbol{\chi}= \mathbf{x_0}$ so that $r_a \to r_1$ and $r_b \to r_2$ which gives a nice closed form solution of

$$\text{tweeter} = \frac{j\omega_2\rho_0 Q_0}{4\pi}\left[\frac{e^{j(\omega_2 t - k_2 r_1)}}{r_1} + \frac{e^{j(\omega_2 t - k_2 r_2)}}{r_2}\right]. \tag{4.7}$$

This solution represents the field coming from two point sources, one a mirror image of the other across the plane $z = 0$. It is this symmetry that allows our solution to satisfy the vanishing normal particle velocity condition over the boundary.

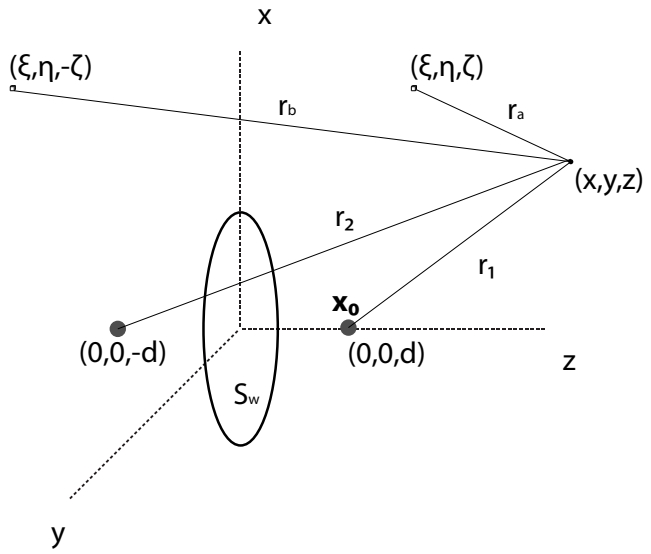

Figure 4.1: Geometry used in evaluating integrals. Note that we are technically only integrating in the region $z \geq 0$; however, due to our Green's function (4.3), we are essentially integrating over all of space. The lengths r_a and r_b are the integration variables while r_1 and r_2 are the fixed distances from the observation point to the tweeter and its image.

4.1.2 Surface Integral - Woofer

The field produced by the woofer is given by the second integral of (4.2). Again, using our momentum equation (2.60) and our boundary condition (3.52) we get that, on the surface S_w

$$\nabla p_1 \cdot \mathbf{n} = -\rho_0 (\mathbf{u}_1 \cdot \mathbf{n})_t = \rho_0 \ddot{B}_1(t) = j\omega_1 \rho_0 b_w e^{j\omega_1 t}. \tag{4.8}$$

Also, on S_w, $r_a = r_b = r$ so our Green's function reduces to

$$G = \frac{\delta(t - \tau - \frac{r}{c})}{2\pi r c^2}, \quad r = \sqrt{(x-\xi)^2 + (y-\eta)^2 + z^2} \tag{4.9}$$

which gives us an integral of

$$\text{woofer} = \frac{j\omega_1 \rho_0 b_w e^{j\omega_1 t}}{2\pi} \int_{S_w} \frac{e^{-jk_1 r}}{r} dS_w. \tag{4.10}$$

This integral is not solvable in general but has various approximating forms and special case solutions.[1] Here we obtain the on-axis solution as it will be a useful

[1] See the introduction in [11] for an in-depth discussion on the subject.

undertaking for the second-order solution. We also derive the farfield solution for a similar reason. Moreover it will serve to justify the Sommerfeld radiation condition at infinity given in Section 3.4.1. The procedure is adapted from [23].

On-axis

When our observation point (x, y, z) is placed on the axis of the woofer our integration is simplified by a change to polar coordinates

$$\begin{aligned} \xi &= \sigma \cos\theta \\ \eta &= \sigma \sin\theta \\ \zeta &= 0 \end{aligned} \tag{4.11}$$

Since $x = y = 0$ the distance r satisfies

$$r^2 = \sigma^2 + z^2 \tag{4.12}$$

The surface element $dS_w = \sigma \, d\theta \, d\sigma$ for $0 \leq \theta \leq 2\pi$ and $0 \leq \sigma \leq a$. Using the equation above for r we have that $rdr = \sigma d\sigma$ where $r_o \leq r \leq r_e$ (see Figure 4.2) so

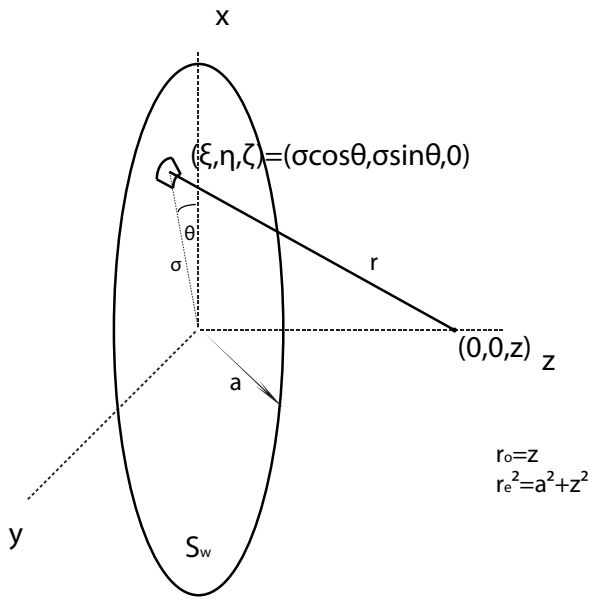

Figure 4.2: Coordinates used in evaluating the surface integral over S_w when observation point is on-axis.

that $dS_w = rdrd\theta$ and the integral becomes

$$\frac{j\omega_1\rho_0 b_w e^{j\omega_1 t}}{2\pi}\int_0^{2\pi}\int_{r_0}^{r_e} e^{-jk_1 r}dr\,d\theta. \tag{4.13}$$

This is easily evaluated to give

$$\text{woofer}_{\text{on-axis}} = \rho_0 b_w c\left[e^{j(\omega_1 t - k_1 r_o)} - e^{j(\omega_1 t - k_1 r_e)}\right]. \tag{4.14}$$

We see then that the solution on the axis of a circular piston is made up of two waves, one due to the edge and one from the centre. Note that as $z \to \infty$, $r_e \approx r_o$ and we are left with a null field. Indeed, we can show that as $z \to \infty$ the solution drops as r^{-1}. It is possible, however, to arrive at this result in general and not just for on-axis observation.

Farfield

The geometry of the general case where the observation point is off-axis is given by Figure 4.3. Due to the circular symmetry of the woofer we can assume that our observation point lies on the plane $y = 0$.

With the change of variables given by (4.11) as well as those for our observation point

$$x = R\sin\beta, \tag{4.15}$$

$$y = 0, \tag{4.16}$$

$$z = R\cos\beta, \tag{4.17}$$

our integration distance r becomes

$$r = \sqrt{R^2 + \sigma^2 - 2\sigma R\sin\beta\cos\theta}. \tag{4.18}$$

Substitution of this value of r into (4.10) yields an unsolvable integral; approximations must therefore be made. In the farfield we assume $R \gg a$. Rewriting our distance r as

$$r = R\sqrt{1 - \frac{2\sigma}{R}\sin\beta\cos\theta + \left(\frac{\sigma}{R}\right)^2} \tag{4.19}$$

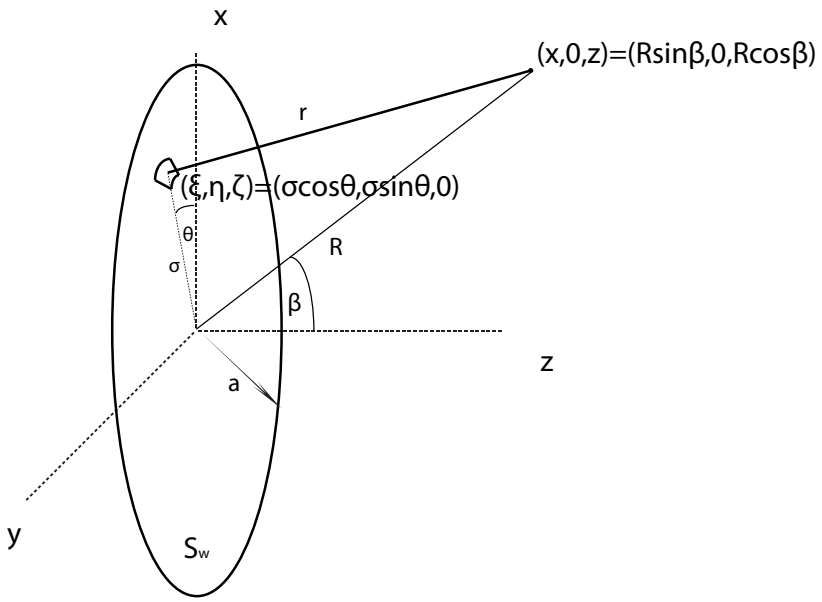

Figure 4.3: Coordinates used in evaluating the surface integral over S_w when observation point is off-axis.

we can neglect the third term using our farfield assumption. We can also approximate $\sqrt{1+x}$ by the first two terms of its Taylor series thus transforming our integration distance to

$$r = R - \sigma \sin\beta \cos\theta. \tag{4.20}$$

We then use this expression in our integral (4.10) but only for the phase component since the attenuation term will not contribute as much change and the integral is more easily computed when $r = R$. This leaves us to evaluate

$$\frac{j\omega_1 \rho_0 b_w e^{j(\omega_1 t - k_1 R)}}{2\pi R} \int_0^a \int_0^{2\pi} e^{jk_1 \sigma \sin\beta \cos\theta} \sigma d\theta d\sigma. \tag{4.21}$$

Using the Hansen formula [33]

$$J_0(x) = \frac{1}{2\pi} \int_{-\pi}^{\pi} e^{jx\cos\theta} d\theta \tag{4.22}$$

where $J_n(x)$ is the n^{th} order Bessel function of the first kind, a quick change of variable and the fact that J_0 is even, the inner integral is evaluated and we are left with

$$\frac{j\omega_1 \rho_0 b_w e^{j(\omega_1 t - k_1 R)}}{R} \int_0^a \sigma J_0(k_1 \sigma \sin\beta) d\sigma. \tag{4.23}$$

Finally, invoking the Bessel identity [44]

$$\int_0^x sJ_0(s)ds = xJ_1(x) \tag{4.24}$$

and a change of variable $u = k_1\sigma\sin\beta \Rightarrow \frac{du}{k_1\sin\beta} = d\sigma$ gives

$$\int_0^a \sigma J_0(k_1\sigma\sin\beta)d\sigma = \frac{1}{(k_1\sin\beta)^2}\int_0^{k_1 a\sin\beta} uJ_0(u)du = \frac{a}{k_1\sin\beta}J_1(k_1 a\sin\beta) \tag{4.25}$$

providing a final expression of

$$\frac{j\omega_1\rho_0 b_w a}{R}\frac{J_1(k_1 a\sin\beta)}{k_1\sin\beta}e^{j(\omega_1 t - k_1 R)}. \tag{4.26}$$

Because of the fact that $\lim_{x\to 0}\frac{J_1(x)}{x} = \frac{1}{2}$ the expression above is often rewritten to give the result

$$\text{woofer}_{\text{off-axis}} = \frac{j\omega_1\rho_0 b_w a^2}{2R}\left(\frac{2J_1(k_1 a\sin\beta)}{k_1 a\sin\beta}\right)e^{j(\omega_1 t - k_1 R)} \tag{4.27}$$

where the term in brackets is called the directivity function [23]. It represents how much the the signal drops off when one moves off the central axis of the woofer. Note that since $0 \le \beta \le \frac{\pi}{2}$ the argument of the directivity function, $k_1 a\sin\beta$, varies between 0 and $k_1 a$ so that as the observation point moves between on-axis ($\beta = 0$) to a position parallel to the baffle ($\beta = \frac{\pi}{2}$) the number of zeroes of the directivity function will depend on the "strength" of $k_1 a$ (refer to Figure 4.4).

For example, we see that for $k_1 a$ less than approximately 4 (more accurately 3.832) the directivity function will not pass through any zeros as its argument varies from 0 to $k_1 a$, that is to say there will not be any nulls in the field as an observer moves from a position on-axis to 90° off-axis. On the other hand, for larger $k_1 a$ it is clear that there will be certain angles which will produce null fields. Indeed, the larger the value of $k_1 a$ the more nulls will be produced.

What does $k_1 a$ represent physically? Since $k_1 = \frac{\omega_1}{c} = \frac{2\pi f_1}{\lambda_1 f_1} = \frac{2\pi}{\lambda_1}$ (with λ_1, f_1 the wavelength and non-angular frequency of the wave respectively) and a is the radius we see that $k_1 a = \frac{2\pi a}{\lambda_1}$ represents the ratio of the circumference of the woofer to the wavelength of the wave it produces. Limiting situations are often categorized as $k_1 a \ll 1$ and $k_1 a \gg 1$.

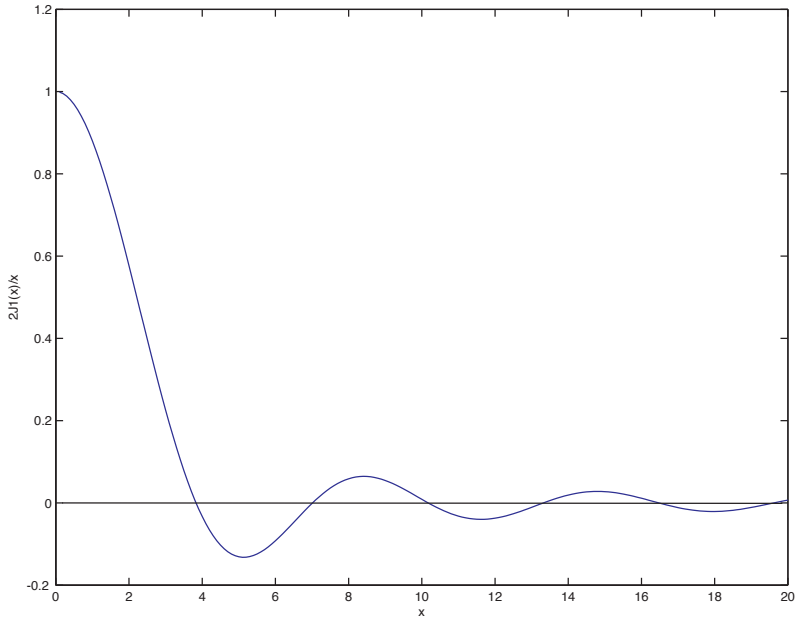

Figure 4.4: Dependence of woofer directivity function on maximum value of argument, $x = k_1 a$

In the first case we have that $circumference \ll wavelength$ which, for a woofer of fixed radius, say 10 cm, would be satisfied for frequencies below approximately 100 Hz. Since $k_1 a \ll 1$ in this instance the woofer produces a field with no nulls and little drop-off as we move off axis (see Figure 4.5).

If we were to take that same woofer and excite it at frequencies above, say, 3000 Hz then we would be in the $k_1 a \gg 1$ regime and would pass through one (if not several) zeroes as we moved off axis. There are now "side lobes" in addition to the "main lobe" of the directivity function. More importantly however is how much amplitude drop-off there is in this case as we can see how quickly and how close the function $\frac{J_1(x)}{x}$ oscillates about 0 once $k_1 a$ is approximately 3 (or once we excite our 10 cm woofer at 1500 Hz). This shows that using an average sized woofer as a high-frequency oscillator produces a highly directional beam of sound.

Figure 4.5 shows various polar plots for increasing values of the parameter $k_1 a$.

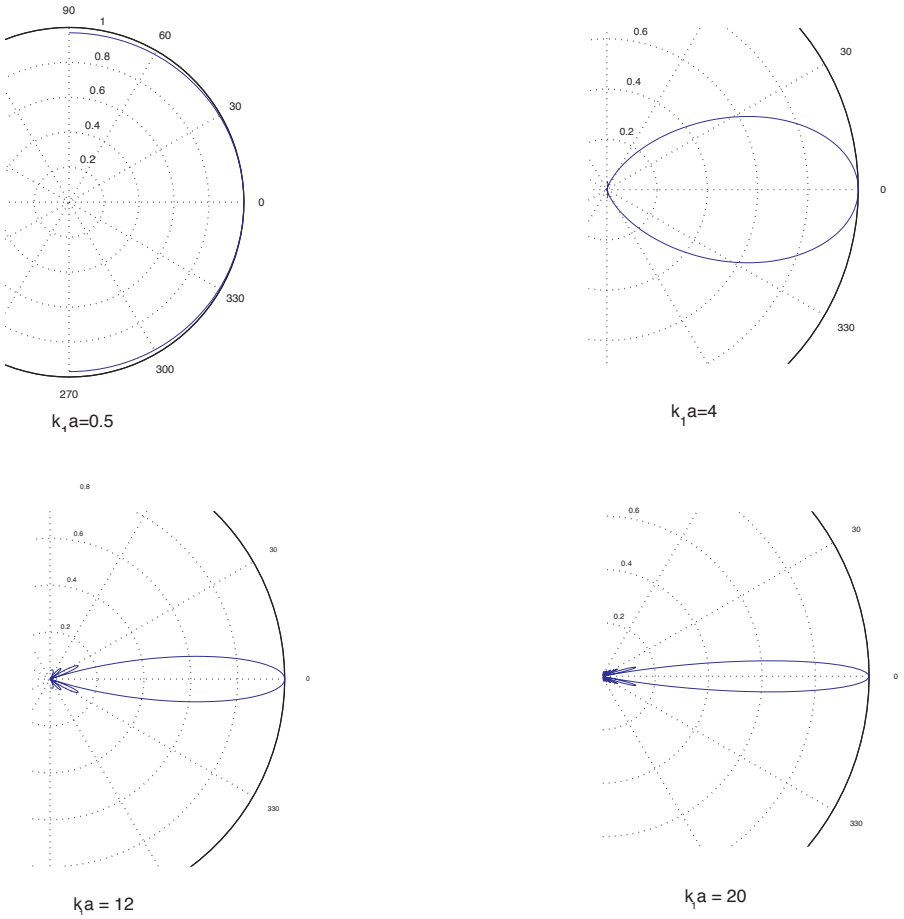

Figure 4.5: Polar plots of directivity function for various parameters $k_1 a$. Here $r = \frac{2J_1(k_1 a \sin\beta)}{k_1 a \sin\beta}$ and $-\frac{\pi}{2} \leq \beta \leq \frac{\pi}{2}$

4.1.3 Final Solution

The first-order pressure field generated by the woofer and tweeter is thus

$$p_1(x,y,z,t) = \frac{j\omega_1 \rho_0 b_w e^{j\omega_1 t}}{2\pi} \int_{S_w} \frac{e^{-jk_1 r}}{r} dS_w + \frac{j\omega_2 \rho_0 Q_0}{4\pi} \left[\frac{e^{j(\omega_2 t - k_2 r_1)}}{r_1} + \frac{e^{j(\omega_2 t - k_2 r_2)}}{r_2} \right] \tag{4.28}$$

where

$$\begin{aligned} r^2 &= (x-\xi)^2 + (y-\eta)^2 + z^2, \\ r_1^2 &= x^2 + y^2 + (z-d)^2, \\ r_2^2 &= x^2 + y^2 + (z+d)^2, \end{aligned} \tag{4.29}$$

where the first integral can be approximated by either (4.14) or (4.27) depending on the situation. In the next section we look at ways of solving the second-order wave equation whose solution depends on the general equation for p_1 (4.28).

4.2 Second-Order

The solution given in the previous section describes the field produced by two pure tones in a multiway speaker setup rather accurately. However, due to the assumed linearity of the solution, not all phenomena will be accounted for. Indeed one can see immediately from (4.28) that only the fundamental frequencies ω_1 and ω_2 will appear in the solution.

This is not necessarily a problem, since, for non-coaxial setups, intermodulation frequencies are essentially inaudible [1]. For coaxial setups however, Klipsch's experiment clearly reveals the presence of sum and difference frequencies in the sound field. As Klipsch's himself put it "*The distortion from the coaxial system was plainly audible; that from the spaced system barely audible.*"

Admittedly, the purpose of this whole endeavour is to mathematically formulate and deduce the experimental results given by Klipsch [1]. Achieving such a goal would allow us to better understand the inherent dependencies.

4.2.1 Change of Variable

Generation of sum and difference frequency tones is governed by our second-order wave equation (3.22) which, for brevity's sake, we will write as

$$p_{2tt} - c^2\nabla^2 p_2 = \psi(x, y, z, t). \tag{4.30}$$

This equation has the general solution (3.78)

$$p_2 = \int_0^T \int_V G\psi(\xi, \eta, \zeta, \tau) dV d\tau + c^2 \int_0^T \int_{S_w} G\nabla p_2 \cdot \mathbf{n}\, dS_w\, d\tau. \tag{4.31}$$

At second-order neither these integrals nor their integrands are trivial. Several authors have investigated solutions to this equation when no boundary is present (i.e., no surface integral, see the following section). The function $\psi(x, y, z, t)$ is often recast into a different form in order to be more manageable [21]. Here we follow the clever substitution given by Dean [45]

$$p_2 = p_2' - \frac{1}{2}\rho_0|\mathbf{u}_1|^2 - \frac{p_1^2}{2\rho_0 c^2} - \frac{p_{1t}}{\rho_0 c^2}\int p_1 dt. \tag{4.32}$$

Substitution of this into our PDE (4.30) and using several vector identities (see Appendix A) gives

$$p_{2tt}' - c^2\nabla^2 p_2' = \frac{\gamma+1}{2\rho_0 c^2}(p_1^2)_{tt} + p_{1t}q(\mathbf{x}, t) + p_1 q_t(\mathbf{x}, t). \tag{4.33}$$

The solution of this equation is still given by (4.31) except with p_2 replaced by p_2' and the function ψ replaced with the right-hand side of (4.33). A modification remains in our surface integral term $\nabla p_2 \cdot \mathbf{n}$ as we are now required to find the equivalent second-order momentum equation of (2.64) for p_2'. We save this calculation for our actual evaluation of the surface integral.

Although we see that (4.33) has reduced the number of integrations necessary to obtain our solution, a problem still remains in evaluating the volume integral. The second and third terms are 'controlled' by the delta function in q; however, as Thierman [46] points out, the first term has no such restriction and we are thus required to integrate our whole first-order solution over the entire semi-infinite range $z \geq 0$ in order to obtain the second-order solution at a single point. Given both the impracticality of performing such an integration and the author's suspicion of the importance of volume nonlinearities when the acoustic pressures used are of such a low magnitude, further simplifications are required.

4.2.2 Bulk Nonlinearities vs. Doppler Effect

Our solution (4.31) is made up of two integrals representing two very different generating mechanisms. The first term deals with the waves produced by the

inherent nonlinearity of the medium while the second deals with that due to the moving boundary. Determining the dominant contribution from either of these phenomena (so called 'bulk nonlinearity' vs. 'Doppler effect') has been the subject of recent research activity.

Separately, there has been no shortage of investigations. In a completely unbounded medium the surface S_w is non-existent and attempts to solve (4.30) date back to the mid 1950s with analyses by Ingard [20] and Westervelt [21] on what is dubbed the 'scattering of sound by sound'.

The method used in these works is to assume a finite volume of interaction away from the observer so that the integration is taken over a bounded region. Although the idea would seem to relate to Case 2 in Figure 3.3, the solution given in that case is not quite correct (see Appendix C). Indeed, even though we assume the effects of interest stem from a fixed region in space, we are still required to include our observation point so as to isolate our field quantity of interest (typically $p(x, y, z, t)$. Compare the solution given by Case 1 to that by Case 2).

The justification for the finite region of integration comes from the assumption that the fundamental field produced is highly directional so that when multiple acoustic beams interact their overlapping regions in space (the source of sum and difference frequencies) must be a restricted volume. A detailed four part investigation is given in [47–50].

For solutions other than those given by plane waves and plane beams Dean [45] computed, by finding a particular solution to the differential equation, solutions based on concentric spherical and cylindrical waves. Exemplary mathematical skill was demonstrated by Sakov and Lyamshev [51, 52] in determining the interaction between non-concentric spherical waves as well as that by plane and spherical waves.

Investigation of the Doppler effect due to the motion of boundaries is encompassed by the surface integral in (4.31). Admittedly, the author was unable to find a single article using such an approach. That is not to say, however, that there is a lack of research into the area. Early work done by Beers and Belar [53] discusses the

distortion produced when a single transducer is excited at two frequencies. Their characterization is based on the standard Doppler formula

$$f_o = \frac{v_o - c}{v_s - c} f_s, \tag{4.34}$$

with c the speed of sound and f_o, v_o, f_s, v_s the frequency and velocity of the observer and the source respectively. In this case, the observer is stationary and the source is the high-frequency wave, ω_2, with a velocity v_s that is oscillatory with angular frequency ω_1.

Allison and Villchur [54] extend the work of Beers and Belar by performing listening tests with actual music and conclude that, for a single radiator, Doppler distortion is inaudible.[2]

Despite this, Butterweck [55] set out to establish the distortion factor for general excitations from a moving piston, assumed to produce plane waves. He points out that in order to provide solutions the analysis is "*confined to the moving boundary effect as the nonlinear bulk phenomena seems to become rather complicated*".

As we have done so far, van Wulfften Palthe [31] maintained the effects of both the medium and the boundary in deriving his solution. Unfortunately not only is the loudspeaker assumed to be a pulsating sphere but the obtained results are rather confusing due to the excessive notation. Attempts to ascertain the dominant distortion effect using the supplied formula proved ineffective.

Motivated by the work of the previous authors, Zóltogórski [56] sought to determine the effect of both forms of nonlinearity (what he calls nonlinear propagation, NP, and moving boundary condition, MBC) in a loudspeaker modelled by a plane wave. Using Burgers' equation he concludes that the distortions caused by the moving boundary are dominant in a low-frequency range adding that

"*special attention should be paid when applying the results to a real loudspeaker, since the real field differs considerably from the assumed field model. A decrease in real acoustic wave amplitude causes NP effects to vanish more quickly than they do*

[2]Recall that the experiments done by Klipsch used a multiway loudspeaker.

in the plane-wave case, although such a decrease does not affect the magnitude of MBC effects".

Characterization of these effects was first given in the important work done by Mujica et al. [18]. Using a basic time delay argument, they deduce that the characteristic magnitude of the Doppler effect is given by the parameter

$$\Delta\Phi_D = 2k_2 A, \tag{4.35}$$

where A is the vibration amplitude of the low-frequency wave (woofer). The excellent work by Zverev and Kalachev [57], confirmed by experiment, showed that the characteristic magnitude of the bulk nonlinear effect is given by

$$\Delta\Phi_{NL} = \frac{(\gamma - 1 + 2\cos\theta)P_1\omega_2 L}{2\rho_0 c^3}\left(\frac{\sin[\frac{k_1 L}{2}(1-\cos\theta)]}{\frac{k_1 L}{2}(1-\cos\theta)}\right) \tag{4.36}$$

where θ is the angle of interaction of the two waves (assumed to be two beams[3]), γ is the ratio of specific heats (as defined right after (2.2)), P_1 is the characteristic pressure amplitude of the low frequency wave and L is the observation distance.

It is then easily seen that the maximum modulation occurs when the waves are collimated ($\theta = 0$) so that our maximum bulk modulation index is given by

$$\Delta\Phi_{NL} = \frac{\gamma + 1}{2\rho_0 c^3} L\omega_2 P_1. \tag{4.37}$$

Using this result, Mujica et al. created the non-dimensional parameter

$$Y = \frac{\Delta\Phi_D}{\Delta\Phi_{NL}} \tag{4.38}$$

and performed various experiments in both air and water[4] to determine the dependence of acoustic waves on both types of nonlinearities.

For our waves in question, we have

[3] A beam is essentially a right prism with the shape of the radiator as its base. With this assumption, each wave is mathematically modeled by a plane wave where the pressure is zero outside of the prism. See the polar plots for large ka in Figure 4.5.

[4] The results in water use a slightly different version, see [18].

- $P_1 = \rho_0 c b_w$ (see for example (4.26) or (4.14))
- $A = \frac{b_w}{\omega_1}$ (see the paragraph at the beginning of Section 4.1)
- $\frac{\omega}{k} = c$

so that our non-dimensional parameter Y reduces to

$$Y = \mu \frac{\lambda_1}{L} \propto \frac{\lambda_1}{L}, \quad \mu = \frac{2\pi}{1+\gamma}. \tag{4.39}$$

For low frequency vibrations of the boundary, $20 \leq f_1 \leq 100$ Hz, the wavelength λ_1 satisfies, $3 \leq \lambda_1 \leq 17$ m, so that for listening distances $L \leq 1$ m our parameter $Y \geq 1$ and the Doppler boundary effect is dominant.

It should be noted that this is indeed a best case scenario for the bulk nonlinear effect due to the fact that $P_1 = \rho_0 c b_w$ is actually the pressure of a plane wave. This can be seen from (4.14) where the second term vanishes in the limit of $r_e \to \infty$ since the edge wave is delayed indefinitely (see [23]). In actuality, for our woofer $P_1 < \rho_0 c b_w$ thus increasing the value of the parameter Y (see the quote by Zóltogórski above). Also, the waves emitted by both the woofer and the point source are hardly collimated beams so that our angle θ in (4.36) is not actually 0 everywhere and our value of $\Delta\Phi_{NL}$ is further reduced thus increasing the parameter Y.

Actual experiments by Mujica et al. lead them to the following conclusions (using our notation)

"*Finally, it is interesting to compare the transition values of* Y *observed with air and water. In the water experiments,* Y *has been varied in the range* $0.11 < Y < 22$ *corresponding to* $30 < f_1 < 6000$ *Hz.* $Y \approx 1$ *corresponds to* $f_1 \approx 700$ *Hz whereas, as shown in Section 3, the Doppler shift is still dominant at much higher frequencies. This shows that the criterion* $Y \approx 1$ *for the transition should be taken with care. It is roughly correct when the waves are one dimensional as for the experiments in air that have been performed in a tube. The experiments in water have been performed in non-confined geometry and both the low and high frequency waves are slightly*

divergent. This decreases the strength of bulk nonlinearities and the Doppler shift thus remains dominant at lower Y i.e. higher frequencies."

Using these results, we therefore focus our attention on solutions of the surface integral, since, in our regime, our Y value is greater than unity and the contributions from the boundary are dominant.

4.2.3 Surface Integral

Our problem of interest then, using our substitution[5] from Section 4.2.1 is to solve

$$p_2' = c^2 \int_0^T \int_{S_w} G \nabla p_2' \cdot \mathbf{n}. \tag{4.40}$$

What is presently required is a formula for $\nabla p_2' \cdot \mathbf{n}$. Currently our momentum equation (2.64) is

$$\nabla p_2 = -\rho_0 \mathbf{u}_{2t} - \frac{p_1}{c^2}\mathbf{u}_{1t} - \rho_0 \left[(\mathbf{u}_1 \cdot \nabla)\mathbf{u}_1\right]. \tag{4.41}$$

Taking the gradient of our substitution (4.32) and applying the result to the above gives

$$\nabla p_2' = -\rho_0 \mathbf{u}_{2t} - \rho_0 \left[(\mathbf{u}_1 \cdot \nabla)\mathbf{u}_1\right] - \frac{p_1 \mathbf{u}_{1t}}{c^2} + \frac{\rho_0}{2}\nabla(|\mathbf{u}_1|^2) + \frac{\nabla(p_1^2)}{2\rho_0 c^2} + \frac{1}{\rho_0 c^2}\nabla(p_{1t}\int p_1 dt). \tag{4.42}$$

Although it may seem that we have made the boundary integral more difficult, if we use the following

- $(\mathbf{u}\cdot\nabla)\mathbf{u} \equiv \frac{1}{2}\nabla(|\mathbf{u}|^2) - \mathbf{u}\times(\nabla\times\mathbf{u})$,
- $\nabla \times \mathbf{u} = 0$ (irrotational),
- $\nabla p_1 = -\rho_0 u_{1t}$ (first-order momentum),
- $\left(\int p_1 dt \mathbf{u}_1\right)_{tt} \equiv p_{1t}\mathbf{u}_1 + 2p_1\mathbf{u}_{1t} + \mathbf{u}_{1tt}\int p_1 dt$,

[5]Based on the arguments from the last section, one may reason that the change of variable is unnecessary since we are focusing on the surface integral. As we will see, the substitution for p_2' also simplifies the boundary condition.

and the fact that the normal is constant in time, our term $p_2' \cdot \mathbf{n}$ simplifies to

$$\nabla p_2' \cdot \mathbf{n} = -\rho_0(\mathbf{u}_2 \cdot \mathbf{n})_t - \frac{1}{c^2}\left(\int p_1 dt(\mathbf{u}_1 \cdot \mathbf{n})\right)_{tt}. \tag{4.43}$$

We now focus our attention on each of the two terms in (4.43).

First term of $\nabla p_2' \cdot \mathbf{n}$

The expression $\rho_0(\mathbf{u}_2 \cdot \mathbf{n})_t$ can be transformed using our boundary condition (2.68) to give

$$\rho_0(w_{1z}B_1(t))_t. \tag{4.44}$$

Unfortunately we are required to compute the function w_1 in order to take its z derivative (that is, we can't simply substitute one of our boundary conditions despite being on the surface $z = 0$). To do this we need to find the particle velocity $\mathbf{u}_1$. We see from our first-order momentum equation (2.60) that $\mathbf{u}_1$ can be computed as

$$\mathbf{u}_1 = -\frac{1}{\rho_0}\int \nabla p_1 dt. \tag{4.45}$$

Performing this operation is not all that mysterious but very cumbersome. From our solution (4.28) we first take the time integral then using the standard ∇ operator in Cartesian coordinates and the chain rule and finally dividing by $-\rho_0$ we arrive at

$$\mathbf{u}_1 = \frac{b_w}{2\pi}e^{j\omega_1 t}\int_{S_w} g(k_1, r)\frac{\mathbf{r}}{r}dS_w + \frac{Q_0}{4\pi}e^{j\omega_2 t}\left(g(k_2, r_1)\frac{\mathbf{r_1}}{r_1} + g(k_2, r_2)\frac{\mathbf{r_2}}{r_2}\right), \tag{4.46}$$

where

$$\begin{aligned} g(k, r) &= e^{-jkr}\left(\frac{jk}{r} + \frac{1}{r^2}\right), \\ \mathbf{r} &= (x - \xi, y - \eta, z), \\ \mathbf{r_1} &= (x, y, z - d), \\ \mathbf{r_2} &= (x, y, z + d), \end{aligned} \tag{4.47}$$

and the non-bold versions are given by the magnitude of these or by (4.29).

Of interest here is the function w_1, the third component of $\mathbf{u}_1$, which we can write as

$$w_1(x,y,z,t) = \frac{b_w}{2\pi}e^{j\omega_1 t}\int_{S_w} g(k_1,r)\frac{z}{r}\,dS_w + \frac{Q_0}{4\pi}e^{j\omega_2 t}\left(g(k_2,r_1)\frac{z-d}{r_1} + g(k_2,r_2)\frac{z+d}{r_2}\right). \tag{4.48}$$

Before taking the z derivative, note that

$$\frac{\partial r}{\partial z} = \frac{z}{r},\ \frac{\partial r_1}{\partial z} = \frac{z-d}{r_1},\ \frac{\partial r_2}{\partial z} = \frac{z+d}{r_2}. \tag{4.49}$$

If we then substitute these into the three locations where they appear above and finally take the z derivative, we get (after several product and chain rule applications)

$$\begin{aligned}
w_{1z} &= Woofer + Tweeter, && (4.50)\\
Woof &= \frac{b_w}{2\pi}e^{j\omega_1 t}\int_{S_w}\left[\frac{\partial g(k_1,r)}{\partial r}\left(\frac{\partial r}{\partial z}\right)^2 + g(k_1,r)\frac{\partial^2 r}{\partial z^2}\right]dS_w, && (4.51)\\
Tweet &= \frac{Q_0}{4\pi}e^{j\omega_2 t}h(k_2,r_1,r_2), && (4.52)\\
h(k_2,r_1,r_2) &= \frac{\partial g(k_2,r_1)}{\partial r_1}\left(\frac{\partial r_1}{\partial z}\right)^2 + g(k_2,r_1)\frac{\partial^2 r_1}{\partial z^2}\\
&+ \frac{\partial g(k_2,r_2)}{\partial r_2}\left(\frac{\partial r_2}{\partial z}\right)^2 + g(k_2,r_2)\frac{\partial^2 r_2}{\partial z^2}. && (4.53)
\end{aligned}$$

Before computing (4.44) we take a moment to discuss our use of complex notation towards our main goal as was mentioned at the beginning of Section 4.1. At first-order, we simply needed to take the real part of our solution to obtain meaningful results; we seek a similar property at second-order. Due to the fact that $\Re(z_1 z_2) \neq \Re(z_1)\Re(z_2)$, before multiplying two first-order quantities we must take their real parts to get the proper results. To this end, consider our expression (4.44). Based on our formula for w_{1z} and that of B_1 we can separate our terms as follows

$$w_{1z}B_1(t) = (\nu_1 + \nu_2)(\upsilon_1) \tag{4.54}$$

where ν_1 and ν_2 are $Woofer$ and $Tweeter$ and υ_1 is $B_1(t)$ (we change the notation in this section in order to better manipulate the complex quantities more easily).

In order to properly compute this expression we are required to take the real parts of each function w_1 and B_1 before multiplying. This can be performed as follows

$$\begin{aligned}\Re(\nu_1+\nu_2)\Re(\upsilon_1) &= \frac{1}{2}(\nu_1+\bar{\nu}_1+\nu_2+\bar{\nu}_2)\frac{1}{2}(\upsilon_1+\bar{\upsilon}_1),\\ &= \frac{1}{4}(\nu_1\upsilon_1+\nu_1\bar{\upsilon}_1)+\frac{1}{2}\left(\frac{\nu_2\upsilon_1+\bar{\nu}_2\bar{\upsilon}_1}{2}\right)+\frac{1}{2}\left(\frac{\nu_2\bar{\upsilon}_1+\bar{\nu}_2\upsilon_1}{2}\right),\\ &= \frac{1}{4}(\nu_1\upsilon_1+\nu_1\bar{\upsilon}_1)+\frac{1}{2}\Re(\nu_2\upsilon_1)+\frac{1}{2}\Re(\nu_2\bar{\upsilon}_1). \qquad (4.55)\end{aligned}$$

The use of subscripts is to denote the frequency of each term. We see from the final expression above that our product $w_{1z}B_1(t)$ will contain two terms from our woofer only (the first harmonic and a dc component, see Thierman [46] for a discussion) and two terms from the combination of the woofer and tweeter frequencies; these are our intermodulation terms. Since our main interest is in describing the sum and difference frequencies we focus our attention on the last two terms.

To avoid any dependence on the actual time we further separate these as follows

$$\nu_2 = Z_2 e^{j\omega_2 t},\ \upsilon_1 = Z_1 e^{j\omega_1 t} \qquad (4.56)$$

where Z_1 and Z_2 are generally complex and depend only on spatial variables. Using these we obtain

$$\frac{1}{2}\Re(\nu_2\upsilon_1) = \frac{1}{2}\Re(Z_1Z_2e^{j\omega_+ t}), \qquad \frac{1}{2}\Re(\nu_2\bar{\upsilon}_1) = \frac{1}{2}\Re(\bar{Z}_1Z_2e^{j\omega_- t}), \qquad (4.57)$$

where $\omega_+ = \omega_2+\omega_1$ and $\omega_- = \omega_2-\omega_1$. This is helpful since, in computing our solution (4.40), we can separate out the time dependence and compute the magnitude of Z_1Z_2 to get a maximum pressure amplitude.[6]

Given the similarities between the forms in (4.57) we will focus on the first one, the sum frequency. One need only take the conjugate of our spatial function Z_1 to obtain the solution for the difference frequency (as well as to use ω_- obviously). We must also not forget to divide our final solution by 2.

[6]For example, say $Z_1Z_2 = a+jb$. Then $\Re((a+jb)e^{j\omega_+ t}) = a\cos(\omega_+ t) - b\sin(\omega_+ t)$ which has a magnitude (or pressure amplitude in our case) of $\sqrt{a^2+b^2}$. Therefore, we can compute the real and imaginary part of Z_1Z_2 separately and then use these to find the maximum amplitude.

Note in doing our expansion (4.55), our terms of interest are combinations of ν_2 and υ_1, that is, $Tweet$ and $B_1(t)$. We can write these as

$$\begin{aligned} \upsilon_1 &= \frac{b_w}{j\omega_1} e^{j\omega_1 t} = Z_1 e^{j\omega_1 t}, && (4.58) \\ \nu_2 &= \frac{Q_0}{4\pi} h(k_2, r_1, r_2) e^{j\omega_2 t} = Z_2 e^{j\omega_2 t}, && (4.59) \end{aligned}$$

which gives our final form of (4.44) for the sum frequency (remembering to take the real part and divide by 2 at the end)

$$\begin{aligned} \rho_0(w_{1z} B_1(t))_t &= \rho_0(Z_1 Z_2 e^{j\omega_+ t})_t, \\ &= \rho_0 j\omega_+ Z_1 Z_2 e^{j\omega_+ t}, \\ \text{sum}_{freq} &= \frac{\rho_0 Q_0 b_w}{4\pi} \left(\frac{\omega_+}{\omega_1}\right) h(k_2, r_1, r_2) e^{j\omega_+ t}, && (4.60) \end{aligned}$$

with h given by (4.53). Since $\bar{Z}_1 = \frac{j b_w}{\omega_1}$, the equivalent version for the difference frequency is given by

$$\text{diff}_{freq} = -\frac{\rho_0 Q_0 b_w}{4\pi} \left(\frac{\omega_-}{\omega_1}\right) h(k_2, r_1, r_2) e^{j\omega_- t}. \quad (4.61)$$

Second term of $\nabla p_2' \cdot \mathbf{n}$

The term $\frac{1}{c^2}\left(\int p_1 dt (\mathbf{u}_1 \cdot \mathbf{n})\right)_{tt}$ is easily obtained due to the first-order boundary condition (2.67). We can separate this product in a similar fashion as was done above with the pressure term containing both frequencies and the boundary term containing only ω_1. First we have

$$\begin{aligned} \mathbf{u}_1 \cdot \mathbf{n} &= -\dot{B}_1(t) = -b_w e^{j\omega_1 t}, && (4.62) \\ \int p_1 dt &= \frac{\rho_0 b_w}{2\pi} e^{j\omega_1 t} \int_{S_w} \frac{e^{-jk_1 r}}{r} dS_w + \frac{\rho_0 Q_0}{4\pi} \left(\frac{e^{-jk_2 r_1}}{r_1} + \frac{e^{-jk_2 r_2}}{r_2}\right) e^{j\omega_2 t} && (4.63) \end{aligned}$$

so that

$$\begin{aligned} \upsilon_1 &= -b_w e^{j\omega_1 t} = Z_1 e^{j\omega_1 t}, && (4.64) \\ \nu_2 &= \frac{\rho_0 Q_0}{4\pi} f(k_2, r_1, r_2) e^{j\omega_2 t} = Z_2 e^{j\omega_2 t}, && (4.65) \\ f(k_2, r_1, r_2) &= \left(\frac{e^{-jk_2 r_1}}{r_1} + \frac{e^{-jk_2 r_2}}{r_2}\right). && (4.66) \end{aligned}$$

Similarly to the section above we can then write (for the sum frequency, recalling what was stated above (4.60))

$$\begin{aligned}\frac{1}{c^2}\left(\int p_1 dt(\mathbf{u}_1\cdot\mathbf{n})\right)_{tt} &= \frac{1}{c^2}(Z_1Z_2e^{j\omega_+t})_{tt}\\ &= -(k_+)^2Z_1Z_2e^{j\omega_+t},\\ \text{sum}_{freq} &= \frac{\rho_0Q_0b_w}{4\pi}(k_+)^2f(k_2,r_1,r_2)e^{j\omega_+t},\end{aligned}\tag{4.67}$$

with f given by (4.66). In this case $\bar{Z}_1 = Z_1$ so the difference frequency has the form

$$\text{diff}_{freq} = \frac{\rho_0Q_0b_w}{4\pi}(k_-)^2f(k_2,r_1,r_2)e^{j\omega_-t}.\tag{4.68}$$

4.2.4 Surface Integral - Final Expression

We can now substitute our expressions (4.60) and (4.67) into (4.43) and then into (4.40) to obtain (for the sum frequency)

$$p_2' = Ac^2\int_{S_w}\int_0^T \frac{\delta(t-\tau-\frac{r}{c})}{2\pi rc^2}\left(\left(\frac{\omega_+}{\omega_1}\right)h(k_2,r_0,r_0)+(k_+)^2f(k_2,r_0,r_0)\right)e^{j\omega_+\tau}\,d\tau\,dS_w\tag{4.69}$$

$$A = -\left(\frac{\rho_0Q_0b_w}{4\pi}\right)\tag{4.70}$$

Here we have used our Green's function (4.9) since we are on the surface S_w. Also, note that on this surface our functions r_1 and r_2 given by (4.29):

$$r_1 = \sqrt{x^2+y^2+(z-d)^2}\tag{4.71}$$

$$r_2 = \sqrt{x^2+y^2+(z+d)^2},\tag{4.72}$$

are transformed into integration distances as $(x,y,z)\rightarrow(\xi,\eta,0)$ over S_w and we get

$$r_1 = r_2 = r_0 = \sqrt{\xi^2+\eta^2+d^2}\tag{4.73}$$

which represents the distance from the tweeter to the integration point on S_w. It is this distance which is crucial in measuring the strength of the intermodulation. For now we have fixed the tweeter on the axis. Shortly we will modify this distance r_0 to account for placing the tweeter off the axis.

With our current distance r_0 our functions f and h simplify to

$$f(k_2, r_0) = \frac{2e^{-jk_2 r_0}}{r_0}, \tag{4.74}$$

$$h(k_2, r_0) = 2\left(\frac{\partial g(k_2, r_0)}{\partial r_0}\left(\frac{\partial r_0}{\partial z}\right)^2 + g(k_2, r_0)\frac{\partial^2 r_0}{\partial z^2}\right). \tag{4.75}$$

Care must be taken in reading the above. The notation is a bit abusive since clearly $r_{0z} = 0$ from (4.73). We must be sure to find r_{1z} and r_{1zz} first before letting $z \to 0$ (likewise for r_2). This is done in the next section.

Evaluating the time integration we can write a final integral expression to be solved for the spatial factor of the sum frequency of p'_2

$$p'_{2+} = -\frac{\rho_0 Q_0 b_w}{4\pi}\left(\frac{e^{j\omega_+ t}}{2\pi}\right)\int_{S_w}\left((k_+)^2 f(k_2, r_0) + \left(\frac{\omega_+}{\omega_1}\right)h(k_2, r_0)\right)\frac{e^{-jk_+ r}}{r}\, dS_w. \tag{4.76}$$

Based on (4.61) and (4.68) we can write a similar integral expression for the difference frequency

$$p'_{2-} = -\frac{\rho_0 Q_0 b_w}{4\pi}\left(\frac{e^{j\omega_- t}}{2\pi}\right)\int_{S_w}\left((k_-)^2 f(k_2, r_0) - \left(\frac{\omega_-}{\omega_1}\right)h(k_2, r_0)\right)\frac{e^{-jk_- r}}{r}\, dS_w. \tag{4.77}$$

4.2.5 Surface Integral - Solutions

Given the impossibility of solving (4.10) in general we note that the expressions given by (4.76) and (4.77) are similar in form with an added spatial factor and are thus also intractable in general. We are thus required to solve this integral numerically, varying parameters to get an idea of the inherent dependencies. We can however obtain a special-case analytic solution if the tweeter and woofer are coaxial and we are in the farfield *and* on-axis. It is hoped that with better mathematical craftiness one can manipulate the integrals to obtain analytic solutions similar to those at first-order (4.14), (4.27).

To obtain the analytic solution described we first simplify our function h. As was mentioned above, the notation $\frac{\partial r_0}{\partial z}$ is shorthand for $\frac{\partial r_1}{\partial z}|_{z\to 0}$ which is not quite

equal to $\frac{\partial r_2}{\partial z}|_{z\to 0}$ since, from (4.49)

$$\frac{\partial r_1}{\partial z}|_{z\to 0} = \frac{-d}{r_0}, \tag{4.78}$$

$$\frac{\partial r_2}{\partial z}|_{z\to 0} = \frac{d}{r_0}, \tag{4.79}$$

however note that our function h has these derivatives squared so they will be equal, hence justifying the first part of (4.75).

Likewise, the second derivatives are given by

$$\frac{\partial^2 r_1}{\partial z^2} = \frac{r_1^2 - (z-d)^2}{r_1^3}, \tag{4.80}$$

$$\frac{\partial^2 r_2}{\partial z^2} = \frac{r_2^2 - (z+d)^2}{r_2^3}, \tag{4.81}$$

which, as $z \to 0$ gives the same function

$$\frac{\partial^2 r_0}{\partial z^2} = \frac{r_0^2 - d^2}{r_0^3}, \tag{4.82}$$

so that using the following

- $g(k_2, r_0) = e^{-jk_2 r_0}\left(\frac{jk_2}{r_0} + \frac{1}{r_0^2}\right)$,
- $\frac{\partial g(k_2,r_0)}{\partial r_0} = e^{-jk_2 r_0}\left(\frac{k_2^2 r_0^2 - 2jk_2 r_0 - 2}{r_0^3}\right)$,
- $\left(\frac{\partial r_0}{\partial z}\right)^2 = \frac{d^2}{r_0^2}$,
- $\frac{\partial^2 r_0}{\partial z^2} = \frac{r_0^2 - d^2}{r_0^3}$,

our function h becomes

$$h(k_2, r_0) = \frac{2e^{-jk_2 r_0}}{r_0^5}\left[r_0^2 + (dk_2 r_0)^2 - 3d^2 + j(k_2 r_0^3 - 3k_2 r_0 d^2)\right]. \tag{4.83}$$

Substituting this, and our expression for f (4.74), into (4.76) leaves us to evaluate

$$p'_{2+} = 2A(t)\int_{S_w} (\text{Coeff})\frac{e^{-j(k_2 r_0 + k_+ r)}}{r\, r_0^5}\, dS_w, \tag{4.84}$$

$$\text{Coeff} \equiv \left[(k_+)^2 r_0^4 + \left(\frac{\omega_+}{\omega_1}\right)\left(r_0^2 + (dk_2 r_0)^2 - 3d^2 + j(k_2 r_0^3 - 3k_2 r_0 d^2)\right)\right], \tag{4.85}$$

$$A(t) \equiv -\frac{\rho_0 Q_0 b_w}{4\pi}\left(\frac{e^{j\omega_+ t}}{2\pi}\right). \tag{4.86}$$

The most general distances r_0 and r are given by[7]

$$r = \sqrt{(x-\xi)^2 + (y-\eta)^2 + z^2}, \tag{4.87}$$

$$r_0 = \sqrt{(\xi - h)^2 + \eta^2 + d^2}. \tag{4.88}$$

Since we are integrating over a circular disk we can make the substitution

$$\begin{aligned} \xi &= \sigma \cos\theta \\ \eta &= \sigma \sin\theta \end{aligned} \tag{4.89}$$

so that our integration distances become

$$r = \sqrt{x^2 + y^2 + z^2 + \sigma^2 - 2x\sigma\cos\theta - 2y\sigma\sin\theta}, \tag{4.90}$$

$$r_0 = \sqrt{\sigma^2 + d^2 - 2h\sigma\cos\theta + h^2}. \tag{4.91}$$

The general solution is then obtained by substituting these into (4.84), changing dS_w to $\sigma\, d\theta\, d\sigma$ and integrating over $0 \le \theta \le 2\pi$, $0 \le \sigma \le a$.

Coaxial, Farfield & On-axis

We can obtain an analytic solution if we assume the tweeter and woofer are coaxial and that the observer is sufficiently far away on this axis. In this case we have the situation as given in Figure 4.6. With the coaxial, on-axis assumption $x = y = h = 0$, we have the following simplifications:

$$r^2 = z^2 + \sigma^2, \tag{4.92}$$

$$r_0^2 = d^2 + \sigma^2, \tag{4.93}$$

$$\Rightarrow r^2 = r_0^2 + z^2 - d^2, \tag{4.94}$$

$$dS_w = 2\pi\sigma d\sigma. \tag{4.95}$$

[7]Here we have included the possibility of the tweeter being off axis by an amount h (not to be confused with our function $h(k, r)$. The use of h is to be consistent with the MATLAB code). Without loss of generality we assume the tweeter would move up the x-axis. Note that this doesn't change any of our derivations since all derivatives were taken with respect to z.

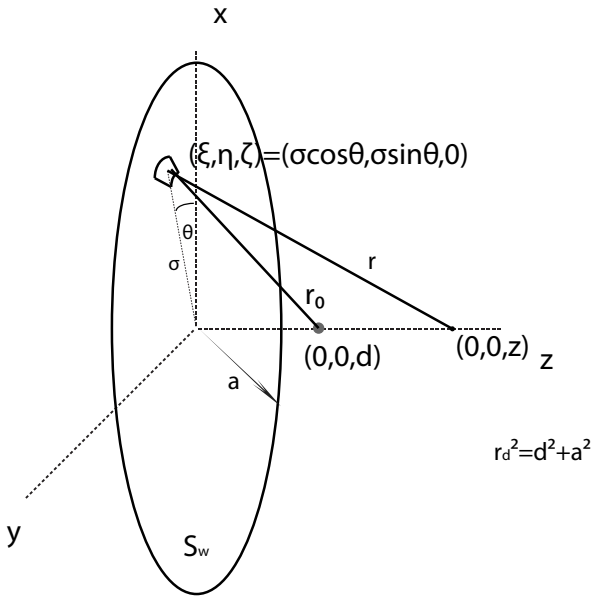

Figure 4.6: On-axis coordinate system for second-order surface integral.

The second of these implies $r_0 dr_0 = \sigma d\sigma$ so that $dS_w = 2\pi r_0 dr_0$. Our integrand no longer depends on θ and our range for r_0 is $d \leq r_0 \leq r_d$ (see Figure 4.6) so that we can write our integral (4.84) in compact form

$$p'_{2+} = -2\left(\frac{\rho_0 Q_0 b_w}{4\pi}\right) e^{j\omega_+ t} \int_d^{r_d} c_p \frac{e^{-jk_2 r_0}}{r_0^{4-p}} \frac{e^{-jk_+\sqrt{r_0^2+z^2-d^2}}}{\sqrt{r_0^2+z^2-d^2}} dr_0,\ p = 0,1,2,3,4. \quad (4.96)$$

The denominator r_0^{4-p} is written as such so that the coefficients c_p correspond to those terms in (4.85) attached to powers of r_0^p. For example $c_0 = -3d^2(\omega_+/\omega_1)$, $c_1 = -j3k_2 d^2(\omega_+/\omega_1)$, $c_4 = (k_+)^2$ and so on.

This integral is still not solvable (to the best of the author's knowledge) so we impose the farfield assumption $z \gg a$. Since we can write

$$\sqrt{r_0^2+z^2-d^2} = z\sqrt{1+\frac{r_0^2-d^2}{z^2}} \quad (4.97)$$

and since $r_0^2 - d^2 = \sigma^2$, our farfield assumption implies that (Taylor expansion)

$$z\sqrt{1+\frac{\sigma^2}{z^2}} \approx z. \quad (4.98)$$

Note that this is similar to the farfield approximation at first-order (4.20) where

$\beta = 0$. This leaves us to evaluate

$$p'_{2+} = -2\left(\frac{\rho_0 Q_0 b_w}{4\pi}\right) e^{j\omega_+ t}\left(\frac{e^{-jk_+ z}}{z}\right)\int_d^{r_d} c_p \frac{e^{-jk_2 r_0}}{r_0^{4-p}} dr_0, \;\; p = 0, 1, 2, 3, 4. \tag{4.99}$$

Again, somewhat remarkably, due to the specific form of the coefficients c_p, all of the exponential integral terms, $E_i(jk_2 r_0)$, that arise from this integration end up cancelling and the integral itself yields

$$\left(\frac{\omega_+}{\omega_1}\right)\left[\left(\frac{d^2 - r_d^2}{r_d^3}\right) e^{-jk_2 r_d} + j\left(\frac{d^2 k_2}{r_d^2} e^{-jk_2 r_d} - k_2 e^{-jk_2 d}\right)\right] + j\frac{(k_+)^2}{k_2}[e^{-jk_2 r_d} - e^{-jk_2 d}]. \tag{4.100}$$

After various attempts, the author could not find a more interesting way to rewrite this expression. The term $d^2 - r_d^2$ is indeed equal to $-a^2$, the radius of the woofer, but that does little to help in creating an enlightening arrangement. Instead it is left the way it is, separated by the scaling factors (ω_+/ω_1) and k_+^2 which correspond to the contributions from the two functions $h(k_2, r_0)$ and $f(k_2, r_0)$, they themselves are a result of the two terms of the boundary condition (4.43). We can compare this solution to the numerical versions to follow to get an idea of the range of validity.

Note that as the radius of the woofer shrinks to 0 the distance from the tweeter to the edge of the woofer, r_d, goes to d so that our expression above vanishes, which is expected. One may be tempted to determine the limiting behaviour as $r_d \to \infty$; however this would invalidate the assumption made in obtaining this solution, namely $z \gg a$.

We can, however, examine the behaviour as $d \to 0$. In this case, $r_d \to a$ and the integral becomes

$$-\left(\frac{\omega_+}{\omega_1}\right)\left[\frac{e^{-jk_2 a}}{a} + jk_2\right] + j\frac{(k_+)^2}{k_2}[e^{-jk_2 a} - 1]. \tag{4.101}$$

Rewriting the first bracket as

$$-\left(\frac{\omega_+}{\omega_1}\right)\left[k_2\frac{\cos(k_2 a)}{k_2 a} - jk_2\frac{\sin(k_2 a)}{k_2 a} + jk_2\right] + j\frac{(k_+)^2}{k_2}[e^{-jk_2 a} - 1] \tag{4.102}$$

we see that if $k_2 a \ll 1$ this expression reduces nicely to

$$-\left(\frac{\omega_+}{\omega_1}\right)\left[k_2\frac{\cos(k_2 a)}{k_2 a}\right]. \tag{4.103}$$

In this case, since k_2 represents the wave number for the high-frequency wave, this limiting situation would only be realistic if the woofer radius were rather small or if the frequency of the tweeter was sufficiently low enough.

The purpose of the previous derivation was to demonstrate that it is indeed possible to obtain an analytic solution given the proper geometry. Perhaps with more mathematical cunning an analytic solution could be obtained in the general farfield as was done at first-order.

4.3 Numerical Investigation of Surface Integral

In this section, more interesting results are obtained via a numerical integration of the general surface integral (4.84)-(4.91). The only assumption that is made in this section is that our observation point is on-axis. The reasons for this are twofold. The first is that, as Olson [58] points out, experimental investigations are in general conducted on the axis of the cone. Secondly, we have been working out solutions to the quantity p_2'. To obtain the final pressure p_2 we must add the correction terms for the sum (or difference) frequency given in (4.32) which is not a trivial matter. For on-axis observation points these terms at least have analytic representations. Computation of these is deferred to Appendix D. The results presented in this section contain the contribution from all terms, that is, p_2' and those terms in (4.32) which affect the sum (or difference) frequency. The MATLAB code used is given in Appendix E.

4.3.1 Experimental Setup and Results

Although motivated by the work of Klipsch [1], his experiments are difficult to compare to the theory due to a lack of knowledge of all the parameters in the setup. To better serve the current undertaking, a baffled coaxial speaker was constructed in a lab environment as shown in Figure (4.7).

The speakers themselves were mounted separately onto their own small sub-baffle and then onto the main baffle so as to be able to switch between a variety of transducer types. The tweeter of a given speaker setup was driven on its own while the woofer was acoustically driven by another large woofer located at the back labelled 'woofer driver' in the diagram. This was done to avoid any electromagnetic coupling between the coils of the tweeter and woofer since, at least for the Uni-Q driver, they are in close proximity and may interfere with one another when a low and high frequency signal is sent through their respective voice-coils.

Two speaker systems were tested, a 20 cm KEF Uni-Q C35 and a superelliptical

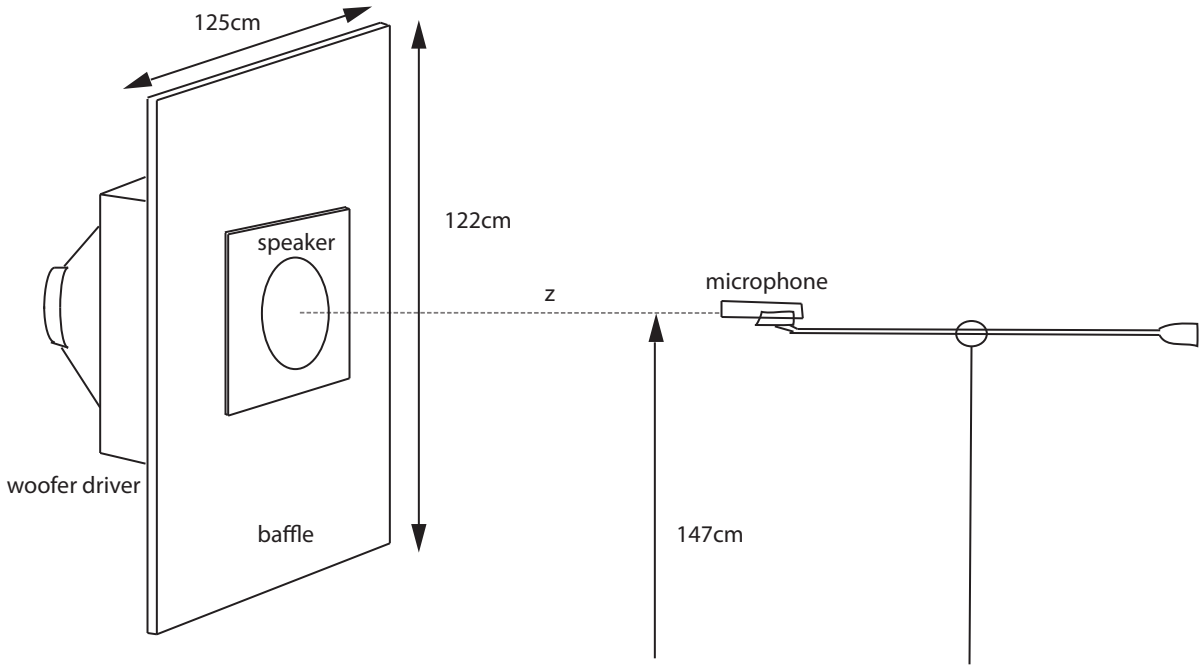

Figure 4.7: Lab setup used for experimental results. Note the speaker is mounted on its own small sub-baffle and then onto the main baffle so that multiple systems can more easily be interchanged. The "speaker" is merely a placeholder for either the pre-made coaxial Uni-Q or our improvised coaxial B139 as seen in Figure 4.8.

KEF B139 woofer with a separately mounted 2.5 cm KEF high-frequency tweeter[8]. The Uni-Q is manufactured as a coaxial loudspeaker and has a standard conical shape with a 1.9 cm tweeter at its centre. The B139, although unfortunately not completely circular in shape, is a perfectly flat woofer. The setup is made coaxial by the mounted tweeter which is held in place by a thin metal beam secured into the smaller rectangular wooden plate, see Figure 4.8.

Unfortunately, due to unforeseen circumstances, not many tests could be conducted. The short list of experimental results is given in Table 4.1. For comparative purposes a table of theoretical results, corresponding to Figures 4.9-4.12, is provided in Table 4.2.

A few comments are in order. First, as Vanderkooy [59] suggests, the closer the microphone to the speakers the more accurate the results should be. This is

[8] A Google image search for 'KEF B139' and 'uni-q speaker' will give respectable image results.

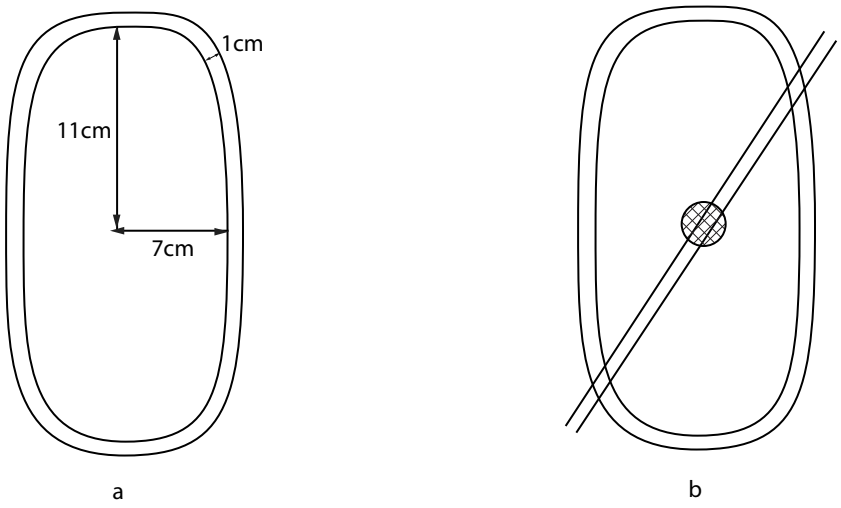

Figure 4.8: Schematic diagram of makeshift coaxial speaker. a) KEF B139 on its own. b) tweeter attached in the front.

Speaker type	f_1 (Hz)	f_2 (kHz)	z-distance (m)	woofer amplitude B (mm)	$P_{\omega_-}/P_{\omega_2}$ (dB)	$P_{\omega_+}/P_{\omega_2}$ (dB)
B139	50	3	1	1	-14.76	-10.41
B139	50	3	0.5	1	-20.03	-17.92
B139	50	3	0.25	1	-20.17	-18.76
B139	50	3	0.25	2	-15.36	-13.95
Uni-Q	30	3	1	1	-28.6	-30.74

Table 4.1: Experimental results.

due to the fact that the boundary effects dominate those due to room reflections and any edge diffraction waves. Therefore those taken at 0.25 m should be most in correspondence with the theory.

The doubling of the amplitude on the B139 from 1 mm to 2 mm resulted in an approximate increase of 5 dB. Given that the amplitude is a scaling factor in our solution (4.84), a doubling of amplitude should lead to an increase of 6 dB. As we will see below, the results are rather sensitive to the smallest changes in the amplitude and so it is likely that our ballpark estimation of 1 mm to 2 mm is a bit off.

Speaker type	f_1 (Hz)	f_2 (kHz)	z-distance (m)	woofer amplitude B (mm)	$P_{\omega_-}/P_{\omega_2}$ (dB)	$P_{\omega_+}/P_{\omega_2}$ (dB)
B139	50	3	1	1	-18.4	-17.6
B139	50	3	0.5	1	-18.9	-18.4
B139	50	3	0.25	1	-20.1	-19.7
B139	50	3	0.25	2	-14.1	-13.7
Uni-Q	30	3	1	1	-29 $\leq \cdot \leq$ -26.5	

Table 4.2: Theoretical results. The range of values for the Uni-Q are from Figure 4.12. A range was used since it was difficult to determine the exact value of d. See the first paragraph of Section 4.3.2.

Finally, the Uni-Q driver has a slight anomaly in that its difference-frequency distortion is actually greater than its sum-frequency distortion. The author is uncertain as to the exact reason for this although given that our lab setup was not perfectly anechoic it could potentially be due to some geometrically caused phase cancellation that only occurs for the sum frequency and not for the difference frequency. More tests should be done on the Uni-Q to better compare the measurements and to determine if this anomaly is present at closer microphone distances. We can state however that the relative difference between the flat B139 and the conical Uni-Q is between 14 and 20 dB. Indeed, the modulation distortion was more audible in the former.

4.3.2 Comparisons Between Theory and Experiment

In order to use our solution (4.84) to determine the theoretical results given in Table 4.2 we must establish the parameters for each model. The Uni-Q has a very small distance d between the tweeter and the woofer. Values in the range $0 \leq d \leq 0.005$ m are appropriate (the woofer is in fact an annular region with the tweeter at its centre). The radius a of the woofer is approximately 10 cm. The B139 setup has a semi-minor axis length of 7 cm and a semi-major axis of 11 cm(see Figure 4.8). For the simulations we approximated the B139 as a 10 cm radius circular piston.

Although this is obviously not completely accurate we will later investigate the dependence of the solution on the radius a. Finally, the tweeter in the B139 setup has a d value of approximately 2.4 cm.

Since we are only interested in relative measurements, we note that all values, unless otherwise stated, are scaled to the first-order, high-frequency acoustic output. Mathematically that means the common factor $\frac{\rho_0 Q_0}{4\pi}$, present at both orders, cancels (see 4.84) and (4.28)). One should therefore note that these quantities do not show up in the code.

B139

Our first comparison is for the B139 setup. Since our measurement of the amplitude of vibration as given in Table 4.1 is subject to human error (it was visually computed while the speaker was moving) our first group of theoretical plots Figures 4.9-4.11 show the relative magnitudes of the intermodulation frequencies as we vary the amplitude of vibration by 0.1 mm increments.

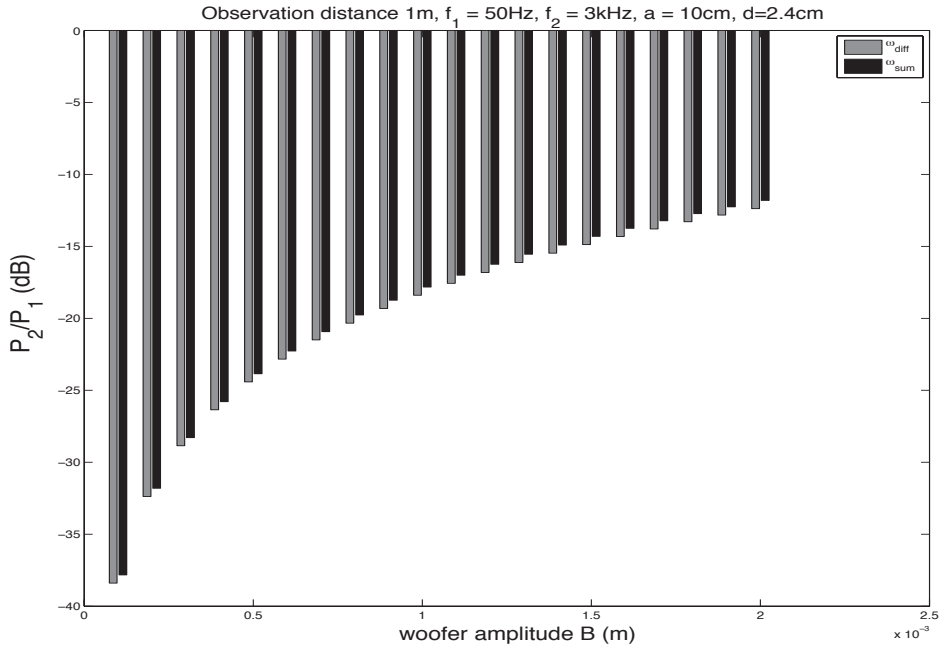

Figure 4.9: Theoretical plot of p_2/p_1 (dB) vs. woofer amplitude B (m). The observation distance is $z = 1$ m. The values at $B = 1$ mm (-18.4 and -17.6) are used in Table 4.2.

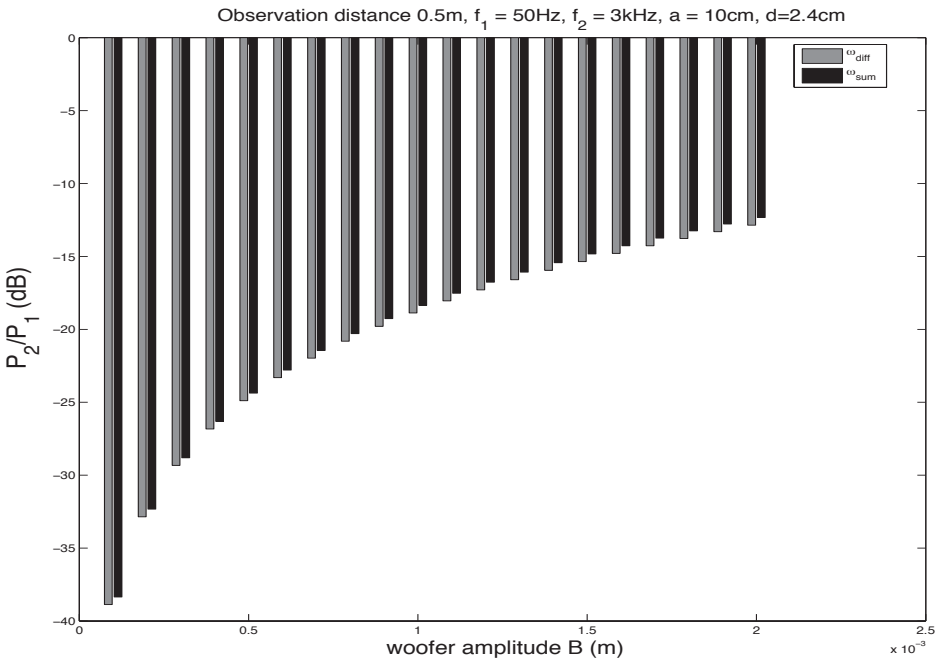

Figure 4.10: Theoretical plot of p_2/p_1 (dB) vs. woofer amplitude B (m). The observation distance is $z = 0.5$ m. The values at $B = 1$ mm (-18.9 and -18.4) are used in Table 4.2.

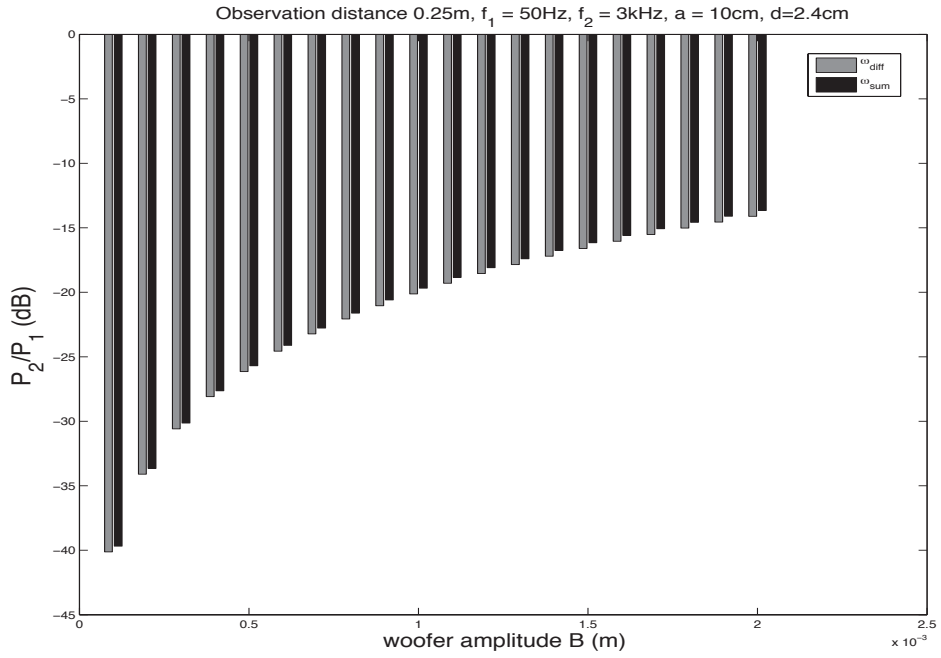

Figure 4.11: Theoretical plot of p_2/p_1 (dB) vs. woofer amplitude B (m). The observation distance is $z = 0.25$ m. The values at $B = 1$ mm (-20.1 and -19.7) and $B = 2$ mm (-14.1 and -13.7) are used in Table 4.2.

Observe how the theoretical values in Figures 4.9-4.11 approach those given by the experiments in Table 4.1 as we move our observation point closer to the baffle confirming what was suggested by Vanderkooy. Increasing the woofer amplitude produces a logarithmic increase in the relative magnitudes of the sum and difference frequencies, which is expected from the definition of sound pressure level (SPL = $20\log_{10}(p_2/p_1)$). The values are in rather good agreement in the case of the flat B139.

Uni-Q

Theoretical results for the Uni-Q are not as easily compared due to the geometrical differences from the mathematical model. Nonetheless we attempt various configurations for comparative purposes. The numerical investigation is performed with continuous values of the parameter $0 < d \leq 0.005$ m as previously mentioned. Also, since the woofer is actually an annular region with inner radius 1 cm, we perform an annular integration where our integration radius σ satisfies $1 \leq \sigma \leq a$ cm. The results of this are shown in Figure 4.12. Excluding the previously mentioned anomaly between the sum and difference frequencies in Table 4.1, it is a bit surprising that the results at 1 m seem to match well with the experiment given the disparity between theory and reality for the B139 at 1 m (first row of Table 4.1 vs. first row of Table 4.2.

Again, it is difficult to make a direct comparison because of the fact that the Uni-Q is in actuality conical in shape and so the normal at each point on the woofer is not simply $\mathbf{n} = (0, 0, -1)$.

Regardless, the results, especially those of the B139, are in rather good agreement so that we may analyze a variety of plots to examine how the intermodulation factors change as we vary the parameters of the model.

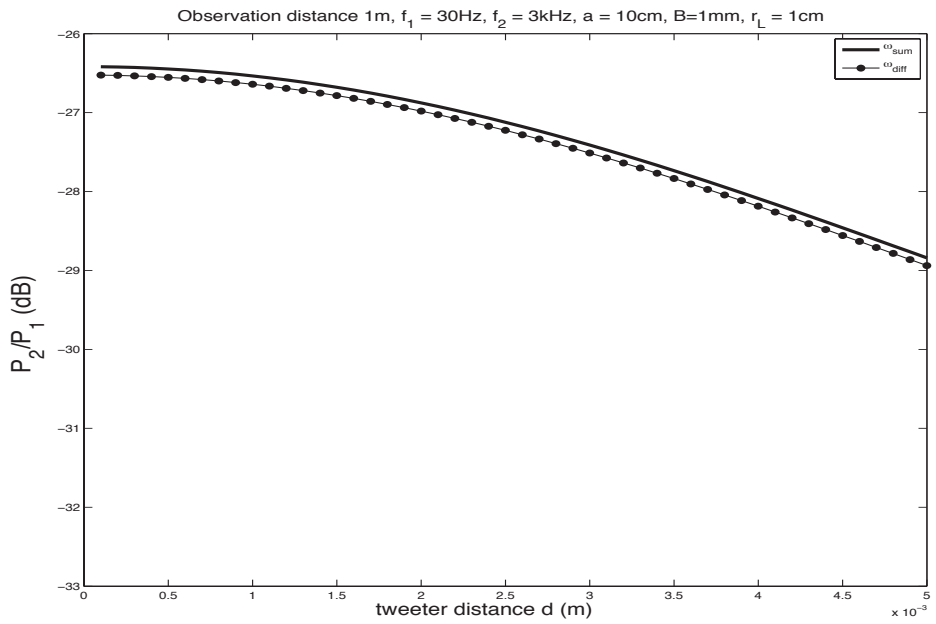

Figure 4.12: Theoretical value of p_2/p_1 (dB) vs tweeter distance from baffle d (m) for Uni-Q. The tweeter distance was varied due to the nature of construction of the Uni-Q speaker. With its tweeter at the centre of the conically shaped woofer, obtaining an exact value for d is difficult.

4.3.3 Theoretical Predictions

In this section a variety simulations are performed to investigate the dependence of the intermodulation factor on various parameter changes. The results to come are strictly theoretical since we were unable to perform the corresponding experiments. Where possible the author attempts to justify some of the observed behaviour. However, many of the plots are not all that intuitive and leave several questions unanswered.

Radius

The first group of plots Figures 4.13-4.17 show the relationship between our solution (4.84) and the radius of the woofer. Note the strong dependence for small values of the parameter a. This is a reflection of the fact that the integration distance r_0 is

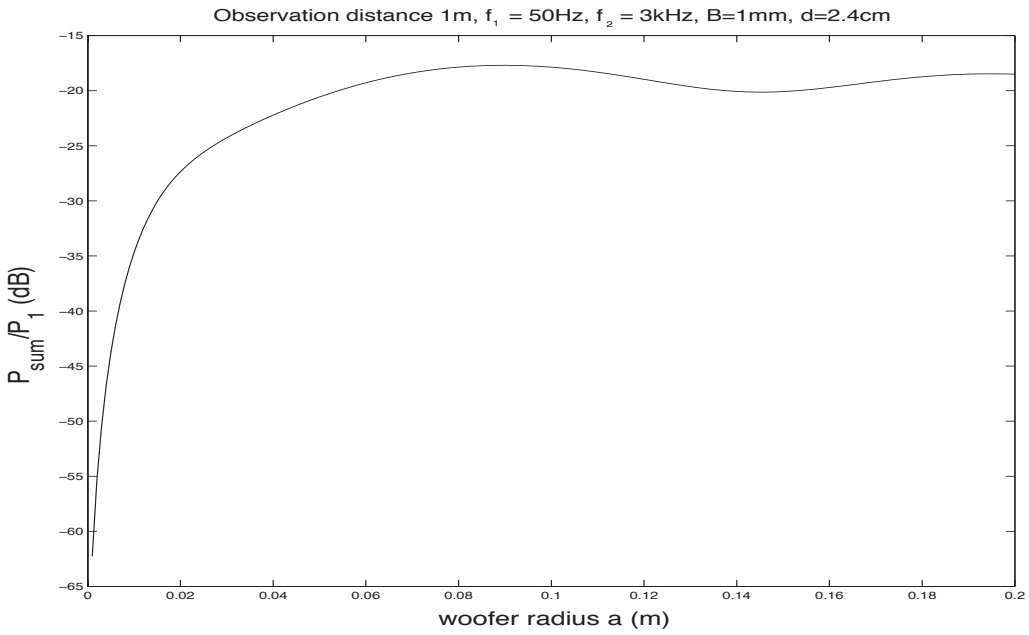

Figure 4.13: Theoretical dependence of relative intermodulation factor p_+/p_1 on radius of woofer for frequency $f_2 = 3$ kHz. Note how this is only for the sum frequency. The difference frequency exhibits similar behaviour.

initially very small and (4.84) has essentially a r_0^{-3} dependence[9]. As a gets bigger (around 0.07 m) and the integration distance r_0 is increased past this point, the added contributions from the integral have a significantly smaller effect by nature of (4.85). The oscillatory behaviour in Figure 4.13 is clearly due to the exponential in (4.84) which is dominantly oscillatory with wavenumber k_2 (giving a wavelength of approximately 11 cm for $f_2 = 3$ kHz). Note that in (4.84) r does not vary much over the integration when our observation distance $z = 1$ m (r being the distance form the observation point to the integration point on the woofer). Indeed the oscillations are dominated by $e^{jk_2 r_0}$. A similar plot, Figure 4.14, with $f_2 = 12$ kHz shows how the wavelength of the oscillations corresponds to the wavelength of f_2 (approximately 3 cm) .

[9]When multiplied by the values in (4.85), the integrand of (4.84) has no more than a r_0^{-3} dependence.

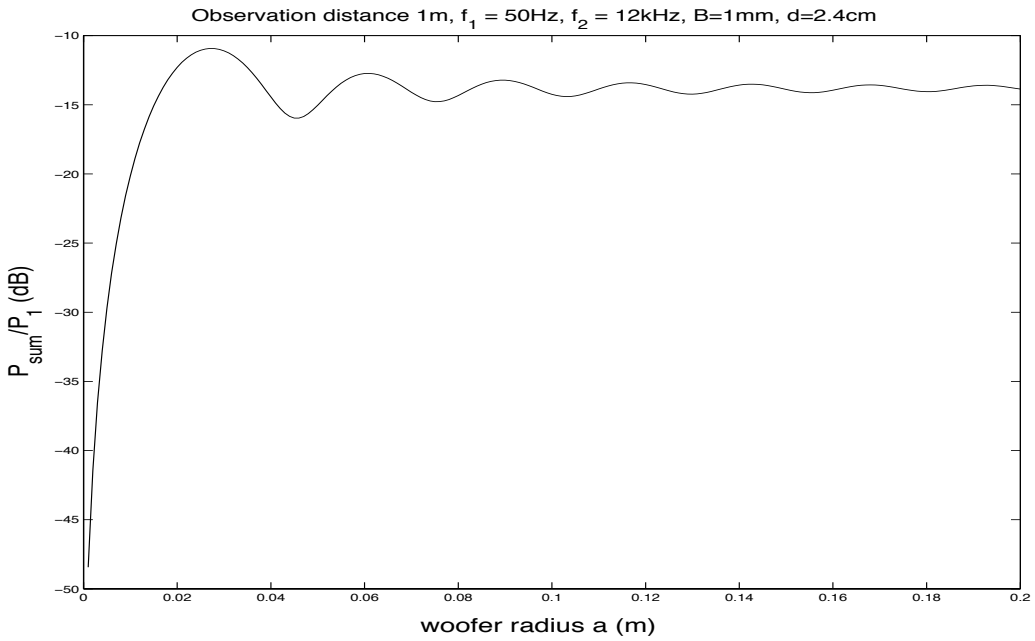

Figure 4.14: Theoretical dependence of relative intermodulation factor p_+/p_1 on radius of woofer for frequency $f_2 = 12$ kHz. This is similar to Figure 4.13 except note the oscillations correspond to the high-frequency f_2.

Some interesting behaviour occurs in Figures 4.15-4.17 which show the dependence of p_{2+}/p_1 on the radius as a is increased up to 2 m (as opposed to the 20 cm of Figures 4.13 and 4.14) for three fixed positions of d (arbitrarily chosen as multiples of the original distance $d = 2.4$ cm).

The author is uncertain as to why there seems to be a generally decreasing trend in Figure 4.15, especially when one considers the two plots Figure 4.16 and Figure 4.17 where we have moved the location of the tweeter to 4.8 cm and 7.2 cm respectively. The overall magnitude decrease in Figures 4.16 and 4.17 compared to Figure 4.15 is likely due to some combination of the larger r_0 values when d is increased as well as the increased p_1 as the tweeter approaches the observation point. The trends for large a however, are not obvious at all. An asymptotic analysis of (4.84) as $a \to \infty$ would perhaps prove fruitful.

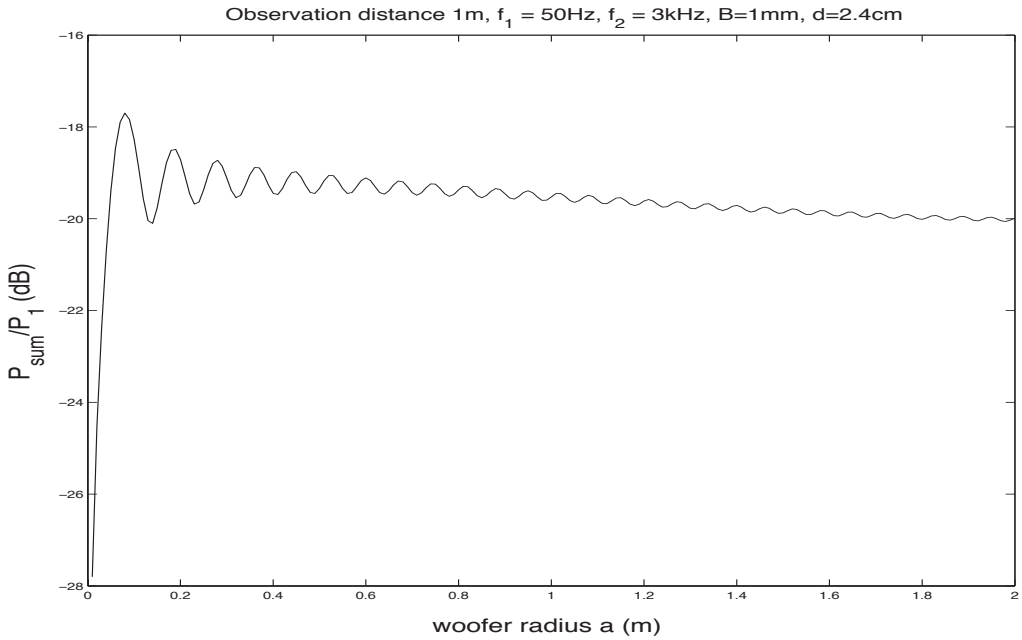

Figure 4.15: Theoretical dependence of intermodulation factor p_+/p_1 on radius of woofer a for $d = 2.4$ cm, $f_2 = 3$ kHz. This is an extended version of Figure 4.13.

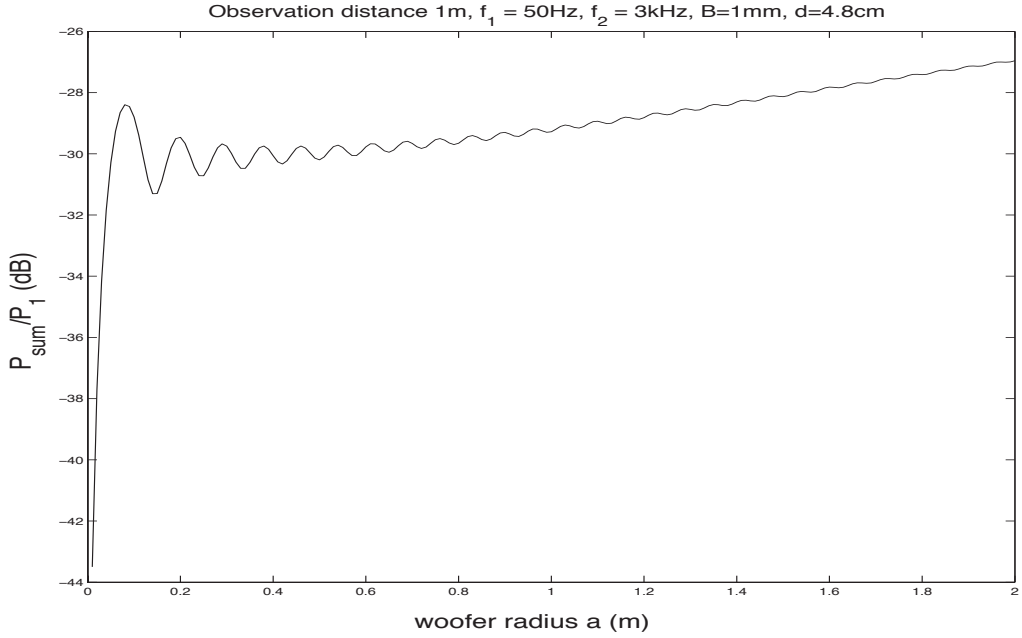

Figure 4.16: Theoretical dependence of intermodulation factor p_+/p_1 on radius of woofer a for $d = 4.8$ cm, $f_2 = 3$ kHz. This is similar to Figure 4.15 with $d = 4.8$ cm.

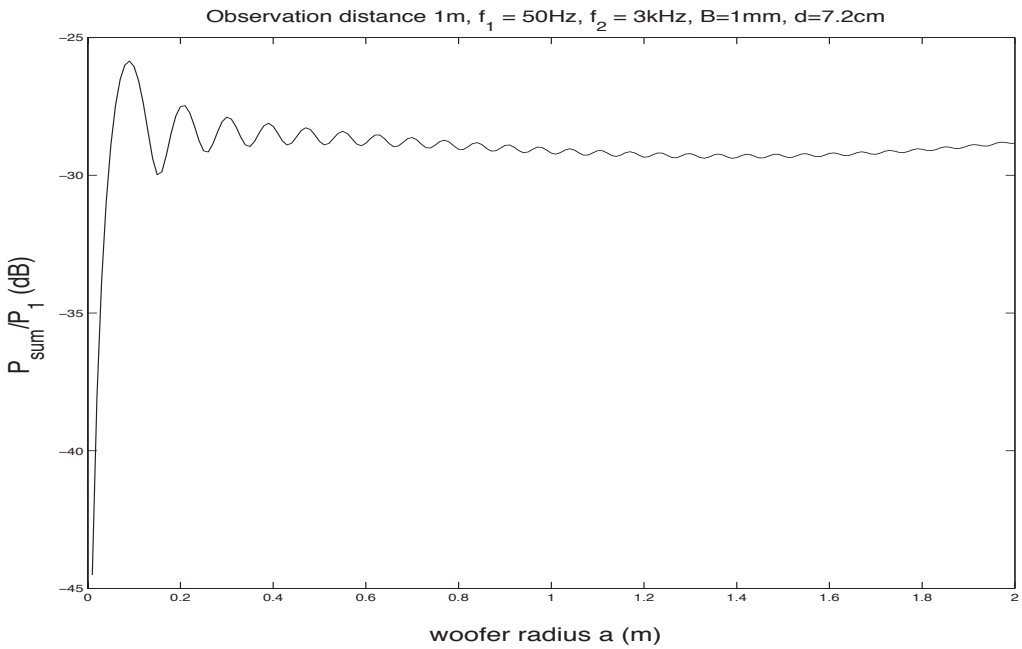

Figure 4.17: Theoretical dependence of intermodulation factor p_+/p_1 on radius of woofer a for $d = 7.2$ cm, $f_2 = 3$ kHz. This is similar to Figure 4.15 with $d = 7.2$ cm.

Tweeter Distance - On-Axis

Other interesting phenomena are exhibited if we vary our distance d for fixed radii. For these simulations however, we only plot the spatial factor p_2 (as opposed to p_2/p_1). The reason for this is that the first-order pressure p_1 fluctuates substantially as we change the value of d (see Figure 4.18).

The oscillatory behaviour of Figure 4.18 is due to the fact that at d values $\frac{\lambda_2}{4}, \frac{3\lambda_2}{4}, \frac{5\lambda_2}{4}$ etc. (λ_2 is the wavelength of the high-frequency wave) the distance between the tweeter and its image source is exactly one half wavelength (or $1\frac{1}{2}, 2\frac{1}{2}$ etc.) so that when we are on-axis the reflected tweeter signal arrives 180° out of phase with the original and thus cancellation occurs. Consequently, to better understand the qualitative behaviour of the intermodulation terms for varying values of d, we avoid plotting the values of p_1.[10]

Figures 4.19-4.21 show that as d increases the general intermodulation factor

[10]Note that this was not a problem for our plots Figures 4.9-4.17 as p_1 was essentially constant in those cases.

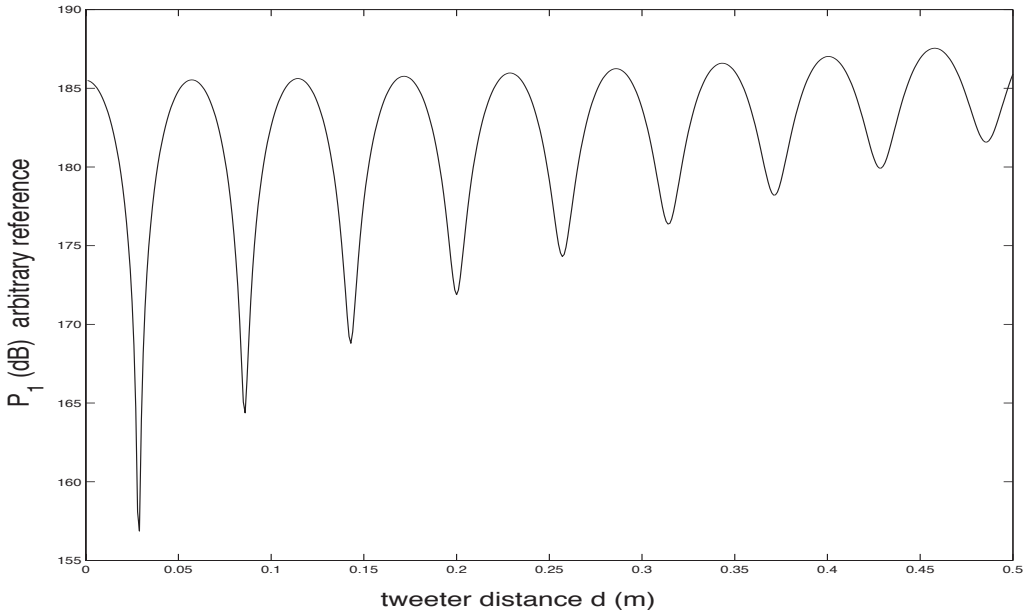

Figure 4.18: Theoretical effect of varying the tweeter distance on the first-order pressure p_1. The units are arbitrary decibel units because we have not calculated Q_0 and thus are lacking the $\rho_0 Q_0/4\pi$ factor. For $f_2 = 3$ kHz the wavelength is approximately 11.4 cm and so the nulls occur at odd multiples of approximately 2.85 cm.

drops, which is expected. There are also some interesting local maxima which seem to occur when the tweeter is positioned at a point on-axis equivalent to the piston radius. For the 30 cm woofer we also see a local minimum appear at around 15 cm (Figure 4.21). To see how these extrema might be affected by the frequencies themselves we plot a similar graph but for $f_2 = 5$ kHz (Figure 4.22).

The qualitative behaviour in Figure 4.22 shows similarities to Figure 4.21 except there seems to be an increasing trend near the end of the graph. To examine this further we extend our range of tweeter distances in Figure 4.23.

The discontinuity at 1 m in Figure 4.23 is due to the correction terms from equation (4.32) which become singular as our tweeter distance moves closer to our observation point. Indeed there is an eventual decreasing trend as d is positioned far enough away, however not before there are significant oscillations as the tweeter is moved between the observer and the boundary. There is also a noticeable drop at around 2 m.

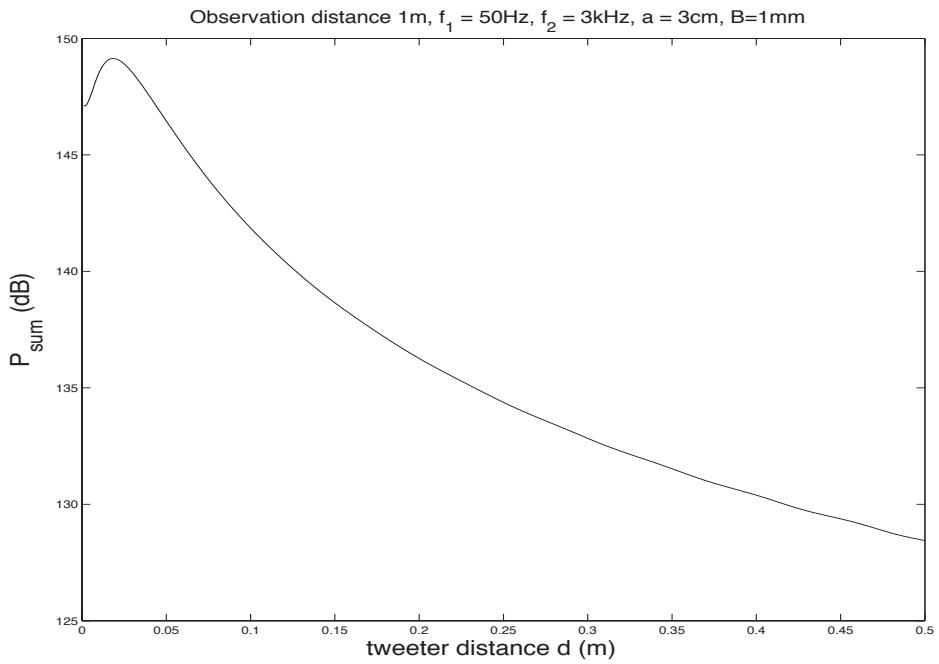

Figure 4.19: Theoretical dependence of sum frequency p_+ on tweeter distance d (arbitrary decibel units) - radius 3 cm.

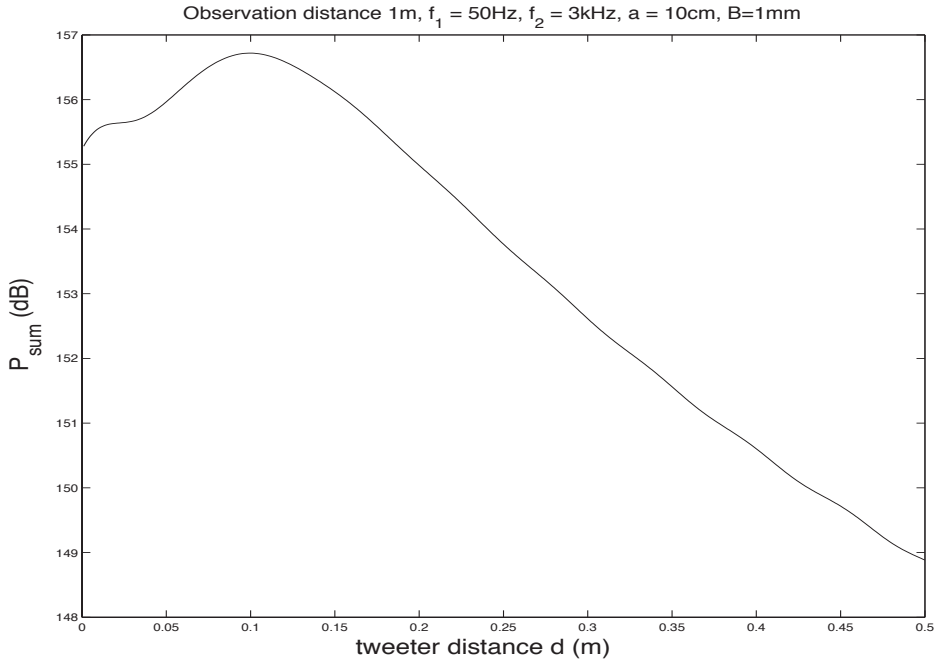

Figure 4.20: Theoretical dependence of sum frequency p_+ on tweeter distance d (arbitrary decibel units) - radius 10 cm.

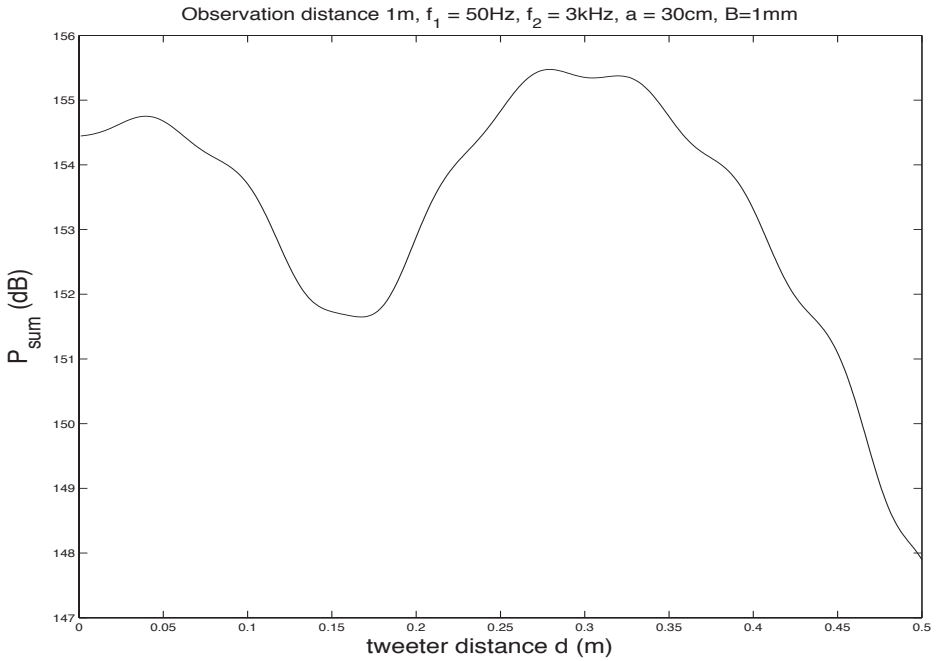

Figure 4.21: Theoretical dependence of sum frequency p_+ on tweeter distance d (arbitrary decibel units) - radius 30 cm.

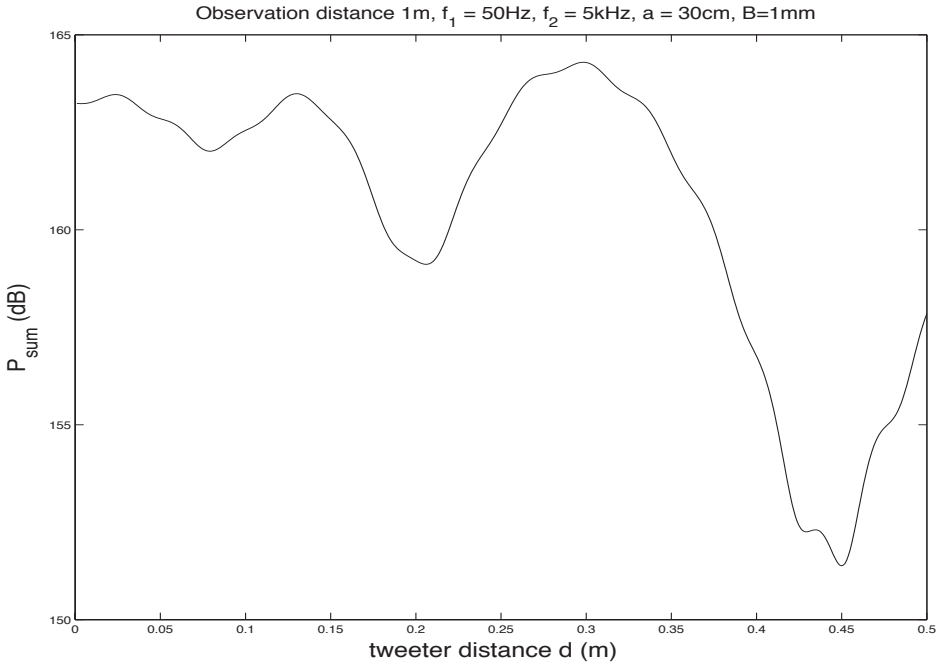

Figure 4.22: Theoretical dependence of sum frequency p_+ on tweeter distance d (arbitrary decibel units) - radius 30 cm. Similar to Figure 4.21 with f_2 now 5 kHz.

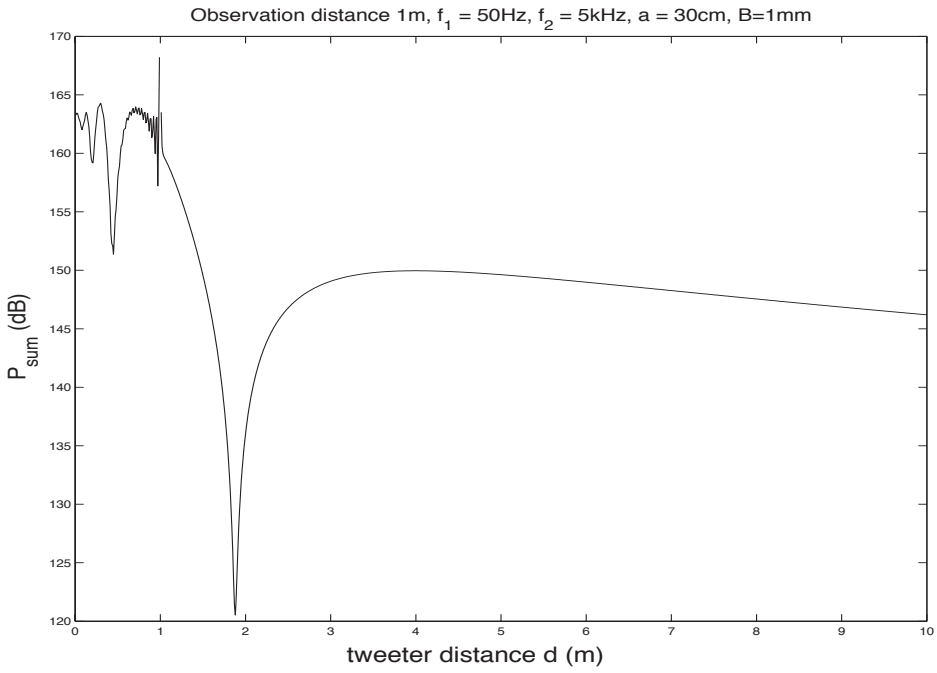

Figure 4.23: Extended theoretical dependence of sum frequency p_+ on tweeter distance d (arbitrary decibel units) - radius 30 cm, $f_2 = 5$ kHz. Similar to Figure 4.22 except we have extended the tweeter distance up to 10 m.

To see what might cause this we plot the same graph without the correction terms in Figure 4.24. Comparison with Figure 4.23 shows that the correction terms seem to cause negligible change in the overall qualitative behaviour of the intermodulation frequency except near the observation point. The large drop at around 2 m is present in both situations and must be the result of some extreme phase cancellation. A similar plot of p_2' (that is, p_2 without the correction terms) for our original frequency $f_2 = 3$ kHz is given in Figure 4.25. Note the position of the apparent null. Predicting this from the integral (4.84) would seem nontrivial given the complexity of the integrand for values of $r_0 = O(1)$.

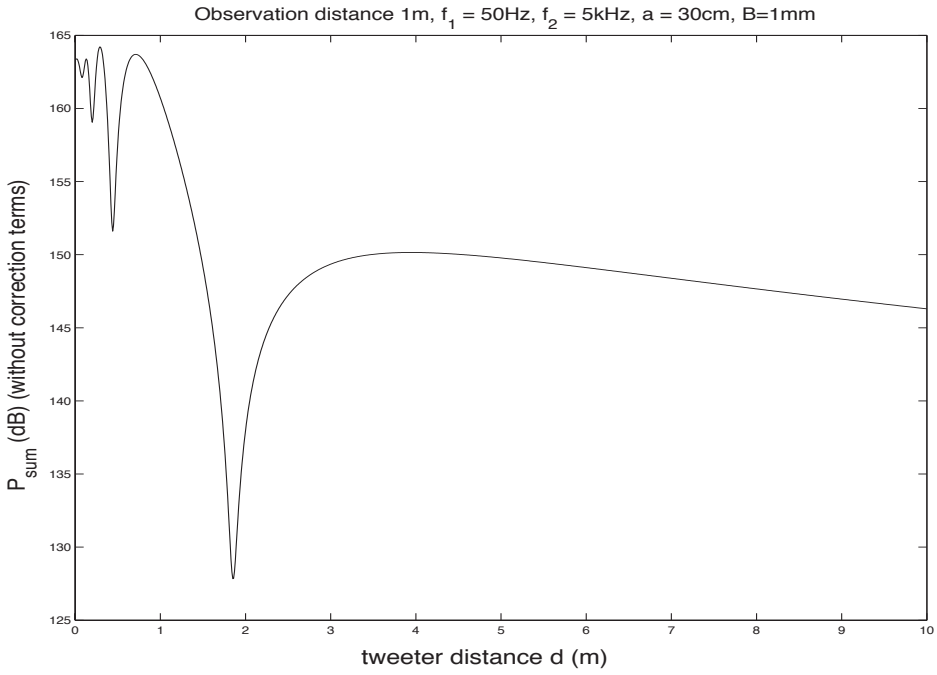

Figure 4.24: Theoretical dependence of sum frequency without correction terms p'_+ on tweeter distance d (arbitrary decibel units) - radius 30 cm, $f_2 = 5$ kHz. Similar to Figure 4.23 except missing the correction terms in (4.32).

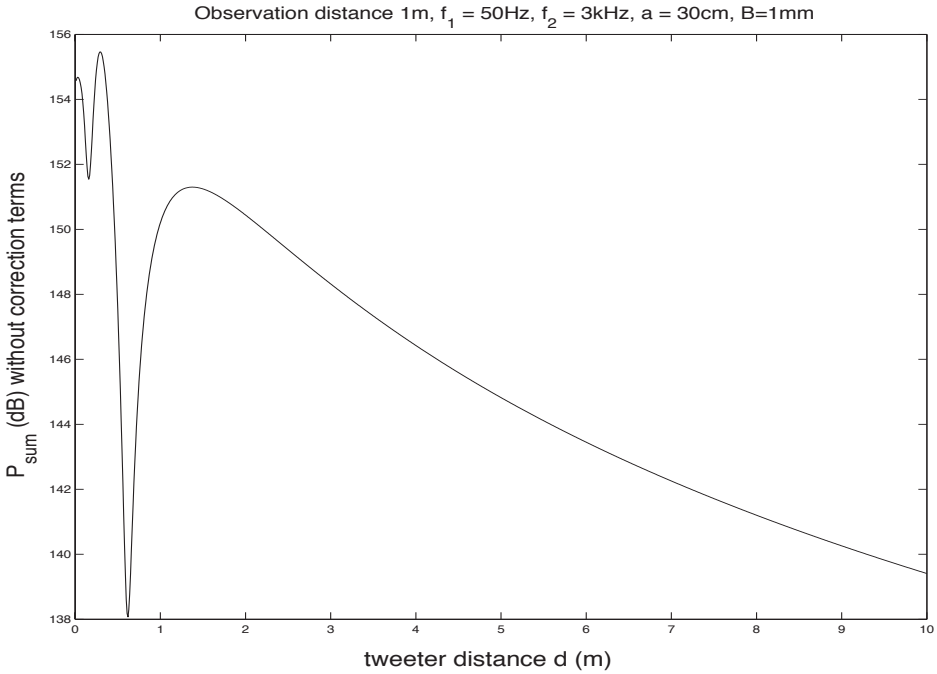

Figure 4.25: Theoretical dependence of sum frequency without correction terms p'_+ on tweeter distance d (arbitrary decibel units) - radius 30 cm, $f_2 = 3$ kHz. Similar to Figure 4.24 except the tweeter is emitting a 3 kHz tone.

Tweeter Distance - Off-Axis

The plots of Figures 4.19-4.25, while interesting, are mostly theoretical since for real speaker setups (coaxial or otherwise) it is unlikely that the tweeter would be positioned so far away. A more useful simulation, and one which should agree with the experiments by Klipsch [1] (at least qualitatively), is to examine the behaviour as the tweeter is moved off the axis. Again for these plots the ordinate is only the pressure p_2 for the same reasons given in the On-Axis Section (although varying the parameter h, which represents our distance off the axis, does not have as strong an effect on p_1 as did varying the d parameter). We first use a d value of 2.4 cm, similar to our B139 setup, and see what happens as h is increased past the edge of the woofer (Figures 4.26-4.28).

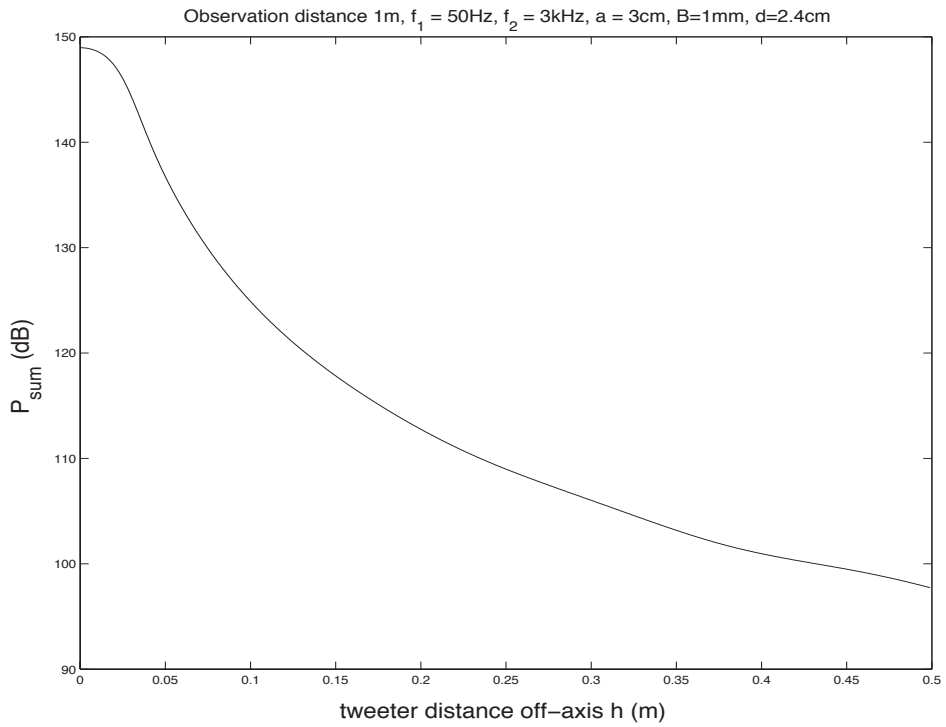

Figure 4.26: Theoretical effect of moving the tweeter off the axis of a woofer with radius 3 cm (arbitrary decibel units). Only the sum frequency p_+ is shown. The horizontal distance d between the tweeter and baffle is 2.4 cm.

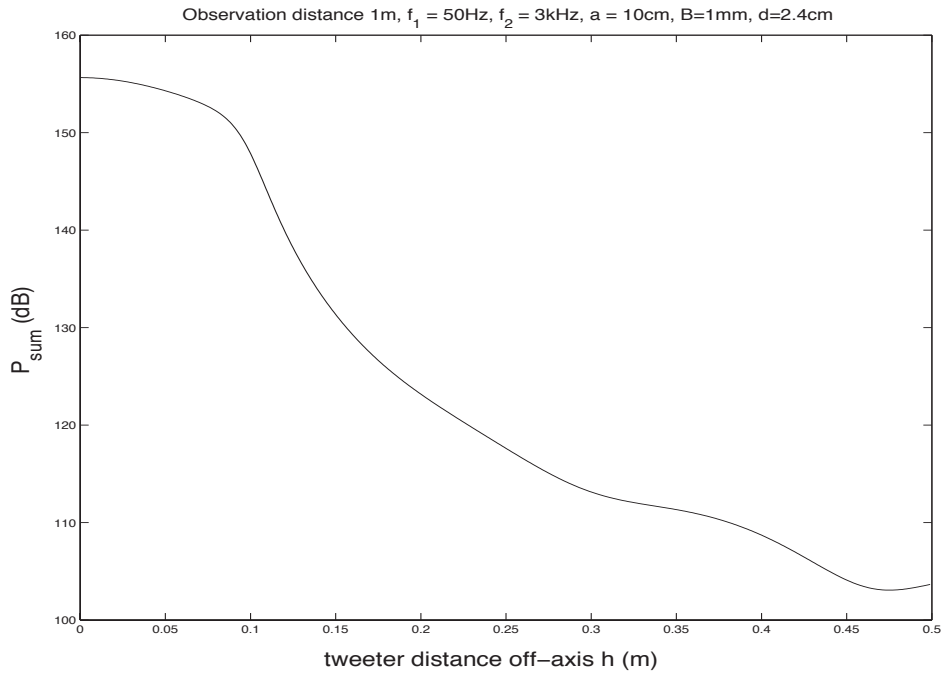

Figure 4.27: Theoretical effect of moving the tweeter off the axis of a woofer with radius 10 cm (arbitrary decibel units). Only the sum frequency p_+ is shown. The horizontal distance d between the tweeter and baffle is 2.4 cm.

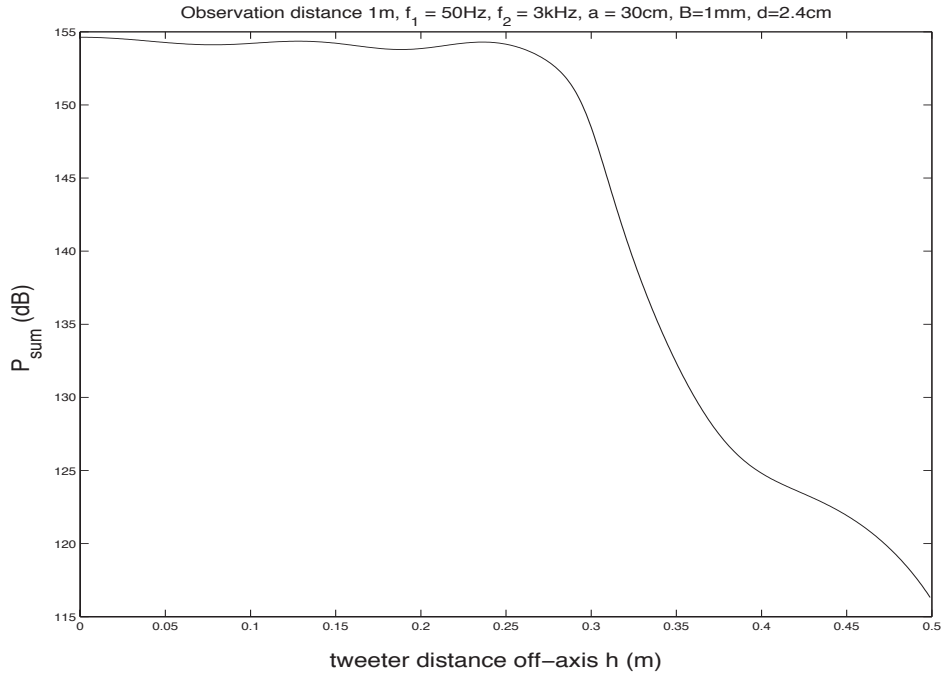

Figure 4.28: Theoretical effect of moving the tweeter off the axis of a woofer with radius 30 cm (arbitrary decibel units). Only the sum frequency p_+ is shown. The horizontal distance d between the tweeter and baffle is 2.4 cm.

As expected the intermodulation factor drops off quite substantially as the tweeter moves past the edge of the woofer. Physically, it would seem that this drop should be stronger the closer the tweeter is to the boundary and weaker as the tweeter is positioned further away. Figures 4.29-4.31 show the behaviour for the same three woofers (radii 3, 10 and 30 cm) when the tweeter is now located 5 mm from the boundary.

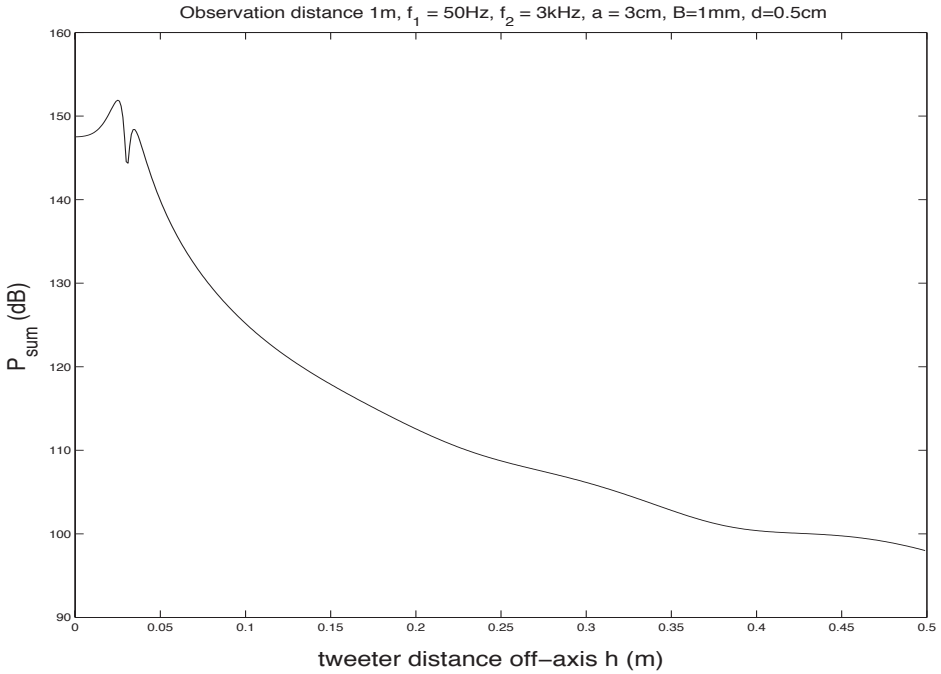

Figure 4.29: Theoretical effect of moving the tweeter off the axis of a woofer with radius 3 cm (arbitrary decibel units). Only the sum frequency p_+ is shown. This is similar to Figure 4.26 except that the horizontal distance d between the tweeter and baffle is now 5 mm.

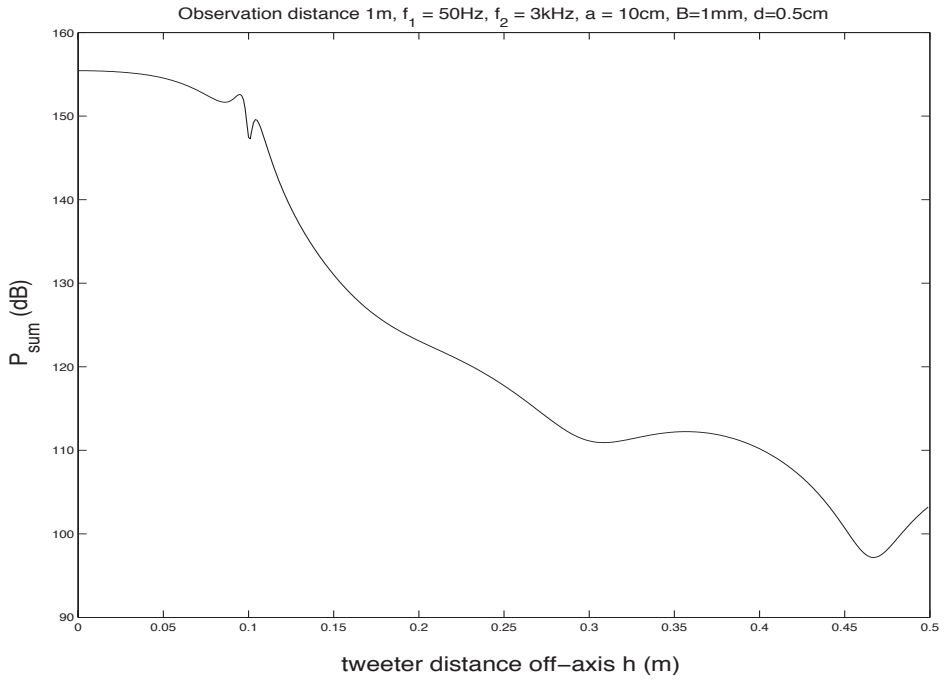

Figure 4.30: Theoretical effect of moving the tweeter off the axis of a woofer with radius 10 cm (arbitrary decibel units). Only the sum frequency p_+ is shown. This is similar to Figure 4.27 except that the horizontal distance d between the tweeter and baffle is now 5 mm.

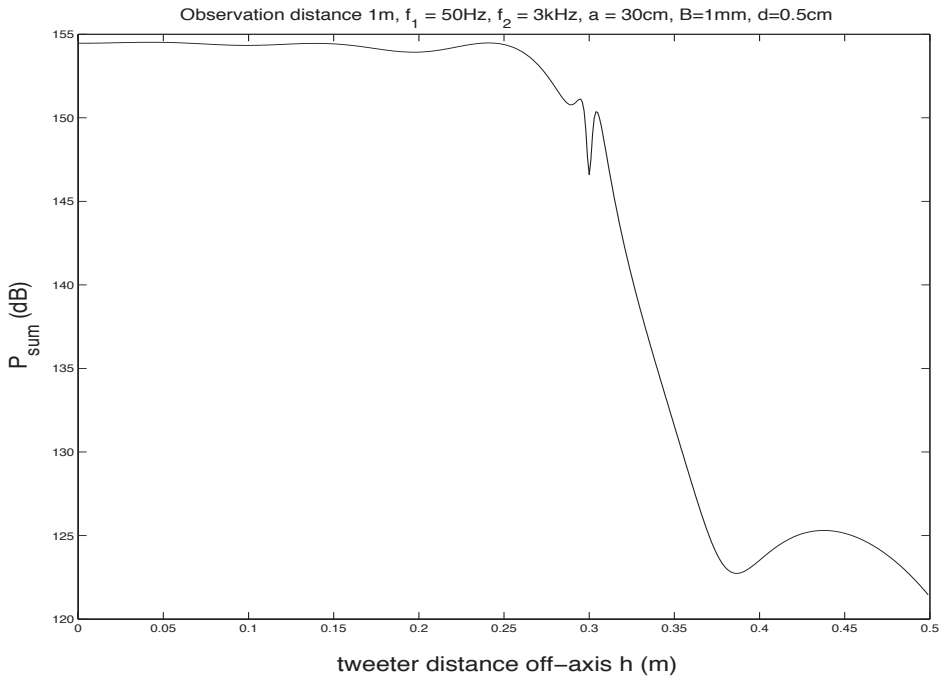

Figure 4.31: Theoretical effect of moving the tweeter off the axis of a woofer with radius 30 cm (arbitrary decibel units). Only the sum frequency p_+ is shown. This is similar to Figure 4.28 except that the horizontal distance d between the tweeter and baffle is now 5 mm.

For comparison, Figure 4.32 shows the result for the 30 cm woofer when the tweeter is now 10 cm from the boundary.

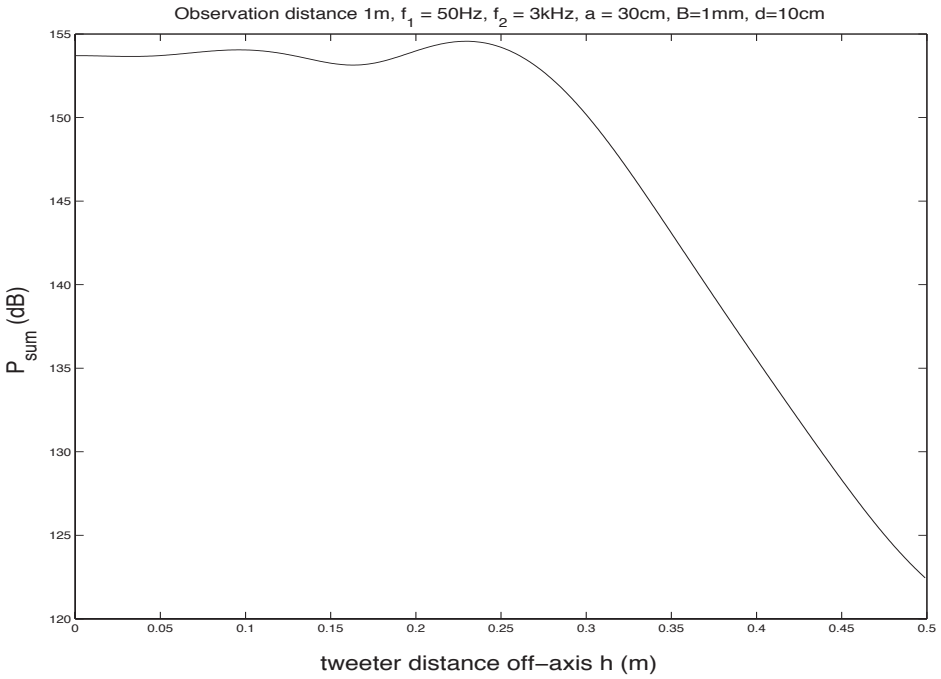

Figure 4.32: Theoretical effect of moving the tweeter off-axis for a woofer with radius 30 cm (arbitrary decibel units). Only the sum frequency p_+ is shown. This is similar to both Figures 4.28 and 4.31 except that the horizontal distance d is now 10 cm.

Indeed Figures 4.29-4.32 show the expected behaviour as the tweeter height is increased beyond the edge of the woofer. Notice the rate of decrease is much quicker for the $d = 5$ mm case (Figure 4.31) than for the $d = 10$ cm case (Figure 4.32). In fact, for the three plots Figures 4.29-4.31, there seems to be a large drop (approx 5 dB) right as the tweeter reaches the edge of the woofer. Interestingly, this drop is quickly followed by a subsequent jump of about 4 dB. Intuition would suggest the initial drop when the tweeter is located so close to the boundary. The subsequent jump however, is not so easily understood. It would be interesting to see if experiments agree with these simulations.

We conclude this section by mentioning that although direct numerical comparisons with the experiments of Klipsch [1] are difficult to perform, the qualitative behaviour of the plots in this section agree with his observations. In other words,

that a coaxial setup ($h = 0$) has a substantially more audible modulation distortion than that of a separated system ($h > a$).

Analytic validity

In this final section we examine the range of validity of the on-axis (both tweeter and observation point) analytic approximation (4.99)-(4.100). We restate the approximation as a single equation

$$\begin{aligned} p'_{2+_{\text{approx}}} &= -2\left(\frac{\rho_0 Q_0 b_w}{4\pi}\right) e^{j\omega_+ t}\,\Gamma(z) \\ \Gamma(z) &= \left(\frac{e^{-jk_+ z}}{z}\right)\left(\frac{\omega_+}{\omega_1}\right)\left[\left(\frac{d^2 - r_d^2}{r_d^3}\right) e^{-jk_2 r_d} + j\left(\frac{d^2 k_2}{r_d^2} e^{-jk_2 r_d} - k_2 e^{-jk_2 d}\right)\right] \\ &\quad + \left(\frac{e^{-jk_+ z}}{z}\right) j\frac{(k_+)^2}{k_2}[e^{-jk_2 r_d} - e^{-jk_2 d}]. \end{aligned} \tag{4.104}$$

to be compared with the exact pressure $p'_{2+_{\text{exact}}}$ given by formula (4.84).

Recall that our derivation of (4.104) was based on the assumption $z \gg a$. We therefore give plots of the error $|p'_{2_{\text{exact}}} - p'_{2_{\text{approx}}}|$ as our observation distance z varies between 0 and 1 m for both the sum and difference frequencies[11]. Figures 4.33 and 4.34 show the expected behaviour for woofers with radii 1 cm and 10 cm respectively. That is, the approximation formula exhibits greater error for the larger radius (figure 4.34, note the different scales).

What may be somewhat surprising, when the radius is further increased to 1 m, is that the magnitude of the error (Figure 4.35) does not differ much from the case $a = 10$ cm (Figure 4.34). Clearly the condition $z \gg a$ is no longer satisfied so there must be other factors involved. We can identify a possible reason for the apparent validity of the approximation even for $z \leq a$ (Figure 4.35) by looking at equation (4.98) and Figures 4.15-4.17. During the initial values of the integration variable σ, the approximation (4.98) is still valid. As $\sigma \to a$, this approximation becomes less and less accurate and the exact distance needs to be used. However, we see

[11] Although (4.104) is only for the sum frequency, following the procedure in Section 4.2.5 using equation (4.77) instead of (4.76) yields a formula for $p'_{2-\text{approx}}$.

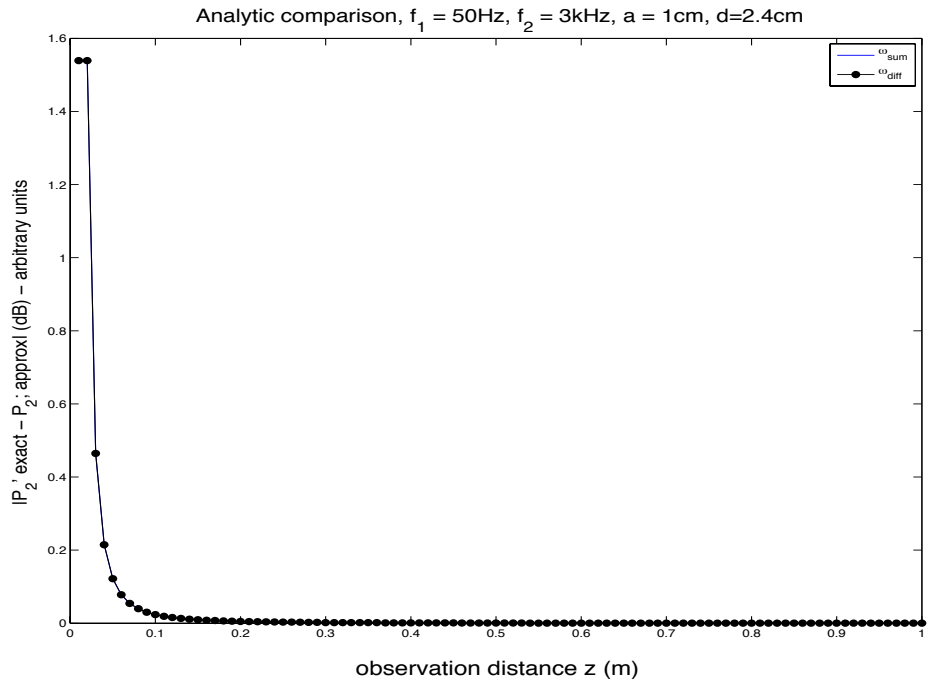

Figure 4.33: Error in analytic approximation $|p'_{2_{\text{exact}}} - p'_{2_{\text{approx}}}|$ as computed from (4.84) and (4.104) respectively (along with the equivalent difference frequency formula). The woofer radius is 1 cm.

from Figures 4.15-4.17 that the contributions from the outer part of the radius are much less significant than those in a small circle approximately $0 \leq \sigma \leq 10$ cm. This would suggest that the condition $z \gg 10$ cm is perhaps more appropriate. We deduce then that for values of z approximately greater than 50 cm (based on Figures 4.15-4.17) the analytic approximation is a good one regardless of radius. A final plot (Figure 4.36) of a 5 m woofer confirms this.

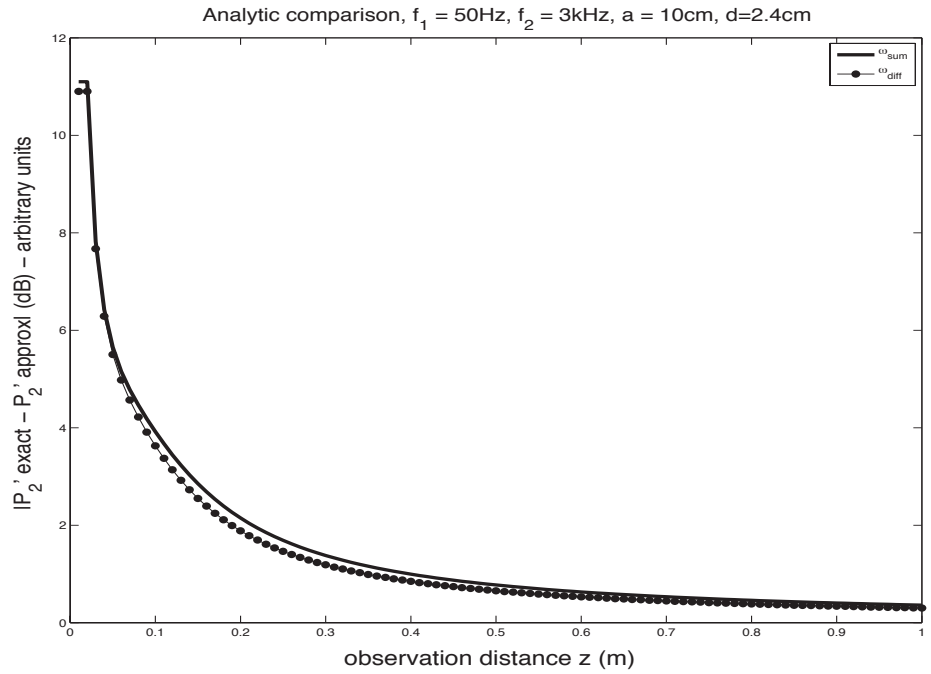

Figure 4.34: Error in analytic approximation $|p'_{2_{\text{exact}}} - p'_{2_{\text{approx}}}|$ as computed from (4.84) and (4.104) respectively. Similar to Figure 4.33 with the woofer radius now 10 cm.

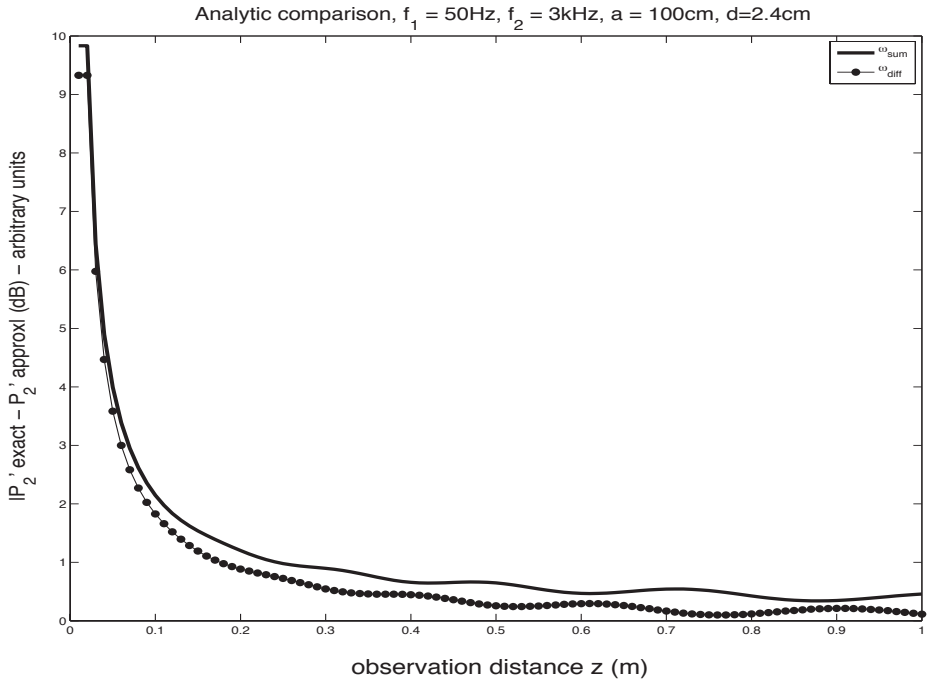

Figure 4.35: Error in analytic approximation $|p'_{2_{\text{exact}}} - p'_{2_{\text{approx}}}|$ as computed from (4.84) and (4.104) respectively. Similar to Figure 4.33 with the woofer radius now 1 m. Note that the condition $z \gg a$ is no longer valid, however the error is still small.

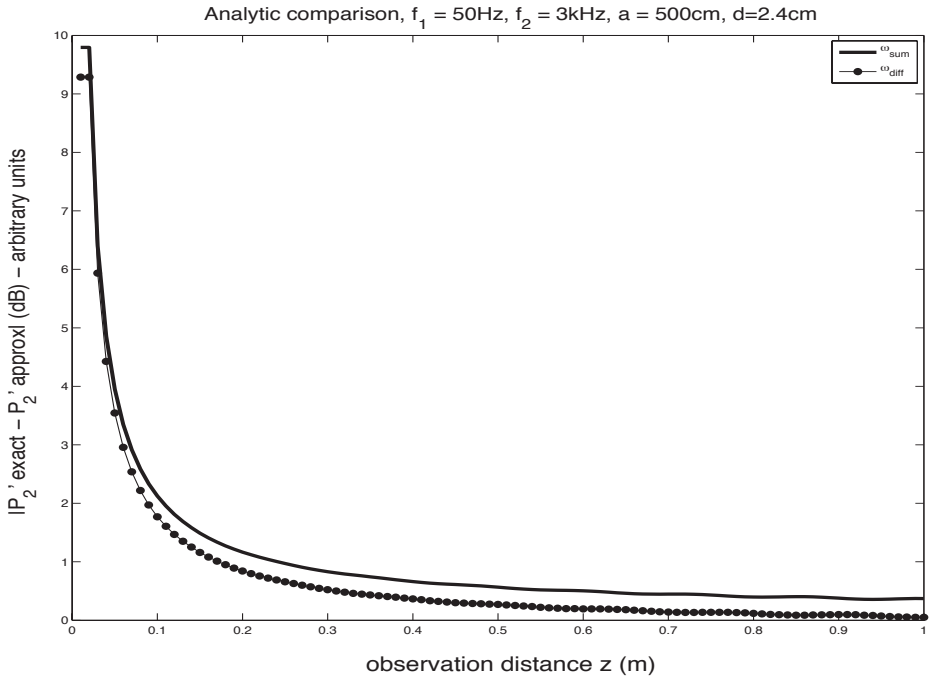

Figure 4.36: Error in analytic approximation $|p'_{2_{\text{exact}}} - p'_{2_{\text{approx}}}|$ as computed from (4.84) and (4.104) respectively. Similar to Figure 4.33 with the woofer radius now 5 m. Here $z < a$ and the approximate formula is still rather good. See the explanation in the text.

Chapter 5

Conclusions

We have established a set of inhomogeneous wave equations, based on the method of successive approximations, to solve for the pressure field of the intermodulation frequencies generated by two interacting acoustic transducers. A dimensionless approach was used in order to be as thorough as possible. Using the Green's function of the wave operator a general solution to the inhomogeneous wave equation was obtained in the form of an integral equation. Employing geometrical simplifications this integral equation was reduced to a matter of quadrature over a semi-infinite volume and a finite surface. To further simplify this integration an argument was made to establish the Doppler effect as the dominant source of sum and difference frequency generation under the current regime. This allowed us to express the solution to the intermodulation frequency component as an integral over the surface of the woofer.

An analytic solution to this integral was obtained for the on-axis, farfield, coaxial case. Numerical simulations however, suggested that the farfield assumption could potentially be relaxed. Comparison between experiment and theory showed that for the parameter values used in the lab, the agreement is rather good. Possible sources of error include room reflections, edge wave diffraction, measurement inaccuracies and geometric disparity. Further experiments would help isolate specific causes.

Using the second-order integral expression (4.84) for the sum and difference fre-

quencies, a numerical investigation was undertaken to observe the dependence of the intermodulation factor on various parameter changes. Several results agreed with intuition although further analysis would seem appropriate for certain observations.

Although it would appear unlikely that a full analytic solution to (4.84) is possible, a general (off-axis) farfield solution similar to the first-order equation (4.27) is potentially attainable. Even without this, however, further experiments to compare with the simulations given in Chapter 4 would prove beneficial.

Appendix A

Vector Identities

Below are some not-so-standard vector identities that have been used in various derivations throughout the text. The latter half are mostly used in the derivation of the reduced wave equation for p_2' (4.33). The functions f, g are scalar, $\mathbf{F}, \mathbf{G}, \mathbf{u}$ are vector.

1. $\nabla \times (f\mathbf{u}) \equiv f\nabla \times \mathbf{u} - \mathbf{u} \times \nabla f$
2. $\nabla \times (\mathbf{F} \times \mathbf{G}) \equiv (\mathbf{G} \cdot \nabla)\mathbf{F} - (\mathbf{F} \cdot \nabla)\mathbf{G} + (\nabla \cdot \mathbf{G})\mathbf{F} - (\nabla \cdot \mathbf{F})\mathbf{G}$
3. $\nabla(\mathbf{F} \cdot \mathbf{G}) \equiv (\mathbf{F} \cdot \nabla)\mathbf{G} + (\mathbf{G} \cdot \nabla)\mathbf{F} + \mathbf{F} \times (\nabla \times \mathbf{G}) + \mathbf{G} \times (\nabla \times \mathbf{F})$
4. $\nabla \cdot (\nabla f \times \nabla g) \equiv 0$
5. $\nabla \times (\nabla \times \mathbf{F}) \equiv \nabla(\nabla \cdot \mathbf{F}) - \nabla^2\mathbf{F}$
6. $\nabla \cdot (\mathbf{F} \times \mathbf{G}) \equiv \mathbf{G} \cdot (\nabla \times \mathbf{F}) - \mathbf{F} \cdot (\nabla \times \mathbf{G})$
7. $(\mathbf{u} \cdot \nabla)\mathbf{u} \equiv \frac{1}{2}\nabla(|\mathbf{u}|^2) - \mathbf{u} \times (\nabla \times \mathbf{u})$
8. $\nabla \cdot [(\mathbf{u} \cdot \nabla)\mathbf{u}] \equiv \frac{1}{2}\nabla^2(|\mathbf{u}|^2) - |\nabla \times \mathbf{u}|^2 + \mathbf{u} \cdot (\nabla \times \nabla \times \mathbf{u})$
9. $\nabla^2(f^2) \equiv 2|\nabla f|^2 + 2f\nabla^2 f$
10. $(f^2)_{tt} \equiv 2(f_t)^2 + 2ff_{tt}$

11. $(\frac{\partial^2}{\partial t^2} - c^2\nabla^2)(f^2) \equiv 2f(f_{tt} - c^2\nabla^2 f) + 2[(f_t)^2 - c^2|\nabla f|^2]$

12. $\frac{\partial^2}{\partial t^2}(|\mathbf{u}|^2) \equiv 2\mathbf{u} \cdot \mathbf{u}_{tt} + 2|\mathbf{u}_t|^2$

13. $(\frac{\partial^2}{\partial t^2} - c^2\nabla^2)(f_t \int f dt) \equiv \int f dt(\frac{\partial^2}{\partial t^2} - c^2\nabla^2)(f_t) + 2f f_{tt} - 2c^2\nabla f_t \cdot \nabla \int f dt + f_t(\frac{\partial^2}{\partial t^2} - c^2\nabla^2)(\int f dt)$

Appendix B

Alternative Derivation of Green's Function for Wave Equation

The following derivation is adapted from [60].

We seek to find the free space Green's function $G = G(\xi, \eta, \zeta, \tau, x, y, z, t)$ solving

$$G_{\tau\tau} - c^2\nabla^2 G = \delta(\xi - x)\delta(\eta - y)\delta(\zeta - z)\delta(\tau - t) \tag{B.1}$$

subject to the condition $G = 0$ for $\tau > t$. Define the spatial Fourier transform pair

$$\mathcal{F}[G] \;:=\; g(k_1, k_2, k_3, \tau, x, y, z, t) = \frac{1}{(\sqrt{2\pi})^3} \int_{-\infty}^{\infty}\int\int G e^{i(k_1\xi + k_2\eta + k_3\zeta)} d\xi d\eta d\zeta \tag{B.2}$$

$$\mathcal{F}^{-1}[g] \;:=\; G(\xi, \eta, \zeta, \tau, x, y, z, t) = \frac{1}{(\sqrt{2\pi})^3} \int_{-\infty}^{\infty}\int\int g e^{-i(k_1\xi + k_2\eta + k_3\zeta)} dk_1 dk_2 dk_3 \tag{B.3}$$

Multiply both sides of (B.1) by $\frac{1}{(\sqrt{2\pi})^3} e^{i(k_1\xi + k_2\eta + k_3\zeta)}$ and integrate over infinite (ξ, η, ζ) space using the properties

- $\mathcal{F}[G_{\tau\tau}] = g_{\tau\tau}$
- $\mathcal{F}[G_{\xi_i\xi_i}] = -k_i^2 g$

and the sifting property of the delta function to get the equation

$$g_{\tau\tau} + c^2k^2g = \frac{1}{(\sqrt{2\pi})^3}e^{i(k_1x+k_2y+k_3z)}\delta(\tau - t) \tag{B.4}$$

where $k = \sqrt{k_1^2 + k_2^2 + k_3^2}$. The condition $G = 0$ for $\tau > t$ can be restated as (see section 3.4.3) $G = G_\tau = 0$ at $\tau = T > t$ which transfers to g as

$$g|_{\tau=T} = \frac{\partial g}{\partial \tau}|_{\tau=T} = 0, \ T > t. \tag{B.5}$$

This ODE (B.4) with time conditions (B.5) has the standard homogeneous solution

$$g_h = c_1 \sin(ck\tau) + c_2 \cos(ck\tau) = c_1u_1(\tau) + c_2u_2(\tau). \tag{B.6}$$

To find a particular solution we employ the method of variation of parameters which, for a second order ODE with inhomogeneous function f, fundamental solutions u_1 and u_2 and Wronskian W, has the solution formula

$$\begin{aligned} g_p &= v_1(\tau)u_1(\tau) + v_2(\tau)u_2(\tau) && \text{(B.7)} \\ v_1(\tau) &= -\int^\tau \frac{u_2(s)f(s)}{W}ds && \text{(B.8)} \\ v_2(\tau) &= \int^\tau \frac{u_1(s)f(s)}{W}ds. && \text{(B.9)} \end{aligned}$$

The lower bound of integration is not important as it yields a constant which will in turn be multiplied by one of our fundamental solutions and can therefore be absorbed into c_1 and c_2.

In our case, the function f is given by

$$f(\tau) = \frac{1}{(\sqrt{2\pi})^3}e^{i\mathbf{k}\cdot\mathbf{x}}\delta(\tau - t) \tag{B.10}$$

where $\mathbf{k} = (k_1, k_2, k_3)$ and $\mathbf{x} = (x, y, z)$ and $W = -ck$. This gives us a particular solution of

$$g_p = \frac{\sin(ck\tau)e^{i\mathbf{k}\cdot\mathbf{x}}}{ck(\sqrt{2\pi})^3}\int^\tau \cos(cks)\delta(s - t)ds - \frac{\cos(ck\tau)e^{i\mathbf{k}\cdot\mathbf{x}}}{ck(\sqrt{2\pi})^3}\int^\tau \sin(cks)\delta(s - t)ds. \tag{B.11}$$

Due to the delta function in our expression for f two cases need to be considered. For $\tau < t$, the integrals vanish and the whole particular solution is simply 0. For $\tau > t$ the integration is easily computed and we thus obtain

$$g_p = 0, \quad \tau < t \tag{B.12}$$

$$g_p = \frac{\sin(ck\tau)\cos(ckt)e^{i\mathbf{k}\cdot\mathbf{x}}}{ck(\sqrt{2\pi}^3)} - \frac{\cos(ck\tau)\sin(ckt)e^{i\mathbf{k}\cdot\mathbf{x}}}{ck(\sqrt{2\pi})^3}, \quad \tau > t \tag{B.13}$$

Using a Heaviside step function this can be rewritten as a single expression which, after a trig simplification, combines with our homogeneous solution g_h to yield

$$g = \frac{\sin[ck(\tau - t)]e^{i\mathbf{k}\cdot\mathbf{x}}}{ck(\sqrt{2\pi})^3} H(\tau - t) + c_1 \sin(ck\tau) + c_2 \cos(ck\tau) \tag{B.14}$$

With a bit of algebra our coefficients c_1 and c_2 are obtained from our conditions (B.5)

$$c_1 = -\frac{\cos(ckt)e^{i\mathbf{k}\cdot\mathbf{x}}}{ck(\sqrt{2\pi})^3} \tag{B.15}$$

$$c_2 = \frac{\sin(ckt)e^{i\mathbf{k}\cdot\mathbf{x}}}{ck(\sqrt{2\pi})^3} \tag{B.16}$$

to give a solution (after another trig identity)

$$g = \frac{\sin[ck(\tau - t)]e^{i\mathbf{k}\cdot\mathbf{x}}}{ck(\sqrt{2\pi})^3} H(\tau - t) + \frac{\sin[ck(t - \tau)]e^{i\mathbf{k}\cdot\mathbf{x}}}{ck(\sqrt{2\pi})^3}. \tag{B.17}$$

Using the fact that sine is odd we can change the sign of the first term by switching the order of t and τ. Then, due to the second term being equal and opposite, we can combine these and switch the Heaviside function to get a final expression

$$g = \frac{\sin[ck(t - \tau)]e^{i\mathbf{k}\cdot\mathbf{x}}}{ck(\sqrt{2\pi})^3} H(t - \tau) \tag{B.18}$$

which trivially satisfies (B.5).

Our next step is to invert this to obtain our function G. Substitution of (B.18) into (B.3) leaves us to integrate

$$G = \frac{H(t - \tau)}{(2\pi)^3} \iiint_{-\infty}^{\infty} \frac{\sin[ck(t - \tau)]e^{i\mathbf{k}\cdot\mathbf{r}}}{ck} dk_1 dk_2 dk_3 \tag{B.19}$$

where we have defined $\mathbf{r} = (x-\xi, y-\eta, z-\zeta)$. This integration is more easily evaluated in spherical coordinates (k, ϕ, θ) defined from

$$k_1 = k\cos\phi \tag{B.20}$$

$$k_2 = k\sin\phi\cos\theta \tag{B.21}$$

$$k_3 = k\sin\phi\sin\theta. \tag{B.22}$$

From these we have the standard transformation $dk_1 dk_2 dk_3 = k^2 \sin\phi d\theta d\phi dk$. Also, we can rewrite $\mathbf{k}\cdot\mathbf{r}$ as $kr\cos\alpha$ where α is the angle between $\mathbf{k}$ and $\mathbf{r}$. To simplify the calculation we place our zenith in the direction of $\mathbf{r}$ (which is fixed during the integration) so that the angle α is actually equal to ϕ. We must then compute

$$G = \frac{H(t-\tau)}{c(2\pi)^3}\int_0^\infty\int_0^\pi\int_0^{2\pi} k\sin[ck(t-\tau)]e^{ikr\cos\phi}\sin\phi d\theta d\phi dk. \tag{B.23}$$

The first of these integrations trivially gives 2π. For the second we have

$$\int_0^\pi e^{ikr\cos\phi}\sin\phi d\phi = -\frac{e^{ikrcos\phi}}{ikr}|_0^\pi = \frac{2\sin(kr)}{kr} \tag{B.24}$$

which leaves us with a final integral of

$$G = \frac{H(t-\tau)}{2\pi^2 rc}\int_0^\infty \sin[ck(t-\tau)]\sin(kr)dk. \tag{B.25}$$

Since $\sin(a)\sin(b) = \frac{1}{2}(\cos(a-b)-\cos(a+b))$, define $t_1 = [c(t-\tau)-r]$ and $t_2 = [c(t-\tau)+r]$ so that our integration becomes

$$G = \frac{H(t-\tau)}{4\pi^2 rc}\int_0^\infty(\cos(kt_1)-\cos(kt_2))dk \tag{B.26}$$

To make this integration meaningful we use the fact that cosine is even and sine is odd and rewrite this as

$$G = \frac{H(t-\tau)}{8\pi^2 rc}\int_{-\infty}^\infty(e^{ikt_1}-e^{ikt_2})dk. \tag{B.27}$$

Finally, invoking the Fourier transform identity [61]

$$\int_{-\infty}^\infty e^{ibk}dk = 2\pi\delta(b) \tag{B.28}$$

we get a final solution of

$$G = \frac{H(t-\tau)}{4\pi rc}[\delta(t_1) - \delta(t_2)] \tag{B.29}$$

To make this match our solution given by equation (3.37) we note that this function is only nonzero when $t - \tau > 0$. Under this condition however, t_2 is always greater than 0 so that $\delta(t_2)$ vanishes. The Heaviside function is then redundant due to the fact that $\delta(t_1)$ is also only nonzero for $t - \tau > 0$. This gives us

$$G = \frac{1}{4\pi rc}\delta(c(t-\tau) - r) \tag{B.30}$$

which is identical to (3.37) upon applying $\delta(ax) = \frac{1}{|a|}\delta(x)$.

Appendix C

Integral solution of Wave Equation for Cases 2 and 3

Here we investigate the derivation of the integral equation for the remaining geometries in figure 3.3. In both situations the derivation follows exactly as in section 3.3 up until equation (3.43). The only difference is the surface S.

Case 2

In this case the surface $S = S_1$ only and we do not have the same ϵ-sphere surrounding the observation point. Because of this, our field quantity of interest, namely $p(x, y, z, t)$ does not appear in isolation and we are left with the modified version of (3.51)

$$0 = \int_V \int_0^T G f d\tau dV + c^2 \int_{S_1} \int_0^T (G\nabla p - p\nabla G) \cdot \mathbf{n} dS_1 d\tau - \int_V (Gp_\tau - G_\tau p) \,|_0^T \quad \text{(C.1)}$$

which is an integral equation to be solved for p.

Case 3

The geometry of this situation is more akin to that of Case 1. The only difference here is that instead of using a full sphere to surround our observation point we

must use a modified volume and shrink its surface to 0. The derivation follows exactly as in section 3.3 up until equation (3.49) where the once trivial integration no longer gives 4π. The actual value of this integral will depend on the solid angle Ω subtended by our observation point subject to the given boundary structure. For example, if the point is on a flat surface our integration is over a hemisphere and we obtain 2π. Similarly, a 90° wall would yield a value of π. The solution is then given by

$$\frac{\Omega}{4\pi}p(x,y,z,t) = \int_V \int_0^T G f d\tau dV + c^2 \int_{S_1} \int_0^T (G\nabla p - p\nabla G)\cdot \mathbf{n} dS_1 d\tau - \int_V (Gp_\tau - G_\tau p)\,|_0^T \tag{C.2}$$

For a more detailed investigation of these integral equations (often called the Helmholtz integral equation) see [62] or [63].

Appendix D

Correction Terms to p_2

Having dealt with p_2' for most of the derivations we return to our original pressure p_2 by means of the substitution (4.32)

$$p_2 = p_2' - \frac{p_1^2}{2\rho_0 c^2} - \frac{p_{1t}}{\rho_0 c^2}\int p_1 dt - \frac{1}{2}\rho_0 |\mathbf{u}_1|^2. \tag{D.1}$$

Calculation of the last three terms is not analytically possible for a general observation point (x, y, z) due to the integral in (4.28). Therefore, the following assumes our observation point to be on axis $(0, 0, z)$. For reference our first-order pressure is given as

$$p_1(x, y, z, t) = \frac{j\omega_1\rho_0 b_w e^{j\omega_1 t}}{2\pi}\int_{S_w}\frac{e^{-jk_1 r}}{r}dS_w + \frac{j\omega_2\rho_0 Q_0}{4\pi}\left[\frac{e^{j(\omega_2 t - k_2 r_1)}}{r_1} + \frac{e^{j(\omega_2 t - k_2 r_2)}}{r_2}\right] \tag{D.2}$$

First term - p_1^2

As in Section 4.2.3, care must be taken when dealing with expressions involving quadratics of complex quantities. Accordingly, we separate the first order pressure p_1 into two terms

$$p_1 = \upsilon_1 + \upsilon_2 \tag{D.3}$$

$$\upsilon_1 = \frac{j\omega_1\rho_0 b_w e^{j\omega_1 t}}{2\pi}\int_{S_w}\frac{e^{-jk_1 r}}{r}dS_w \tag{D.4}$$

$$\upsilon_2 = \frac{j\omega_2\rho_0 Q_0}{4\pi}\left[\frac{e^{j(\omega_2 t - k_2 r_1)}}{r_1} + \frac{e^{j(\omega_2 t - k_2 r_2)}}{r_2}\right]. \tag{D.5}$$

Calculation of p_1^2 is then

$$\begin{aligned} p_1^2 &= [\Re(\upsilon_1 + \upsilon_2)]^2 && \text{(D.6)} \\ &= \frac{1}{4}(\upsilon_1 + \bar{\upsilon}_1 + \upsilon_2 + \bar{\upsilon}_2)^2 && \text{(D.7)} \\ &= \frac{1}{4}(\upsilon_1 + \bar{\upsilon}_1)^2 + \frac{1}{4}(\upsilon_2 + \bar{\upsilon}_2)^2 + \frac{1}{2}(\upsilon_1\upsilon_2 + \overline{\upsilon_1\upsilon_2} + \upsilon_1\bar{\upsilon}_2 + \bar{\upsilon}_1\upsilon_2). && \text{(D.8)} \end{aligned}$$

Of interest is the last bracket which is responsible for the sum and difference frequency tones. It can be separated and rewritten as

$$\frac{1}{2}(\upsilon_1\upsilon_2 + \overline{\upsilon_1\upsilon_2} + \upsilon_1\bar{\upsilon}_2 + \bar{\upsilon}_1\upsilon_2) = \overbrace{\Re(\upsilon_1\upsilon_2)}^{\text{sum freq}} + \overbrace{\Re(\bar{\upsilon}_1\upsilon_2)}^{\text{diff freq}}. \qquad \text{(D.9)}$$

Letting $\upsilon_1 = Y_1 e^{j\omega_1 t}$ and $\upsilon_2 = Y_2 e^{j\omega_2 t}$ the amplitude of the sum frequency is then given by the magnitude of $Y_1 Y_2$; that of the difference frequency by the magnitude of $\bar{Y}_1 Y_2$ (see the comments after equation (4.57). We thus have

$$\begin{aligned} Y_1 Y_2 &= -\frac{\rho_0^2 Q_0 b_w}{8\pi^2}(\omega_1\omega_2)\left[\int_{S_w}\left(\frac{e^{-j(k_1 r + k_2 r_1)}}{r r_1} + \frac{e^{-j(k_1 r + k_2 r_2)}}{r r_2}\right) dS_w\right] && \text{(D.10)} \\ \bar{Y}_1 Y_2 &= \frac{\rho_0^2 Q_0 b_w}{8\pi^2}(\omega_1\omega_2)\left[\int_{S_w}\left(\frac{e^{j(k_1 r - k_2 r_1)}}{r r_1} + \frac{e^{j(k_1 r - k_2 r_2)}}{r r_2}\right) dS_w\right]. && \text{(D.11)} \end{aligned}$$

This is the general form of the spatial factor for the sum and difference frequencies of p_1^2. We have not yet restricted ourselves to the on-axis solution since the form given above will reappear in the following section.

Second term - $p_{1t}\int p_1 dt$

Arriving at the sum and difference contributions in this case is similar to that given above except we have four kinds of terms instead of two. Again we must take the real parts before doing the multiplication so that

$$\Re(p_{1t})\Re(\int p_1 dt) = \frac{1}{4}(z_1 + \bar{z}_1 + z_2 + \bar{z}_2)(v_1 + \bar{v}_1 + v_2 + \bar{v}_2) \qquad \text{(D.12)}$$

where the the v_i, z_i are computed from (D.2) and given as

$$z_1 = -\frac{\rho_0 b_w \omega_1^2}{2\pi} \int_{S_w} \frac{e^{j(\omega_1 t - k_1 r)}}{r} dS_w \tag{D.13}$$

$$z_2 = -\frac{\rho_0 Q_0 \omega_2^2}{4\pi} \left[\frac{e^{j(\omega_2 t - k_2 r_1)}}{r_1} + \frac{e^{j(\omega_2 t - k_2 r_2)}}{r_2} \right] \tag{D.14}$$

$$v_1 = \frac{\rho_0 b_w}{2\pi} \int_{S_w} \frac{e^{j(\omega_1 t - k_1 r)}}{r} dS_w \tag{D.15}$$

$$v_2 = \frac{\rho_0 Q_0}{4\pi} \left[\frac{e^{j(\omega_2 t - k_2 r_1)}}{r_1} + \frac{e^{j(\omega_2 t - k_2 r_2)}}{r_2} \right]. \tag{D.16}$$

Expanding (D.12) and separating out the intermodulation terms we have

$$\Re(p_{1t})\Re(\int p_1 dt)_{\pm} = \overbrace{\frac{1}{2}\Re(v_1 z_2) + \frac{1}{2}\Re(v_2 z_1)}^{\text{sum frequency}} + \overbrace{\frac{1}{2}\Re(\bar{v}_1 z_2) + \frac{1}{2}\Re(v_2 \bar{z}_1)}^{\text{difference frequency}}. \tag{D.17}$$

Using the substitutions

$$v_1 = V_1 e^{j\omega_1 t},\ v_2 = V_2 e^{j\omega_2 t},\ z_1 = Z_1 e^{j\omega_1 t},\ z_2 = Z_2 e^{j\omega_2 t} \tag{D.18}$$

we have the two spatial factors for the sum frequency

$$V_1 Z_2 = -\frac{\rho_0^2 Q_0}{8\pi^2}(\omega_2^2) \left[\int_{S_w} \left(\frac{e^{-j(k_1 r + k_2 r_1)}}{r r_1} + \frac{e^{-j(k_1 r + k_2 r_2)}}{r r_2} \right) dS_w \right] \tag{D.19}$$

$$V_2 Z_1 = -\frac{\rho_0^2 Q_0}{8\pi^2}(\omega_1^2) \left[\int_{S_w} \left(\frac{e^{-j(k_1 r + k_2 r_1)}}{r r_1} + \frac{e^{-j(k_1 r + k_2 r_2)}}{r r_2} \right) dS_w \right] \tag{D.20}$$

and those for the difference frequency

$$\bar{V}_1 Z_2 = -\frac{\rho_0^2 Q_0}{8\pi^2}(\omega_2^2) \left[\int_{S_w} \left(\frac{e^{j(k_1 r - k_2 r_1)}}{r r_1} + \frac{e^{j(k_1 r - k_2 r_2)}}{r r_2} \right) dS_w \right] \tag{D.21}$$

$$V_2 \bar{Z}_1 = -\frac{\rho_0^2 Q_0}{8\pi^2}(\omega_1^2) \left[\int_{S_w} \left(\frac{e^{j(k_1 r - k_2 r_1)}}{r r_1} + \frac{e^{j(k_1 r - k_2 r_2)}}{r r_2} \right) dS_w \right]. \tag{D.22}$$

Computing sum and difference contributions of $\frac{1}{2\rho_0 c^2} p_1^2 + \frac{1}{\rho_0 c^2} p_{1t} \int p_1 dt$

The total contribution to the sum frequency is given by the coefficient $\frac{1}{2\rho_0 c^2}$ times equation (D.10) plus $\frac{1}{\rho_0 c^2}$ times $\frac{1}{2}$ from in front of the real part of (D.17) and equations (D.19) and (D.20). The difference frequency is similar except we use equations (D.11),(D.21) and (D.22).

We note that the bracketed terms in all of (D.10), (D.11) and (D.19)-(D.22) are identical for their respective frequencies. Also the c^2 in the denominator of the coefficients transforms all the ω terms into their respective wavenumbers k. Combining all of these we obtain final expressions for the spatial factors of the sum and difference frequencies of the two middle terms of (D.1):

$$\text{Sum freq} = -\frac{\rho_0 Q_0}{16\pi^2}(k_1^2 + k_1 k_2 + k_2^2)\left[\int_{S_w}\left(\frac{e^{-j(k_1 r + k_2 r_1)}}{r r_1} + \frac{e^{-j(k_1 r + k_2 r_2)}}{r r_2}\right) dS_w\right] \tag{D.23}$$

$$\text{Diff freq} = -\frac{\rho_0 Q_0}{16\pi^2}(k_1^2 - k_1 k_2 + k_2^2)\left[\int_{S_w}\left(\frac{e^{j(k_1 r - k_2 r_1)}}{r r_1} + \frac{e^{j(k_1 r - k_2 r_2)}}{r r_2}\right) dS_w\right]. \tag{D.24}$$

The on-axis solution is easily obtained from these since in this case we have (see Section 4.1.2) $dS_w = 2\pi r dr$ for $z \le r \le r_e$ and the integral is easily computed.

Third term - $|\mathbf{u}_1|^2$

Determining the square of the magnitude of the velocity vector is achieved by computing $\mathbf{u}_1 \cdot \mathbf{u}_1$. It easier in this case to assume from the beginning that we are on-axis as our vector function then simplifies substantially.

The expression for the first-order velocity is given by equation (4.46)

$$\mathbf{u}_1 = \frac{b_w}{2\pi} e^{j\omega_1 t}\int_{S_w} g(k_1, r)\frac{\mathbf{r}}{r} dS_w + \frac{Q_0}{4\pi} e^{j\omega_2 t}\left(g(k_2, r_1)\frac{\mathbf{r_1}}{r_1} + g(k_2, r_2)\frac{\mathbf{r_2}}{r_2}\right) \tag{D.25}$$

with the r values give by (4.47). On-axis we have $x = y = 0$ so that the velocity can be written as

$$\mathbf{u}_1 = \frac{b_w}{2\pi} e^{j\omega_1 t}\int_{S_w} \frac{g(k_1, r)}{r}(-\xi, -\eta, z) dS_w + \frac{Q_0}{4\pi} e^{j\omega_2 t}\left(\frac{g(k_2, r_1)}{r_1}(0, 0, z - d) + \frac{g(k_2, r_2)}{r_2}(0, 0, z + d)\right). \tag{D.26}$$

If we let $\xi = \sigma\cos\theta$ and $\eta = \sigma\sin\theta$ then since our distance r does not depend on the angle θ the x and y components of the surface integral vanish as a result of integrating over $0 \le \theta \le 2\pi$. We are therefore left with a single nonzero component

w_1 given by

$$\mathbf{u}_{1_{\text{on-axis}}} = w_1 = \frac{b_w}{2\pi} e^{j\omega_1 t} \int_{S_w} \frac{g(k_1, r)}{r} z dS_w + \frac{Q_0}{4\pi} e^{j\omega_2 t} \left(\frac{g(k_2, r_1)}{r_1}(z-d) + \frac{g(k_2, r_2)}{r_2}(z+d) \right). \tag{D.27}$$

Using the definition of $g(k, r)$ from equation (4.47) and the substitution $dS_w = \sigma d\theta d\sigma = r dr d\theta = 2\pi r dr$ our surface integral becomes

$$\int_{S_w} \frac{g(k_1, r)}{r} z dS_w = -2\pi z \left(\frac{e^{jk_1 r}}{r} \right) |_z^{r_e}. \tag{D.28}$$

The final form of the on-axis velocity is then

$$w_1 = b_w z e^{j\omega_1 t} \left[\frac{e^{-jk_1 z}}{z} - \frac{e^{-jk_1 r_e}}{r_e} \right] + \frac{Q_0 e^{j\omega_2 t}}{4\pi} \left[\frac{g(k_2, r_1)}{r_1}(z-d) + \frac{g(k_2, r_2)}{r_2}(z+d) \right]. \tag{D.29}$$

As before we let $w_1 = s_1 + s_2 = S_1 e^{j\omega_1 t} + S_2 e^{j\omega_2 t}$ so that as with p_1^2 when we compute $\Re(w_1)\Re(w_1)$ our intermodulation terms are given by $\Re(s_1 s_2)$ and $\Re(\bar{s}_1 s_2)$. We therefore obtain, for the spatial factor of the sum and difference frequencies:

$$S_1 S_2 = \frac{b_w Q_0 z}{4\pi} \left[\frac{e^{-jk_1 z}}{z} - \frac{e^{-jk_1 r_e}}{r_e} \right] \left[\frac{g(k_2, r_1)}{r_1}(z-d) + \frac{g(k_2, r_2)}{r_2}(z+d) \right] \tag{D.30}$$

$$\bar{S}_1 S_2 = \frac{b_w Q_0 z}{4\pi} \left[\frac{e^{jk_1 z}}{z} - \frac{e^{jk_1 r_e}}{r_e} \right] \left[\frac{g(k_2, r_1)}{r_1}(z-d) + \frac{g(k_2, r_2)}{r_2}(z+d) \right]. \tag{D.31}$$

All that remains is to include the coefficient term $\frac{\rho_0}{2}$ when calculating the intermodulation frequency of choice.

Final comments

Recall from the footnote below equation (4.57) that once we have separated the expressions as we have above (that is, in complex form $z_1 = Z_1 e^{j\omega_1 t}, s_2 = S_2 e^{j\omega_2 t}$ etc.) what remains is to collect the spatial functions of either the sum or difference frequency and calculate the magnitude of the spatial factor. All of this is performed in the MATLAB code in the next appendix.

Appendix E

MATLAB Code for Evaluating Surface Integral

The following is the MATLAB code used to perform the simulations given in Chapter 4. If one were to scan the code carefully and compare it with the equations given in that chapter there are two notable omissions. The first is the factor $\frac{\rho_0 Q_0}{4\pi}$. For those plots where we computed the relative change p_1/p_2 this factor cancels altogether. For the plots of just p_2 (or p_2') the decibel units are specified to be arbitrary because of this missing factor. The qualitative behaviour of the graph is unaffected.

The other omission is the factor 2 which comes from our integral solution (4.84). This is simply because it cancels with the 1/2 from our complex separation (4.55).

The code is not all that user-friendly since to investigate the dependence of the pressure on any given parameter, one must comment out the sections of the other parameters. Also the name of the routine `plot_harmonics` is a bit of a misnomer since the sum and difference frequencies are technically not harmonics.

Finally, we originally had our z-axis as the x-axis and this was only recently changed for the written thesis. To avoid any errors the code here still uses x instead of z.

plot_harmonics

This function is used to plot the dependence of p_2/p_1 (or just p_2) on various parameters. The actual computation of both p_1 and p_2 is in the subsequent routines.

```
function ret = plot_harmonics
b = 0.001; %1mm amplitude
f1 = 50; %woofer frequency
f2 = 3000; %tweeter frequency
w1 = 2*pi*f1;
w2 = 2*pi*f2;
bw = w1*b;%woofer velocity
c = 343; %speed of sound
k1 = w1/c;
k2 = w2/c;
%w =  w2+w1;
%k = w/c;
a = 0.3; %radius of woofer
d = 0.024; %tweeter distance
h = 0; %tweeter distance off-axis
x = 1; %observation point 1m away


% progress bar %
wtbar = waitbar(0, 'Calculating...');



%%%%%%%%%%%%%%%%%%%%Vary h parameter%%%%%%%%%%%%%%%%%%%%%
% last = 500;
% p2_h = zeros(1,last);
% p2_h_d = zeros(1,last);
% p1_h = zeros(1,last);
% incr = 0.001; %1mm
% for i=0:last-1;
%     %calculate p2 for sum frequency
%     h = incr*(i);
%     [re im] = surface_integral(x,d,a,h,f1,f2,true);
%     z = [re im];
%     [re_corr im_corr] = correction(b,d,h,x,true);
%     re_p2 = bw*z(1)/(2*pi) - re_corr;
%     im_p2 = bw*z(2)/(2*pi) - im_corr;
%     max_p2 = sqrt(re_p2^2 + im_p2^2);
%     p2_h(i+1) = max_p2;
%
% %     %calculate p2 for difference frequency
```

```
% %     h = incr*(i);
% %     [re_d im_d] = surface_integral(x,d,a,h,f1,f2,false);
% %     z_d = [re_d im_d];
% %     [re_corr_d im_corr_d] = correction(b,d,h,x,false);
% %     re_p2_d = bw*z_d(1)/(2*pi) - re_corr_d;
% %     im_p2_d = bw*z_d(2)/(2*pi) - im_corr_d;
% %     max_p2_d = sqrt(re_p2_d^2 + im_p2_d^2);
% %     p2_h_d(i+1) = max_p2_d;
%
%     %calculate p1
%     p1_h(i+1) = first_pressure(x,d,h,f2);
%
%     %update waitbar
%     waitbar(i/last);
% end
%  x_axis = 0:incr:(last-1)*incr;
% ref = 2*10^(-5);
%  %plot(x_axis,p1_h,x_axis,p2_h);
% % plot(x_axis,20*log10(p2_h./p1_h));
%  plot(x_axis,20*log10(p2_h/ref));
% title(['Observation distance ',num2str(x),'m, f_1 = ',num2str(f1),'Hz, f_2 = ',num2str(f2/1000),'kHz, ...
% a = ',num2str(a*100),'cm, B=',num2str(b*1000),'mm, d=',num2str(d*100),'cm']);
%  xlabel('tweeter distance off-axis h (m)');
%  ylabel('P_{sum} (dB)');
%%%%%%%%%%%%%%%%%%%%Vary d parameter%%%%%%%%%%%%%%%%%%%%
 last = 1000;
 incr = 0.01; %0.1mm increments
 p2_h = zeros(1,last); %sum frequency
 p2_h_d = zeros(1,last); %diff frequency
 p1_h = zeros(1,last);
 if h < a
     for i=1:last;
     %calculate p2 for sum frequency
     d = incr*(i);
     [re im] = surface_integral(x,d,a,h,f1,f2,true);
     z = [re im];
     [re_corr im_corr] = correction(b,d,h,x,true);
     re_p2 = bw*z(1)/(2*pi) - re_corr;
     im_p2 = bw*z(2)/(2*pi) - im_corr;
     max_p2 = sqrt(re_p2^2 + im_p2^2);
     p2_h(i) = max_p2;

      %calculate p2 for difference frequency
      [re_d im_d] = surface_integral(x,d,a,h,f1,f2,false);
      z_d = [re_d im_d];
```

```
     [re_corr_d im_corr_d] = correction(b,d,h,x,false);
     re_p2_d = bw*z_d(1)/(2*pi) - re_corr_d;
     im_p2_d = bw*z_d(2)/(2*pi) - im_corr_d;
     max_p2_d = sqrt(re_p2_d^2 + im_p2_d^2);
     p2_h_d(i) = max_p2_d;


    %calculate p1
    p1_h(i) = first_pressure(x,d,h,f2);

    %updatewaitbar
    waitbar(i/last);


    end
    x_axis = incr:incr:incr*last;
else
    for i=0:last-1;
    %calculate p2 for sum frequency
    d = incr*(i);
    [re im] = surface_integral(x,d,a,h,f1,f2,true);
    z = [re im];
    [re_corr im_corr] = correction(b,d,h,x,true);
    re_p2 = bw*z(1)/(2*pi) - re_corr;
    im_p2 = bw*z(2)/(2*pi) - im_corr;
    max_p2 = sqrt(re_p2^2 + im_p2^2);
    p2_h(i+1) = max_p2;

    %calculate p2 for difference frequency
     [re_d im_d] = surface_integral(x,d,a,h,f1,f2,false);
    z_d = [re_d im_d];
    [re_corr_d im_corr_d] = correction(b,d,h,x,false);
    re_p2_d = bw*z_d(1)/(2*pi) - re_corr_d;
    im_p2_d = bw*z_d(2)/(2*pi) - im_corr_d;
     max_p2_d = sqrt(re_p2_d^2 + im_p2_d^2);
     p2_h_d(i) = max_p2_d;
     %calculate p1
     p1_h(i+1) = first_pressure(x,d,h,f2);

    %updatewaitbar
    waitbar(i/last);

    end
    x_axis = 0:incr:incr*(last-1);
end
```

```
 ref = 2*10^(-5);

% plot(x_axis,20*log10(p1_h/ref));
 plot(x_axis,20*log10(p2_h/ref));
% p_sum = 20*log10(p2_h./p1_h);
%p_diff = 20*log10(p2_h_d./p1_h);
%plot(x_axis,p_sum,x_axis,p_diff);
 title(['Observation distance ',num2str(x),'m, f_1 = ',num2str(f1),'Hz, f_2 = ',num2str(f2/1000),'kHz, ...
  a = ',num2str(a*100),'cm, B=',num2str(b*1000),'mm']);
 xlabel('tweeter distance d (m)');
 ylabel('P_{sum} (dB)');
 %%%%%%%%%%%%%%%%%%%%Vary b parameter%%%%%%%%%%%%%%%%%%%%%
%  last = 20;
%  b_incr = 0.0001; %0.1mm
%  decibels = zeros(last,2);
%
%  for i=1:last;
%      %calculate p2
%      b = b_incr*(i);
%
%      %calculate p1
%      p1 = first_pressure(x,d,h,f2);
%      %decibels(i,2) = 20*log10( p1/(2*10^(-5)) );
%
%      %calculate sum frequency
%      [re im] = surface_integral(x,d,a,h,f1,f2,true);
%      z = [re im];
%      [re_corr im_corr] = correction(b,d,h,x,true);
%      re_p2 = -b*w1*z(1)/(2*pi) - re_corr;
%      im_p2 = -b*w1*z(2)/(2*pi) - im_corr;
%      max_p2 = sqrt(re_p2^2 + im_p2^2);
%      decibels(i,2) = 20*log10( max_p2/p1 );
%
%      %calculate difference frequency
%      [re im] = surface_integral(x,d,a,h,f1,f2,false);
%      z = [re im];
%      [re_corr im_corr] = correction(b,d,h,x,false);
%      re_p2 = -b*w1*z(1)/(2*pi) - re_corr;
%      im_p2 = -b*w1*z(2)/(2*pi) - im_corr;
%      max_p2 = sqrt(re_p2^2 + im_p2^2);
%      decibels(i,1) = 20*log10( max_p2/p1 );
%
%
%
```

```
%      %updatewaitbar
%      waitbar(i/last);
%
%
%
%  end
%
%  if last == 1
%      x_axis = [0 b_incr];
%  else
%      x_axis = b_incr:b_incr:b_incr*last;
%  end
%  bar(x_axis,decibels,'group');
%  title(['Observation distance ',num2str(x),'m, f_1 = ',num2str(f1),'Hz, f_2 = ',num2str(f2/1000),'kHz, ...
% a = ',num2str(a*100),'cm, d=',num2str(d*100),'cm']);
%  xlabel('woofer amplitude B (m)');
%  ylabel('P_2/P_1 (dB)');

 %%%%%%%%%%%%%%%%%%%%Vary a parameter%%%%%%%%%%%%%%%%%%%%%%
%  last = 200;
%  a_incr = 0.001; %1mm
%  a = a_incr;
%  decibels = zeros(last,2);
%
%  for i=1:last;
%      %calculate p2
%      a = a + a_incr;
%      [re im] = surface_integral(x,d,a,h,f1,f2,true);
%      z = [re im];
%      [re_corr im_corr] = correction(b,d,h,x,true);
%      re_p2 = b*w1*z(1)/(2*pi) - re_corr;
%      im_p2 = b*w1*z(2)/(2*pi) - im_corr;
%      max_p2 = sqrt(re_p2^2 + im_p2^2);
%      decibels(i,2) = 20*log10( (max_p2)/(2*10^(-5)) );
%      %calculate p1
%      p1 = first_pressure(x,d,h,f2);
%      decibels(i,1) = 20*log10( p1/(2*10^(-5)) );
%
%
%      %updatewaitbar
%      waitbar(i/last);
%
%
%
%  end
```

```
%  x_axis = a_incr:a_incr:a_incr*last;
%  plot(x_axis,decibels(:,2)-decibels(:,1));
%  title(['Observation distance ',num2str(x),'m, f_1 = ',num2str(f1),'Hz, f_2 = ',num2str(f2/1000),'kHz, ...
%  B=',num2str(b*1000),'mm, d=',num2str(d*100),'cm']);
%  xlabel('woofer radius a (m)');
%  ylabel('P_{sum}/P_1 (dB)');

  %bar(x_axis,decibels,'group','r');


 %%%%%%%%%%%%%%%%%%Vary x parameter (compare to analytic solution)%%%%%%%%%
 % do not use correction terms since comparing p2'_exact to p2'_approx and
 % correction terms blow up as x moves toward tweeter. Also, they are
 % independent of the method used
%  last = 100;
%  x_incr = 0.01;
%  decibels = zeros(last,4);
%  ref = 2*10^(-5);
%  x=x_incr;
%
%  for i=1:last;
%      %calculate p2
%
%      %calculate sum frequency
%      [re im] = surface_integral(x,d,a,h,f1,f2,true);
%      z = [re im];
%      re_p2 = -b*w1*z(1)/(2*pi);
%      im_p2 = -b*w1*z(2)/(2*pi);
%      max_p2 = sqrt(re_p2^2 + im_p2^2);
%      decibels(i,1) = 20*log10( max_p2/ref );
%       w = w1+w2; k=w/c;
%
%       %analytic solution sum frequency
%       rd = sqrt(a^2 + d^2);
%       temp = (w/w1)*(d^2/rd^3*cos(k*x+k2*rd) + d^2*k2/rd^2*sin(k*x+k2*rd)-cos(k*x + k2*rd)/rd ...
%  - k2*sin(k*x + k2*d)) + k^2/k2*(sin(k*x  + k2*rd) - sin(k*x + k2*d));
%       temp = temp/x;
%       %imaginary part
%       temp2 = (w/w1)*(-d^2/rd^3*sin(k*x+k2*rd) + d^2*k2/rd^2*cos(k*x+k2*rd)+sin(k*x + k2*rd)/rd ...
%  - k2*cos(k*x + k2*d)) + k^2/k2*(cos(k*x  + k2*rd) - cos(k*x + k2*d));
%       temp2 = temp2/x;
%       max_approx_sum = b*w1*sqrt(temp^2 + temp2^2);
%       decibels(i,2) = 20*log10( max_approx_sum/ref );
%
%   %%%%%%%%%%%%%%%%%%%%%%%%%%%%%%%%%%%%%%%%%%%%%%%%%%%%%%%%%%%%%%%%%%%%
```

```
%
%      %calculate difference frequency
%      [re_d im_d] = surface_integral(x,d,a,h,f1,f2,false);
%      z_d = [re_d im_d];
%      re_p2_d = -b*w1*z_d(1)/(2*pi);
%      im_p2_d = -b*w1*z_d(2)/(2*pi);
%      max_p2_d = sqrt(re_p2_d^2 + im_p2_d^2);
%      decibels(i,3) = 20*log10( max_p2_d/ref );
%       w = w2-w1; k=w/c;
%
%
%       %analytic approximation difference frequency
%       %real part
%
%       rd = sqrt(a^2 + d^2);
%       temp = -(w/w1)*(d^2/rd^3*cos(k*x+k2*rd) + d^2*k2/rd^2*sin(k*x+k2*rd)-cos(k*x + k2*rd)/rd ...
% - k2*sin(k*x + k2*d)) + k^2/k2*(sin(k*x  + k2*rd) - sin(k*x + k2*d));
%       temp = temp/x;
%       %imaginary part
%       temp2 = -(w/w1)*(-d^2/rd^3*sin(k*x+k2*rd) + d^2*k2/rd^2*cos(k*x+k2*rd)+sin(k*x + k2*rd)/rd ...
%  - k2*cos(k*x + k2*d)) + k^2/k2*(cos(k*x  + k2*rd) - cos(k*x + k2*d));
%       temp2 = temp2/x;
%       max_approx_d = b*w1*sqrt(temp^2 + temp2^2);
%       decibels(i,4) = 20*log10( max_approx_d/ref );
%
%
%      %updatewaitbar
%      waitbar(i/last);
%
%     x = x_incr*i;
%
%
%  end
%
%  x_axis = x_incr:x_incr:x_incr*last;
%  %bar(x_axis,decibels,'group');
%
%  plot(x_axis,abs(decibels(:,1)-decibels(:,2)),x_axis,abs(decibels(:,3)-decibels(:,4)));
%  title(['Analytic comparison, f_1 = ',num2str(f1),'Hz, f_2 = ',num2str(f2/1000),'kHz, ...
% a = ',num2str(a*100),'cm, d=',num2str(d*100),'cm']);
%  xlabel('observation distance x (m)');
%  ylabel('P_2 exact - P_2 approx (dB) - arbitrary units');
%
 %close waitbar
 close(wtbar);
```

```
function [re_corr im_corr] = correction(b,d,h,x,sum)
    rx = sqrt(a^2 + x^2);
    r1 = sqrt( (x-d)^2 + h^2 );
    r2 = sqrt( (x+d)^2 + h^2 );   %for on axis observation

    %pressure terms
    if sum
        re_corr = (1/(2*r1*k1))*(sin(k1*rx+k2*r1) - sin(k1*x+k2*r1)) + (1/(2*r2*k1))*(sin(k1*rx+k2*r2) ...
        -sin(k1*x+k2*r2));
        im_corr = (1/(2*r1*k1))*(cos(k1*rx+k2*r1) - cos(k1*x+k2*r1)) + (1/(2*r2*k1))*(cos(k1*rx+k2*r2) ...
        -cos(k1*x+k2*r2));
        factor = (-b*w1/c^2)*(w1^2 + w1*w2 + w2^2);
        re_corr = factor*re_corr;
        im_corr = factor*im_corr;
    else %difference frequency
        re_corr = (1/(2*r1*k1))*(sin(k1*rx-k2*r1) - sin(k1*x-k2*r1)) + (1/(2*r2*k1))*(sin(k1*rx-k2*r2) ...
        -sin(k1*x-k2*r2));
        im_corr = (1/(2*r1*k1))*(cos(k1*rx-k2*r1) - cos(k1*x-k2*r1)) + (1/(2*r2*k1))*(cos(k1*rx-k2*r2) ...
        -cos(k1*x-k2*r2));
        factor = (-b*w1/c^2)*(w1^2 - w1*w2 + w2^2);
        re_corr = factor*re_corr;
        im_corr = -factor*im_corr;
    end
    %velocity term
    if sum
        re_u1 = (k2/(r1^2))*(-sin(k1*rx+k2*r1)/rx +sin(k1*x+k2*r1)/x) - cos(k1*rx+k2*r1)/(rx*r1^3) ...
         + cos(k1*x+k2*r1)/(x*r1^3);
        re_u1 = b*w1*x*(x-d)*re_u1/2;
        re_u2 = (k2/(r2^2))*(-sin(k1*rx+k2*r2)/rx +sin(k1*x+k2*r2)/x) - cos(k1*rx+k2*r2)/(rx*r2^3) ...
         + cos(k1*x+k2*r2)/(x*r2^3);
        re_u2 = b*w1*x*(x+d)*re_u2/2;
        re_u = re_u1+re_u2;

        im_u1 = (k2/(r1^2))*(-cos(k1*rx+k2*r1)/rx +cos(k1*x+k2*r1)/x) + sin(k1*rx+k2*r1)/(rx*r1^3) ...
         - sin(k1*x+k2*r1)/(x*r1^3);
        im_u1 = b*w1*x*(x-d)*im_u1/2;
        im_u2 = (k2/(r2^2))*(-cos(k1*rx+k2*r2)/rx +cos(k1*x+k2*r2)/x) + sin(k1*rx+k2*r2)/(rx*r2^3) ...
         - sin(k1*x+k2*r2)/(x*r2^3);
        im_u2 = b*w1*x*(x+d)*im_u2/2;
        im_u = im_u1 + im_u2;
```

```
        else %difference frequency
            re_u1 = (k2/(r1^2))*(sin(k1*rx-k2*r1)/rx - sin(k1*x-k2*r1)/x) - cos(k1*rx-k2*r1)/(rx*r1^3)  ...
            + cos(k1*x-k2*r1)/(x*r1^3);
            re_u1 = b*w1*x*(x-d)*re_u1/2;
            re_u2 = (k2/(r2^2))*(sin(k1*rx-k2*r2)/rx - sin(k1*x-k2*r2)/x) - cos(k1*rx-k2*r2)/(rx*r2^3) ...
            + cos(k1*x-k2*r2)/(x*r2^3);
            re_u2 = b*w1*x*(x+d)*re_u2/2;
            re_u = re_u1+re_u2;

            im_u1 = (k2/(r1^2))*(-cos(k1*rx-k2*r1)/rx +cos(k1*x-k2*r1)/x) - sin(k1*rx-k2*r1)/(rx*r1^3) ...
             + sin(k1*x-k2*r1)/(x*r1^3);
            im_u1 = b*w1*x*(x-d)*im_u1/2;
            im_u2 = (k2/(r2^2))*(-cos(k1*rx-k2*r2)/rx +cos(k1*x-k2*r2)/x) - sin(k1*rx-k2*r2)/(rx*r2^3) ...
            + sin(k1*x-k2*r2)/(x*r2^3);
            im_u2 = b*w1*x*(x+d)*im_u2/2;
            im_u = im_u1 + im_u2;
        end

        re_corr = re_corr + re_u;
        im_corr = im_corr + im_u;
    end%correction

end%plot_harmonics
```

first_pressure

This function computes the first order pressure for on-axis observation

```
function p1_max = first_pressure(x,d,h,f2)


w2 = 2*pi*f2;
c = 343;
k2 = w2/c;

r1 = sqrt( (x-d)^2 + h^2 );
r2 = sqrt( (x+d)^2 + h^2 ); %for on axis observation
re = sin(k2*r1)/r1 + sin(k2*r2)/r2;
im = cos(k2*r1)/r1 + cos(k2*r2)/r2;
re = w2*re;
im = w2*im;
p1_max = sqrt(re^2 + im^2);

end
```

surface_integral

This function computes our surface integral (4.84) for on-axis observation

```
function [re im] = surface_integral(x,d,a,h,f1,f2,sum)
c = 343;
w1 = 2*pi*f1;
w2 = 2*pi*f2;
k1 = w1/c;
k2 = w2/c;
if sum
    w = w2+w1;
else %difference frequency
    w = w2 - w1;
end
k = w/c;
tol = exp(-12);
re = dblquad(@re_intgrnd,0,a,0,2*pi,tol,@equad);
im = dblquad(@im_intgrnd,0,a,0,2*pi,tol,@equad);
```

```
    function z = re_intgrnd(sigma,theta)
        r0 = sqrt(d^2+sigma.^2 - 2*sigma*h*cos(theta) + h^2);
        ra = sqrt (x^2 + sigma.^2);
        I1 = cos(k2*r0 + k*ra).*(1./r0.^3 +(d*k2)^2./r0.^3 - 3*d^2./r0.^5) ...
         + sin(k2*r0 + k*ra).*(k2./r0.^2 - 3*k2*d^2./r0.^4);
        if sum
            I1 = I1*(w/w1);
        else %difference frequency
            I1 = -I1*(w/w1);
        end

        I2 = cos(k2*r0 + k*ra)./r0;
        I2 = I2*k^2;
        I = (I1 + I2)./ra;
        z = I.*sigma;
    end %re_integrnd

    function z = im_intgrnd(sigma,theta)
        r0 = sqrt(d^2+sigma.^2 - 2*sigma*h*sin(theta) + h^2);
        ra = sqrt (x^2 + sigma.^2);
        I1 = -sin(k2*r0 + k*ra).*(1./r0.^3 +(d*k2)^2./r0.^3 - 3*d^2./r0.^5) ...
         + cos(k2*r0 + k*ra).*(k2./r0.^2 - 3*k2*d^2./r0.^4);
```

```
        if sum
            I1 = I1*(w/w1);
        else %difference frequency
            I1 = -I1*(w/w1);
        end
        I2 = -sin(k2*r0 + k*ra)./r0;
        I2 = I2*k^2;
        I = (I1+I2)./ra;
        z = I.*sigma;
    end %im_integrnd
end%surface_integral
```

equad

This is simply a wrapper function in order to use the `quadgk` quadrature routine in the `dblquad` command of the previous `surface_integral` function. This quadrature method was used solely based on the recommendation by MATLAB.

```
function q = equad(fun,a,b,tol,trace,varargin)

q = quadgk(@(x)fun(x,varargin{:}),a,b,'AbsTol',tol, 'Waypoints', linspace(a,b,10),'MaxIntervalCount',8000);
```

References

[1] P. Klipsch. A note on modulation distortion: coaxial and spaced tweeter - woofer loudspeaker system. *J. Audio Eng. Soc.*, 24(3), April 1976. iii, 58, 76, 93, 97

[2] Robert T. Beyer. *Physical Acoustics: Principles and Methods*, volume 2B, chapter 10. Academic Press, 1965. 1

[3] Wikipedia. Loudspeaker — wikipedia, the free encyclopedia, 2009. [Online; accessed 26-January-2009]. 1

[4] H.F Olson. Loudspeakers. In *Proc. IRE*, page 730, May 1961. 1

[5] J. Chernof. Principles of loudspeaker design and operation. *IRE Transactions on Audio*, 5(5 Part 1):117–127, 1957. 2

[6] J.W.S. Rayleigh. *The Theory of Sound*, volume 2, 1896. reprinted by Dover, New York, 2nd edition, 1945. 2

[7] J.C. Lockwood and J.G. Willette. High-speed method for computing the exact solution for the pressure variations in the nearfield of a baffled piston. *J. Acoust. Soc. Am.*, 53:735, 1973. 2

[8] M. Greenspan. Piston radiator: Some extensions of the theory. *J. Acoust. Soc. Am*, Jan. 1979.

[9] B. Newberry and J. Rose. An approximation for the on-axis field of an elliptical piston transducer. *J. Acoust. Soc. Am.*, Jan. 1989.

[10] J. Kelly and R. McGough. An annular superposition integral for axisymmetric radiators. *J. Acoust. Soc. Am.*, Jan. 2007.

[11] T.D. Mast and F. Yu. Simplified expansions for radiation from a baffled circular piston. *J. Acoust. Soc. Am.*, 118:3457, 2005. 51

[12] Joe Zemanek. Beam behavior within the nearfield of a vibrating piston. *J. Acoust. Soc. Am.*, 50:136, 1971.

[13] T. Lawu, M. Tabei, and M. Ueda. Fast converging binomial series for radiation field calculation. *J. Acoust. Soc. Am.*, 98:2819, 1995. 2

[14] J. Timko. The mathematical modeling of a coaxial speaker, 2003. R.A. Report, University of Waterloo. 3

[15] A. Gutfraind. Point-plane model of coaxial loudspeakers, 2002. R.A. Report, University of Waterloo. 3

[16] Frazier Speakers. Coaxial loudspeakers: Separating facts from hype. White Paper (undated). 3

[17] J.C. Piquette and A.L. Van Buren. Censor's acoustical doppler effect analysis-is it a valid method? *J. Acoust. Soc. Am.*, page 1681, Oct. 1987. 4

[18] N. Mujica, R. Wunenburger, and S. Fauve. Scattering of a sound wave by a vibrating surface. *The European Physical Journal B-Condensed Matter*, Jan. 2003. 4, 62

[19] M. Lighthill. On Sound Generated Aerodynamically. I. General Theory. *Proceedings of the Royal Society of London. Series A*, Jan. 1952. 4

[20] U. Ingard and David C. Pridmore-Brown. Scattering of sound by sound. *J. Acoust. Soc. Am.*, 28(3):367, 1956. 4, 60

[21] P.J. Westervelt. Scattering of sound by sound. *J. Acoust. Soc. Am.*, 29:199, 1957. 4, 59, 60

[22] A.L. Thuras, R.T. Jenkins, and H.T. O'Neil. Extraneous frequencies generated in air carrying intense sound waves. *J. Acoust. Soc. Am.*, 6:173, 1935. 4

[23] David T. Blackstock. *Fundamentals of Physical Acoustics*. Wiley & Sons Inc., 2000. 6, 7, 9, 11, 15, 23, 52, 55, 63

[24] Pijush K. Kundu. *Fluid Mechanics*, chapter 3-5. Elsevier Inc., 3rd edition, 2004. 6, 15

[25] Lawrence E. Kinsler. *Fundamentals of Acoustics*. Wiley & Sons, 3rd edition, 1982. 6

[26] F.V. Hunt. Notes on the exact equations governing the propagation of sound in fluids. *J. Acoust. Soc. Am.*, 27(6):1019, 1955. 6

[27] A.D. Pierce. *Acoustics: An Introduction to Its Physical Principles and Applications*. McGraw-Hill Book Company, 1981. 7, 22, 23, 25, 26

[28] Wikipedia. Speed of sound — wikipedia, the free encyclopedia, 2009. [Online; accessed 21-February-2009]. 8

[29] J. Borwick. *Loudspeaker and Headphone Handbook*. Butterworths, 1988. 8

[30] P. M. Morse and K. U. Ingard. *Theoretical Acousics*. McGraw-Hill, Inc., 1968. 9, 10, 22, 23, 40

[31] D.W. van Wulfften Palthe. Doppler effect in loudspeakers. *Acustica*, 28, 1973. 9, 61

[32] F.J. Fahy. *Sound Intensity*, page 14. E & FN Spon, 2nd edition, 1995. 12

[33] E. Skudrzyk. *The Foundations of Acoustics*. Springer-Verlag, 1971. 17, 40, 54

[34] Wikipedia. Fundamental solution — wikipedia, the free encyclopedia, 2009. [Online; accessed 10-March-2009]. 17

[35] Wikipedia. Spherical coordinate system — wikipedia, the free encyclopedia, 2009. [Online; accessed 5-March-2009]. 23

[36] Wikipedia. Lewy's example — wikipedia, the free encyclopedia, 2009. [Online; accessed 11-March-2009]. 28

[37] Wikipedia. Malgrange-Ehrenpreis theorem — wikipedia, the free encyclopedia, 2009. [Online; accessed 11-March-2009]. 29

[38] M.D. Greenberg. *Application of Green's Functions in Science and Engineering*. Prentice-Hall, 1971. 30

[39] D.G. Crighton, A. P. Dowling, J.E. Ffowcs Williams, M. Heckl, and F.G. Leppington. *Modern Mehods in Analytical Acoustics – Lecture Notes*. Springer-Verlag, 1992. 35, 36

[40] J. Wainwright and G.Tenti. Calculus 4 – course notes for AMATH231. Department of Applied Mathematics – University of Waterloo, 2003. 35

[41] E.G. Williams. *Fourier Acoustics — Sound Radiation and Nearfield Acoustical Holography*. Academic Press, 1999. 40

[42] A. Sommerfeld. *Partial Differential Equations in Physics*. Academic Press, Inc., 1949. translated by E.G. Straus. 41

[43] Eugene Gutkin and Paul K Newton. The method of images and Green's function for spherical domains. *J. Phys. A: Math. Gen.*, 37(50):11989–12003, Dec 2004. 41, 46

[44] Eric W. Weisstein. "Bessel function of the first kind." from mathworld–a Wolfram web resource. 55

[45] L.W. Dean III. Interactions between sound waves. *J. Acoust. Soc. Am.*, 34:1039, 1962. 59, 60

[46] J.S Thierman. *Sources of Difference Frequency Sound in a Dual-Frequency Imaging System with Implications for Monitoring Thermal Surgery*. PhD thesis, MIT, 2004. 59, 67

[47] J. Tjøtta and S. Tjøtta. Interaction of sound waves. part i: Basic equations and plane waves. *J. Acoust. Soc. Am.*, page 1425, Jan. 1987. 60

[48] J. Tjøtta and S. Tjøtta. Interaction of sound waves. part ii: Plane wave and real beam. *J. Acoust. Soc. Am.*, page 1429, 1987.

[49] J. Tjøtta and S. Tjøtta. Interaction of sound waves. part iii: Two real beams. *J. Acoust. Soc. Am.*, 83:487, 1988.

[50] J. Berntsen, J. Tjøtta, and S. Tjøtta. Interaction of sound waves. part iv: Scattering of sound by sound. *J. Acoust. Soc. Am.*, page 1969, Jan. 1989. 60

[51] P.V. Sakov. Nonlinear interaction of nonconcentric spherical waves. *Sov. Phys. Acoust.*, 38(2):180, 1992. 60

[52] L. M. Liamshev and P. V. Sakov. Nonlinear interaction of plane and spherical waves. *Akusticheskii Zhurnal*, 34:485–490, June 1988. 60

[53] G. Beers and H. Belar. Frequency-modulation distortion in loudspeakers. *Proc. IRE*, 31(4):132 – 138, Apr 1943. 60

[54] R. Allison and E. Villchur. On the magnitude and audibility of fm distortion in loudspeakers. *J. Audio Eng. Soc.*, 30(10):694, October 1982. 61

[55] H.J. Butterweck. About the Doppler effect in acoustic radiation from loudspeakers. *Acustica*, 63:77, 1987. 61

[56] B. Zóltogórski. Moving boundary conditions and nonlinear propagation as sources of nonlinear distortions in loudspeakers. *J. Audio Eng. Soc.*, 41(9), 1993. 61

[57] V.A. Zverev and A.I. Kalachev. Modulation of sound by sound in the intersection of sound waves. *Sov. Phys. Acoustics*, 16(2), 1970. 62

[58] H.F. Olson. *Acoustical Engineering*. Professional Audio Journals, Inc., 1991. 76

[59] J. Vanderkooy. University of Waterloo, Physics Department, Canada. Personal Communication. 77

[60] E. Zauderer. *Partial Differential Equations of Applied Mathematics*. John Wiley & Sons, 1983. 106

[61] M.C.M. Wright, editor. *Lecture Notes on the Mathematics of Acoustics*. Imperial College Press, 2005. 109

[62] R.T. Kessel. The Exterior Helmholtz Integral Equation and it's Approximate Solution For Acoustic Radiation Problems. Master's thesis, University of Waterloo, 1989. 112

[63] O. von Estorff, editor. *Boundary Elements in Acoustics*. WIT Press, 2000. 112